

30/10/96 (1996) 2^e ex

Validation and application of soil acidification models at local, national and European scale

A compilation of articles on the models NuCSAM, ReSAM and SMART

**J. Kros
J.E. Groenenberg
C. van der Salm
W. de Vries
G.J. Reinds**

Report 98

25 OKT. 1996

DLO Winand Staring Centre, Wageningen, 1996



CENTRALE LANDBOUWCATALOGUS

0000 0754 8718

ISBN 921691

ABSTRACT

J. Kros, J.E. Groenenberg, C. van der Salm, W. de Vries and G.J. Reinds, 1996. *Validation and application of soil acidification models on local, national and European scales; a compilation of articles on the models NuCSAM, ReSAM and SMART*, 1996. Wageningen (The Netherlands), DLO Winand Staring Centre. Report 98. 158 pp.; 25 Figs; 51 Tables; 85 Refs; 2 Annexes.

An overview is given of three dynamic soil acidification models for application on different spatial scales. NuCSAM, the model for the local scale, was validated on data from two intensively monitored research sites. Results of annual average soil solution concentrations and fluxes calculated with the validated NuCSAM model agreed well with those of the national-scale model ReSAM and to a lesser extent with those of the European-scale model SMART. Various deposition scenarios for SO_x, NO_x and NH_x on soils were evaluated with the three acidification models.

Keywords: atmospheric deposition, environmental protection, simulation model

ISSN 0927-4537

©1996 DLO Winand Staring Centre for Integrated Land, Soil and Water Research (SC-DLO), P.O. Box 125, NL-6700 AC Wageningen (The Netherlands).
Phone: 31 317474200; fax: 31 317424812; e-mail: postkamer@sc.dlo.nl

No part of this publication may be reproduced or published in any form or by any means, or stored in a data base or retrieval system, without the written permission of the DLO Winand Staring Centre.

Project 7240

Rep98.IS\07-96

Contents

	page
Preface	13
Summary	15
1 Introduction	19
References	21
2 Validation and application of a nutrient cycling and soil acidification model to an intensively monitored douglas fir site	23
2.1 Introduction	23
2.2 Model description	24
2.2.1 Model structure	24
2.2.2 Hydrology	24
2.2.3 Nutrient cycling	27
2.2.4 Geochemical process formulations	30
2.2.5 Forest growth	32
2.3 Model calibration	33
2.3.1 Derivation of input data	36
2.3.1.1 Site description	36
2.3.1.2 Hydrology	36
2.3.1.3 Soil chemistry	38
2.3.1.4 Forest growth	41
2.3.2 Results	42
2.3.2.1 Hydrology	42
2.3.2.2 Soil chemistry	44
2.4 Scenario analyses	49
2.4.1 Derivation of input data	49
2.4.1.1 Deposition scenarios	49
2.4.1.2 Hydrology	51
2.4.1.3 Soil chemistry	52
2.4.2 Results	56
2.4.2.1 Hydrology for the 'Veluwe' region	56
2.4.2.2 Soil chemistry for the 'Veluwe' region	57
2.4.3 Comparison of results for the three deposition scenarios	59
2.5 General discussion and conclusions	61
2.5.1 Model validation	61
2.5.2 Scenario analyses	62
2.5.3 Uncertainties	62
2.5.4 Recommendations for future research	63
2.5.5 Major conclusions	63
References	65

3	Application of the model NuCSAM to the Solling spruce site	71
3.1	Introduction	71
3.2	Model principles and key equations	71
3.2.1	Model structure	71
3.2.2	Hydrological processes	72
3.2.3	Biogeochemical processes	72
3.3	Derivation of input data	73
3.3.1	Hydrological data	73
3.3.2	Biogeochemical data	75
3.4	Results and discussion	76
3.4.1	Hydrology	76
3.4.2	Biogeochemistry	78
3.5	Conclusions	82
	References	83
4	Uncertainties in long-term predictions of forest soil acidification due to neglecting seasonal variability	85
4.1	Introduction	85
4.2	Models used	86
4.2.1	ReSAM	86
4.2.2	NuCSAM	87
4.3	Methods and data	88
4.3.1	Approach	88
4.3.2	The Solling site	89
4.3.3	Deposition data and scenarios	89
4.3.4	Hydrological data	89
4.3.5	Biogeochemical data	90
4.4	Results and discussion	93
4.4.1	Validation of NuCSAM	93
4.4.2	Long-term predictions with ReSAM and NuCSAM	96
4.5	Conclusions	102
	References	105
5	Application of soil acidification models with different degrees of process description on an intensively monitored spruce site	107
5.1	Introduction	107
5.2	Models used	108
5.2.1	SMART	109
5.2.2	ReSAM	109
5.2.3	NuCSAM	110
5.3	Methods and data	110
5.3.1	Methods	110
5.3.2	Hydrological data	112
5.3.3	Geochemical data	113
5.3.4	Biological data	114
5.4	Results and discussion	119
5.4.1	Influence of vertical resolution	120
5.4.2	Influence of process description	121

5.4.3 Influence of temporal resolution	122
5.5 Conclusions	123
References	125
6 Scenario studies on soil acidification at different spatial scales	127
6.1 Introduction	127
6.2 The models NuSCAM, ReSAM and SMART	128
6.2.1 Process descriptions	131
6.3 Validation and application of the models at various scales	131
6.3.1 Studies on a local scale	131
6.3.1.1 Methodology	131
6.3.1.2 Model validation	132
6.3.1.3 Model predictions	134
6.3.2 Studies on a national scale	136
6.3.2.1 Methodology	136
6.3.2.2 Model validation	137
6.3.2.3 Model predictions	138
6.3.3 Studies on a european scale	139
6.3.3.1 Methodology	139
6.3.3.2 Model predictions	140
6.4 Discussion and conclusions	141
6.4.1 Evaluation of model predictions	141
6.4.2 Limitations of the models	142
6.4.3 Use of the models to predict chemical time bombs	143
References	145
7 General discussion and conclusions	147
 Tables	
2.1 NuCSAM model parameters that were calibrated	35
2.2 Vegetation dependent hydrologic parameter values for the Speulderbos site	37
2.3 Parameters of the Mualem-Van Genuchten functions to describe the soil physical properties.	38
2.4 Gaines Thomas exchange coefficients (mol l^{-1}) ^{z-2} and cation exchange capacity ($\text{mmol}_c \text{ kg}^{-1}$)	39
2.5 Parameters for weathering of silicates	39
2.6 Parameters for the calculation of weathering of oxalate extractable Al	40
2.7 Sulphate and phosphate sorption capacities as a function of depth, calculated according to Eqn. (45) and (46)	40
2.8 Values for soil-layer independent model parameters	41
2.9 Tree growth parameters as derived from data for plot 1 measured by Jans <i>et al.</i> (1994) and data for the soil plot (Olsthoorn, 1991)	41
2.10 Data on biomass and element contents of needles, roots and stems of Speuld stand	42
2.11 Simulated water balance terms for the Speuld experimental forest	43

2.12	NuCSAM Performance criteria for the discrepancy between observed and measured soil water contents	44
2.13	Performance of NucSAM during the observation period	48
2.14	Major element fluxes of the simulated element budgets for NO_3^- , NH_4^+ , Al^{3+} and Ca^{2+} for the soil component.	48
2.15	Total acid deposition ($\text{mol}_c \text{ ha}^{-1} \text{ a}^{-1}$) for generic Scots pine (SP) and Douglas fir (DF) stands in Drenthe (situated in the Northern Netherlands), Veluwe (Central Netherlands) and North Limburg (Southern Netherlands).	49
2.16	Parameters of the Mualem-Van Genuchten functions to describe the soil physical properties for a Cambic podzol and a Haplic arenosol	51
2.17	Hydrological parameter values for generic Douglas fir on a Cambic podzol and Scots pine on a Haplic arenosol	52
2.18	Element contents in primary minerals, hydroxides and the adsorption complex for the generic Cambic podzol and the Haplic arenosol	53
2.19	Values used for overall model parameters for Douglas fir on a Cambic podzol and Scots pine on a Haplic arenosol	54
2.20	Elovich constants for Al dissolution, base cation weathering rate constants and Gaines Thomas exchange constants of the Cambic podzol and the Haplic arenosol used in the simulation	54
2.21	Initial stand structure conditions for generic Douglas fir and Scots pine	55
2.22	Data on biomass and element contents of leaves, fine roots and stems for the generic Douglas fir and Scots pine	55
2.23	Average simulated water balance for Douglas fir on a Cambic podzol (DFCP) and Scots pine on a Haplic arenosol (SPHA) in the 'Veluwe' region for the period 1980-2050	56
2.24	Annual simulated fluxes of NO_3^- and NH_4^+ for generic Douglas fir on a Cambic Podzol for region 'Veluwe', and for 1990 and 2010.	57
2.25	Mean predicted soil parameters at 20 cm depth simulated by NuCSAM between 1990 and 2000, and between 2040 and 2050 for generic Douglas fir on a Cambic podzol and generic Scots pine on a Haplic arenosol	61
3.1	Parameters used to calculate interception	74
3.2	Water retention and hydrological conductivity characteristics used in the simulation	74
3.3	Values for the crop factor and root uptake distribution used in the simulation	74
3.4	Values for soil-layer independent model parameters used in the simulation based on the Solling data set	76
3.5	Elovich constants for Al dissolution, base cation weathering rate constants, Gaines Thomas exchange constants and SO_4 sorption parameters used in the simulation	76
4.1	Values for biogeochemical model parameters used in the NuCSAM and ReSAM simulations	90
4.2	Monthly distribution fractions (unitless) for litterfall (<i>lf</i>), root decay (<i>rd</i>), mineralization (<i>mi</i>) and root uptake (<i>ru</i>) as used in NuCSAM	91
4.3	Constants for Al dissolution, base cation weathering rate constants and Gaines Thomas exchange constants, SO_4^{2-} sorption parameters used in ReSAM and NuCSAM	92
4.4	Soil properties used for NuCSAM and ReSAM	93

4.5	Performance of the two models during the observation period expressed as the Normalized Mean Absolute Error	96
5.1	Overview of the considered processes	108
5.2	Statistical measures for evaluation of model results	112
5.3	Average drainage fluxes and water contents used in NuCSAM, ReSAM and SMART	113
5.4	Soil properties used for NuCSAM, ReSAM and SMART	113
5.5	Elovich constants for Al dissolution, base cation weathering rate constants and Gaines Thomas exchange constants, SO ₄ sorption parameters used in the simulation by NuCSAM and ReSAM	115
5.6	Values for soil-layer independent model parameters used in the simulation based on the Solling dataset	116
5.7	Geochemical parameters for SMART	116
5.8	Normalized mean Absolute Error (NMAE) and Coefficient of Residual MASS (CRM) for simulated concentrations	120
6.1	Characteristics of the dynamic soil acidification models used at the DLO Winand Staring Centre	129
6.2	Processes and process formulations included in NuCSAM, ReSAM and SMART	130
6.3	Statistical measures for evaluation of model results	132
6.4	Normalized Mean Absolute Error (NMAE) and Coefficient of Residual MASS (CRM) for simulated SO ₄ , NO ₄ and Al concentrations with NuCSAM, ReSAM, and SMART at Speuld	134
6.5	Average values used for the potential acid deposition in 2010 and 2050 for three scenarios.	136
6.6	Median values of soil solution parameters measured in the field and simulated by ReSAM	137
6.7	Transfer functions between soil properties and soil characteristics	140
6.8	Possibilities and limitations of the models NuCSAM, ReSAM and SMART	143

Figures

2.1	Accumulated simulated throughfall for the years 1988 and 1989	43
2.2	Comparison of observed and simulated water contents in the 0-50 and 50-100 cm soil layers for the year 1989	44
2.3	Simulations of soil water chemistry by NuCSAM for 20 cm depth	46
2.4	Simulations of soil water chemistry by NuCSAM for 90 cm depth	47
2.5	Deposition scenarios for Scots Pine and Douglas fir stands in the Veluwe	50
2.6	Simulated soil water chemistry for Douglas fir on a Cambic podzol and for Scots pine on a Haplic arenosol (right) in the 'Veluwe' region at 20 cm (left) and at 90 cm (right)	58
2.7	Simulated pH at 20 cm depth for Scots pine on a Haplic arenosol (top) and Douglas fir on a Cambic podzol (bottom) for scenario 'Drenthe', 'Veluwe' and 'N-Limburg'	60
3.1	Measured and simulated throughfall (cm) for the whole year (top) and the summer period (bottom)	77
3.2	Simulated (—) and measured (+) pF-values at 10 (left) and 100 cm (right) depth and simulated (—) and measured (+) Cl concentrations	

	at 10 (left) and 90 cm (right) depth	78
3.3	Simulated (—) and average measured (+) concentrations of SO ₄ and NO ₃ at 10 cm (left) and 90 cm (right) depth	79
3.4	Simulated (—) and average measured (+) concentrations of Mg, Al and pH at 10 cm (left) and 90 cm (right) depth	80
3.5	Changes in flux-weighted Al and Ca concentration, molar Al/Ca ratio and pH in the 0-10 cm (left) and 80-100 cm (right) layers for the 'business as usual' (BU) and 'improved environment' (IE) scenarios	81
4.1	Simulated and observed concentrations of Cl ⁻ , Al ³⁺ , Al ³⁺ /Ca ²⁺ ratio, SO ₄ ²⁻ , NO ₃ ⁻ and NH ₄ ⁺ at 10 cm (left-hand side) and 90 cm (right-hand side) depth	94/95
4.2	Flux-weighted annual averaged concentrations simulated with NuCSAM and with ReSAM of Al ³⁺ , SO ₄ ²⁻ , NO ₃ ⁻ , NH ₄ ⁺ and Al ³⁺ /Ca ²⁺ ratio at 10 cm (left-hand side) and 90 cm (right-hand side) depth, under the Business as Usual scenario.	97
4.3	Flux-weighted annual averaged concentrations simulated with NuCSAM and with ReSAM of Al ³⁺ , SO ₄ ²⁻ , NO ₃ ⁻ , NH ₄ ⁺ and Al ³⁺ /Ca ²⁺ ratio at 10 cm (left-hand side) and 90 cm (right-hand side) depth, under the Improved Environment scenario.	98
4.4	Cumulative leaching fluxes of Al ³⁺ , SO ₄ ²⁻ , NO ₃ ⁻ and NH ₄ ⁺ at 10 cm (left-hand side) and 90 cm (right-hand side) depth as simulated with NuCSAM and ReSAM, using the Business as Usual scenario	100
4.5	Cumulative leaching fluxes of Al ³⁺ , SO ₄ ²⁻ , NO ₃ ⁻ and NH ₄ ⁺ at 10 cm (left-hand side) and 90 cm (right-hand side) depth as simulated with NuCSAM and ReSAM, using the Improved Environment scenario	101
5.1	Measured and simulated SO ₄ and Cl concentrations and leaching at 10 (left) and 90 cm depth (right)	117
5.2	Measured and simulated NO ₃ and NH ₄ concentrations and leaching at 10 (left) and 90 cm depth (right)	118
5.3	Measured and simulated Al and BC concentrations and leaching at 10 (left) and 90 cm depth (right)	119
6.1	Observed and simulated concentrations with NuCSAM, ReSAM and SMART of SO ₄ , NO ₃ and Al at Solling at 10 cm depth (left) and 90 cm depth (right)	133
6.2	Flux-weighted annual average concentrations simulated with NuCSAM and with ReSAM of SO ₄ , NO ₃ , Al and Al/Ca ratio at Speuld at 10 cm depth (left) and 90 cm depth (right), for the period 1970-2090 under the Improved Environment scenario.	135
6.3	The percentage of Dutch forest soils exceeding a critical Al concentration of 0.2 mol _c m ⁻³ (A) and a critical molar Al/Ca ratio of 1.0 in the topsoil (B) in response to three scenarios	138
6.4	Trends in total emissions of SO ₂ , NO _x and NH ₃ in Europe for three scenarios	139
6.5	Temporal development of the forested area in Europe (%) with Al concentrations above 0.2 mol _c m ⁻³ (A) and molar Al/BC ratios above 1.0 (B) in response to three scenarios	141

Annexes

- 1 Annotation of used symbols in Chapter 3 151
- 2 Description of the most important processes included in SMART, ReSAM and NuCSAM 153

Preface

This report is the final report of the project *Extension of the model ReSAM towards a soil acidification model on stand level*. The research was part of and funded by the third phase of the Dutch Priority Programme on Acidification. The main part of this report have been included, in part or in whole, in the following publications:

- Tiktak, A., J.J.M. van Grinsven, J.E. Groenenberg, C. van Heerden, P.H.M. Janssen, J. Kros, G.J.M. Mohren, C. van der Salm, J.R. van de Veen and W. de Vries, 1995. Application of three Forest-Soil-Atmosphere models to the Speuld experimental forest. RIVM Report no. 733001003, Bilthoven, Netherlands. (Chapter 2)
- Groenenberg, J.E., J. Kros, C. van der Salm and W. de Vries, 1995. Application of the model NUCSAM to the Solling spruce site. *Ecological Modelling*, 83: 97-107. (Chapter 3)
- Kros, J., J.E. Groenenberg, W. de Vries and C. van der Salm, 1995. Uncertainty due to time resolution in long term predictions of forest soil acidification. *Water Air and Soil Pollution* 79: 353-375. (Chapter 4)
- Salm, C. van der, J. Kros, J.E. Groenenberg, W. de Vries and G.J. Reinds, 1995. Validation of soil acidification models with different degrees of process aggregation on an intensively monitored spruce site. In: S. Trudgill (Ed.): *Solute modelling in catchment systems*, John Wiley, Chichester: 327-346. (Chapter 5)
- De Vries, W., J. Kros, J.E. Groenenberg, G.J. Reinds, C. van der Salm and M. Posch, 1995. Scenario studies on soil acidification at different spatial scales. In: J.F.T. Schoute, P.A. Finke, F.R. Veeneklaas & H.P. Wolfert (eds.), *Scenario studies for the rural environment*. Kluwer, Dordrecht, Netherlands. *Environment & Policy* 5: 169-188. (Chapter 6)

This study was carried out during the period 1991 - 1994 at the DLO Winand Staring Centre and was focused on the validation and application of the soil acidification model ReSAM and the extended version (NuCSAM). Together with three other modelling projects: (i) calibration of the DAS modules (RIVM), (ii) modification of the forest-soil model SoilVeg (RIVM) and (iii) extension and validation of the forest growth model ForGro (IBN-DLO), it was aimed either to validate or to improve scientific justification for the DAS module.

Moreover, this report was extended with two chapters, which include results about the soil acidification model SMART, which was developed for applications at a European scale. Basically these chapters were no project results as such, but it was considered useful to include them in the final report.

Summary

During the last decade various soil acidification models have been developed at the DLO Winand Staring Centre to evaluate long-term soil response to deposition scenarios at a national scale (ReSAM) and a European scale (SMART). An important shortage of these models is that they are only partly validated, because of the lack of sufficient long-term (> 50 a) observations. A thorough validation, using available short-term (< 10 a) observations from intensively monitored sites is hardly possible because these models do not account for day-to-day variability observed at these sites. In order to use these data from intensively monitored sites for model validation, ReSAM was extended towards a model at stand-level by incorporation of:

- (i) a hydrological module to simulate daily soil water contents and soil water fluxes in both upward and downward direction;
- (ii) a heat transport module to simulate the seasonal variation of soil temperatures with depth;
- (iii) a solute transport module to simulate upward and downward solute transport;
- (iv) temperature dependence in the formulations for biogeochemical processes to simulate these processes on a daily basis;
- (v) dissolution of iron and cycling of phosphorous;
- (vi) a more detailed description of mineralization;
- (vii) a chemical equilibrium module, EPIDIM (Groenendijk, 1995), to account for ion speciation.

The model thus derived is called the Nutrient Cycling and Soil Acidification Model (NuCSAM). This model was used for an indirect validation of the regional model ReSAM. Furthermore, NuCSAM was developed to be linked with an extended version of the forest growth model FORGRO to simulate effects of nutrient limitations on forest growth.

First, the results of the newly developed stand-level model NuCSAM were directly compared to the observations from two sites. The two intensively monitored sites used for validation were:

- (i) a Douglas fir stand in the Speulderbos, Netherlands;
- (ii) a Norway Spruce stand at Solling, Germany.

Subsequently, the results of the stand-level model NuCSAM were compared to those of the regional model ReSAM.

A brief description of the NuCSAM model and a calibration of the model to the Speulderbos Douglas fir stand is presented in Chapter 2. Results show a reasonable good fit of NuCSAM to the Speulderbos observations. However, problems exist for the pH and Ca concentration in the topsoil and Cl in the subsoil. Long-term (60 y) impacts of acid deposition of three deposition scenarios on two generic forest soil combinations were also evaluated with NuCSAM. Scenario analyses show a fast response of the Al and SO₄ concentration after a decrease in SO_x deposition, a time-delay in decrease of the NO₃ concentration resulting from a decrease in NO_x deposition and higher soil solution concentrations below Douglas fir.

The NuCSAM application to a Spruce site at Solling (Chapter 3), Germany, took place within the scope of a workshop on comparison of forest soil atmosphere models. Simulated trends and dynamics in the concentrations of SO_4 , Al and base cations and pH between 1973 and 1991 compared favourably with observed time series during that period. Dynamics and concentrations of NO_3 in the subsoil were, however, overestimated. Scenario analyses for the period 1990-2090 for two deposition scenarios showed ongoing acidification (pH decrease) of the soil at continuation of present acid load, whereas a rapid response of soil solution chemistry to deposition reduction was simulated. However, there was a long time delay before favourable Al/Ca ratios were reached.

Uncertainty caused by the neglect of seasonal variability in long-term predictions was investigated by a comparison of long-term simulations with ReSAM and NuCSAM (Chapter 4). Two deposition scenarios for the period 1990-2090 were evaluated. The models were parameterized and validated by using data from the intensively monitored spruce site at Solling, Germany. Although both the seasonal and the interannual variation in soil solution parameters were large, the trend in soil solution parameters simulated with ReSAM and NuCSAM corresponded well. The leaching fluxes were almost similar. Generally it appeared that the uncertainty due to time resolution in long-term predictions of annual average concentrations was relatively small.

A comparison between the one-layer soil acidification model SMART, the multi-layer model ReSAM (both with a time resolution of one year) and the multi-layer soil acidification model NuCSAM (with a temporal resolution of one day) was made using data from the intensively monitored spruce site at Solling, Germany (Chapter 5). Simulated concentrations and leaching fluxes were compared with measured values at this site during the period 1973-1991. The major aim was to study the influence of model simplifications, especially with respect to process formulation and the reduction of temporal and vertical resolution, on the simulation of soil solution concentrations. Results showed that all models were able to simulate most of the concentrations during the examined period reasonably. However, the one-layer model, SMART, had some difficulties to simulate strong changes in soil solution concentrations due to a lower retardation in the soil system.

Chapter 6 presents an overview of the various studies made with three dynamic soil acidification models, i.e. SMART, developed for application at a European scale, ReSAM, a national scale model and NuCSAM, a site scale model. The uncertainties in model predictions and the use of the models in acidification abatement policies is addressed and the various strong and weak points of the model are evaluated. Furthermore, the limitations and possibilities to use the models in other scenario studies, such as changes in land use, hydrology and heavy metal deposition are discussed.

The major conclusions of this research are (Chapter 7):

- (i) The daily based model NuCSAM reproduces the main features of the concentration variations over time for most elements in both Speuld and Solling.
- (ii) The capability of the yearly based model ReSAM to simulate observed flux-weighted annual averaged concentrations (and ratios) is comparable or even better than NuCSAM.

- (iii) Long-term predictions of annual average concentrations with ReSAM and NuCSAM show general agreement. This implies that ignoring seasonal variation of weather conditions does not have a large impact on the long-term response of soil solution chemistry to deposition. ReSAM, is thus acceptable for making long-term annual average predictions.

1 Introduction

Information on the long-term effects of acid deposition on soils is very important for the formulation of policies for emission reductions. Models are an important tool to assist decision makers in evaluating the effectiveness of abatement strategies. During the first two phases of the Dutch Priority Programme on Acidification (DPPA), the integrated Dutch Acidification Systems (DAS) model has been developed (Heij and Schneider, 1991). This model aims at evaluating the long-term effectiveness of acidification abatement strategies on a number of receptor systems (forests, forest-soils, heathland and aquatic ecosystems). The model describes the complete causality chain from emissions to effects in a regionalized way. Within DAS the forest soil model ReSAM (De Vries *et al.*, 1995) forms an important effect module. The temporal resolution of all DAS modules is one year.

The DAS model was used for scenario analysis at the end of the 2nd phase of DPPA (Heij and Schneider, 1991; Tiktak *et al.*, 1992). The scenarios were based on abatement strategies announced in the National Dutch Environmental Policy Plan Plus. Some conclusions with respect to forest soils and forests, based on results from ReSAM, were:

- (i) deposition reduction leads to a fast (almost instantaneous) improvement in soil solution chemistry, i.e. an increase in pH and a decrease of the Al/Ca and NH_4/K ratio's;
- (ii) the exceedance of the critical Al concentration in the soil solution decreased from about 75% of the total forest area now to 40% in 2000, the exceedance of the critical Al/Ca ratio reduced from about 65% to 40%;
- (iii) a reduction of the acid deposition to $1200 \text{ mol}_c \text{ ha}^{-1} \text{ a}^{-1}$ was needed to stop the exhaustion of the pool of secondary aluminium compounds. These compounds provide an important pool for buffering protons.

An important shortage remaining at the end of the 2nd phase of DPPA, was that the integrated modules were not or only partly validated. ReSAM was validated against a regional data-set containing data from 150 forest stands (De Vries *et al.*, 1992). However, because this data-set only contained one observation for each stand, validation of the predicted changes in time could not be carried out. None of the modules were applied to the stand level, which is the most appropriate level for validating this type of models because intensive monitoring is carried out at this level. The yearly average concentrations as calculated with ReSAM, however, cannot be compared directly to site measurements as these show high temporal dynamics. In principle, though, a comparison on stand-level is possible by generating flux-weighted annual averaged concentrations from the observed concentration. ReSAM, which aims at predicting long-term changes, cannot be validated with results from relatively short (3-10 a) monitoring programmes alone. Therefore, it was considered necessary to derive a stand-level model from ReSAM, which can be used for validation and scientific justification for the regional DAS module ReSAM. The model thus derived is called the Nutrient Cycling and Soil Acidification Model (NuCSAM). Furthermore, NuCSAM was developed to be linked with an extended version of the forest growth model ForGro (Mohren, 1987) to simulate effects of nutrient limitations on forest growth (Mohren, 1995).

With the use of NuCSAM validation of ReSAM has been carried out in two steps. The first step was to compare the results of the daily based stand-level model NuCSAM with observations. The second step was to compare the results of the flux-weighted annual average concentrations with the validated stand-level model NuCSAM with those of the regional model ReSAM. Two intensively monitored sites were used for validation:

- (i) A Dutch Douglas fir stand in the Speulderbos (one of the so called experimental AciForN sites). Data on forest hydrology, soil chemistry and tree growth were available for the period 1986-1990 (Heij and Schneider, 1991; Evers *et al.*, 1987).
- (ii) A Norway Spruce stand at Solling (Germany). Monitoring data were available for the period 1973-1991. The data-set, which focused on soil chemistry and nutrient cycling, is very suitable for validation of the models over a longer time span (Bredemeier *et al.*, 1995; Tiktak *et al.*, 1995).

In addition, NuCSAM was used to assess the long-term development of soil solution chemistry (in particular Al concentration in the soil solution, Al/Ca ratio, content of secondary aluminium compounds and nutrient status) and forest growth. This goal was achieved by performing scenario analyses for the following two generic forest-soil combinations: (i) Douglas fir on a Cambic podzol and (ii) Scots pine on a Haplic arenosol. For both combinations, model simulations were carried out with deposition scenarios that are representative for Dutch regions with low, average and high deposition rates, respectively. It was assumed that in a clean region, the target acid deposition load of $1400 \text{ mol}_c \text{ ha}^{-1} \text{ a}^{-1}$ (NMP+) is reached in 2010, whereas in average and polluted regions these loads are reached in 2050 and 2100, respectively.

At the DLO Winand Staring Centre also a one layer soil acidification model was developed for applications at a European scale. This model, SMART (De Vries *et al.*, 1989) is part of the integrated model RAINS (Regional Acidification INFORMATION and Simulation model; Alcamo *et al.*, 1990). As with ReSAM, SMART has a temporal resolution of one year and a very simple hydrologic description. Consequently, amongst other things, these models do not include seasonal dynamics. In order to characterize the effects of model simplification on soil and soil solution chemistry, this report includes a comparison of an application of the models SMART, ReSAM and NuCSAM to the Solling Spruce site. Furthermore various studies on model validation and uncertainties in model predictions with SMART, ReSAM and NuCSAM are reviewed and the strong and weak points of the model are evaluated.

Chapter 2 provides a full description of the NuCSAM model and a calibration on the Speulderbos site and scenario analyses. Chapter 3 presents the results of the application on the Solling site, which was carried out as part of an international workshop on comparison of Forest-Soil-Atmosphere Models (Van Grinsven *et al.*, 1995). A comparison between the long-term results of ReSAM and NuCSAM is given in Chapter 4. A comparison of the three acidification models NuCSAM, ReSAM and SMART, using the Solling data-set, is given in Chapter 5. Chapter 6 gives an overview of the various model studies (validation and scenario studies) carried out with NuCSAM, ReSAM and SMART, on a local scale, a national scale and a European scale respectively. Chapter 7 summarizes the most important results and gives the conclusions and recommendations.

References

- Alcamo, J., R. Shaw and L. Hordijk, 1990. The RAINS model of acidification. Science and Strategies in Europe. Dordrecht, The Netherlands, Kluwer Academic Publishers, 402 pp.
- Bredemeier, M, A. Tiktak and C. van Heerden, 1995. The Solling spruce site: Background information on the data set. *Ecol. Model.* 83:7-15.
- De Vries, W., E.E.J.M. Leeters, C.M. Hendriks, W. Balkema, M.M.T. Meulenbrugge, R. Zwijnen and J.C.H. Voogd, 1992. Soil and soil solution composition of 150 forest stands in the Netherlands in 1990. In: T. Schneider (ed.). Acidification research. Evaluation and policy making. Elsevier Science Publ., Amsterdam, Netherlands, 535-536.
- De Vries, W., J. Kros and C. van der Salm, 1995. Modelling the impact of nutrient cycling and acid deposition on forest soils. *Ecol. Model.* 79:231-234.
- Evers, P.W., C.J.M. Konsten and A.W.M. Vermetten, 1987. Acidification research on Douglas fir forests in the Netherlands (ACIFORN project). Proc. Symp. Effects of Air Pollution on Terrestrial and Aquatic Ecosystems. Grenoble, 887-909.
- Heij, G.J. and T. Schneider, 1991. Acidification research in the Netherlands. Final report of the Dutch Priority Programme on Acidification. *Studies in Environmental Science* 46, Elsevier, Amsterdam, 771 pp.
- Mohren, G.M.J., 1995. Simulatie van effecten van luchtverontreiniging en bodemverzuring op naaldbossen: toepassingen van een geïntegreerd opstandsmodeel. IBN-DLO, IBN-rapport 167, Wageningen, Netherlands, 194 pp.
- Tiktak, A., A.H. Bakema, K.F. de Boer, J.W. Erisman, J.J.M. van Grinsven, C. van Heerden, G.J. Heij, J. Kros, F.A.A.M. de Leeuw, J.G. van Minnen, C. van der Salm, J.C.H. Voogd and W. de Vries, 1992. Scenario analysis with the Dutch Acidification Systems (DAS) model: an example for forests and forest soils. In: T. Schneider (ed.). Acidification research: evaluation and policy applications. *Studies in Environmental Science* 50, Elsevier, Amsterdam, 319-340.
- Tiktak, A., M. Bredemeier and C. van Heerden, 1995. The Solling data-set: Site characteristics and deposition scenarios. *Ecol. Model.* 83:17-34.
- Van Grinsven, J.J.M., C.T. Driscoll and A. Tiktak, 1995. Comparison of Forest-Soil-Atmosphere models and application to the Norway spruce site in Solling, Germany. *Ecol. Model.* 83:1-6.

Chapter 2 is based on:

Tiktak, A., J.J.M. van Grinsven, J.E. Groenenberg, C. van Heerden, P.H.M. Janssen, J. Kros, G.J.M. Mohren, C. van der Salm, J.R. van de Veen and W. de Vries, 1995. Application of three Forest-Soil-Atmosphere models to the Speuld experimental forest. RIVM Report no. 733001003, Bilthoven, Netherlands.

2 Validation and application of a nutrient cycling and soil acidification model to an intensively monitored douglas fir site

Abstract

A brief description of the NuCSAM model and a calibration of the model to the Speulderbos Douglas fir stand is presented. Results show a reasonable good fit of NuCSAM to the Speulderbos observations. However, problems exist for the pH and Ca concentration in the topsoil and Cl in the subsoil. Long-term (60 y) impacts of acid deposition of three deposition scenarios on two generic forest soil combinations were also evaluated with NuCSAM. Scenario analyses show a fast response of the Al and SO₄ concentration after a decrease in SO_x deposition, a time-delay in decrease of the NO₃ concentration resulting from a decrease in NO_x deposition and higher soil solution concentrations below Douglas fir.

2.1 Introduction

Several hypotheses that link forest growth and forest vitality to air pollution, atmospheric deposition, soil acidification and disturbed nutrient cycling have been developed. Examples are the Al-toxicity hypothesis (Ulrich, 1983) and the nitrogen saturation hypothesis (Skeffington, 1988). Such hypothetical effect relationships can be tested by applying a mechanistic and comprehensive simulation models. As a first step, the integrated Dutch Acidification Systems (DAS) model has been developed during the Dutch Priority Programme on Acidification (DPPA; Heij and Schneider, 1991). This model aims at evaluating the long-term effectiveness of acidification abatement strategies on a number of receptor systems (forests, forest-soils, heathland and aquatic ecosystems). The model describes the complete causality chain from emissions to effects in a regionalized way. An important effect module within DAS is the forest soil model ReSAM (De Vries *et al.*, 1995a), which has a temporal resolution of one year.

One major limitation of the regional model ReSAM is, however, the difficulty to validate it at the stand level (which is the most appropriate level for validating this type of models as most measurements are carried out at this particular level of detail), since yearly average concentrations cannot be compared directly to (biweekly or monthly) monitoring measurements, which show high temporal dynamics. Furthermore, the regional model ReSAM, which aims at predicting long-term changes, cannot be validated with results from relatively short (3-10 a) monitoring programmes. In order to overcome this limitation, during the third phase of DPPA ReSAM was extended towards a stand-level model with a higher temporal resolution. The model thus derived is called the Nutrient Cycling and Soil Acidification model (NuCSAM). In addition NuCSAM was coupled with ForGro (Mohren, 1987; Mohren *et al.*, 1993), a process-oriented model that includes the essentials of whole-tree physiology, to simulate effects of nutrient limitations on forest growth.

One of the most important reasons for developing NuCSAM was validation and scientific justification for the regional model ReSAM. Validation of ReSAM was carried out in two steps. First, the results of the stand-level model NuCSAM were directly compared to measurements at a Norway Spruce stand at Solling (Germany) for which monitoring data were available for the period 1969-1990 (Groenenberg *et al.*, 1995; cf Chapter 3). Secondly, the results of the stand-level model NuCSAM were compared to results of the regional model ReSAM, using data of the intensively monitored Solling site (Kros *et al.*, 1995; cf Chapter 4).

In this Chapter, emphasis is given to the description of the model NuCSAM, and application the application of the model to a Dutch Douglas fir stand in the Speulderbos (one of the so called experimental AciForN sites). Data on forest hydrology, soil chemistry and tree growth were available for the period 1986-1990 (Heij and Schneider, 1991; Evers *et al.*, 1987). Furthermore, the results of scenario analyses are presented which represents the present targets of the Dutch environmental policy (Keizer, 1994).

2.2 Model description

2.2.1 Model structure

NuCSAM simulates the major hydrological and biogeochemical processes in the forest canopy, litter layer, and mineral soil. The change in soil solution and solid phase chemistry is calculated from a set of mass balance equations, describing the input, output and interactions in each compartment. Vertical heterogeneity is taken into account by differentiating between soil layers. The soil layers are considered as homogeneous compartments of constant density and the constituent input mixes completely within each soil layer.

2.2.2 Hydrology

To simulate soil water fluxes, soil water contents, etc. an adapted version of the SWATRE model (Belmans *et al.*, 1983) was used as hydrological submodel.

Potential evapotranspiration

Potential transpiration is calculated by multiplying the reference evapotranspiration according to Makkink (1957) by an empirical, season dependent crop factor. For conditions in the Netherlands, the Makkink equation is written as:

$$E_r = \frac{\beta}{\lambda} \cdot \frac{s}{s+\gamma} \cdot K\downarrow \cdot f_s \quad (1)$$

in which E_r (m d^{-1}) is the Makkink reference evapotranspiration, s ($\text{g g}^{-1} \text{K}^{-1}$) is derivative of the saturation water vapour pressure temperature curve, γ ($\text{g g}^{-1} \text{K}^{-1}$) is psychrometer constant, $K\downarrow$ (W m^{-2}) is global radiation, λ (J g^{-1}) is specific heat of

evaporation and β (-) is empirical constant related to the geographical latitude, which for conditions in the Netherlands is equal to 0.65.

Canopy interception

A relatively simple empirical one-layer canopy-interception submodel is used. Water is supplied to the canopy by precipitation and lost by throughfall and evaporation of intercepted water:

$$A_{wc} = A_{wc} + \Delta t \cdot (P - TF - E_i) \quad (2)$$

where A_{wc} (m) is amount of water intercepted by the canopy, P (m d^{-1}) is daily precipitation, TF (m d^{-1}) is daily throughfall, E_i (m d^{-1}) is evaporation of intercepted water and Δt (d) is time-step (which is one day).

The amount of water intercepted is calculated by using a coefficient of free throughfall in combination with a threshold value.

The calculation of the interception evaporation is based on Gash (1979). An analytical approximation is used to calculate daily interception. However, unlike the original Gash model, NuCSAM uses daily evaporation rates instead of yearly average evaporation rates. As evaporation rates are lower during rainfall, empirical correction factors have been introduced for the dry and wet part of the day. First the amount of rainfall required to saturate the canopy, P_s (m), is calculated:

$$P_s = - \frac{A_{wc,max}}{E_r \cdot fE_{wet}} \cdot \ln \left(1 - \frac{E_r \cdot fE_{wet}}{\bar{R}} \cdot \frac{1}{sc} \right) \cdot \bar{R} \quad (3)$$

where sc (-) the soil cover fraction, $A_{wc,max}$ (m) the maximum amount of water stored in the canopy, E_r (m d^{-1}) the reference evapotranspiration, fE_{wet} (-) a correction factor for the evaporation rate during rainfall, \bar{R} (m d^{-1}) the average rainfall intensity and P (m) the precipitation. The interception evaporation is now calculated as:

$$\begin{aligned} \text{if } P < P_s : \quad E_i &= P \cdot sc \\ \text{if } P \geq P_s : \quad E_i &= P_s \cdot sc + \left(\frac{E_r \cdot fE_{wet}}{\bar{R}} \right) \cdot (P - P_s) \end{aligned} \quad (4)$$

The canopy water storage at the end of the day is calculated as:

$$A_{wc} = A_{wc,o} \cdot \exp \left(- \frac{E_r \cdot fE_{dry}}{A_{wc,max}} \cdot t_d \right) \quad (5)$$

where A_{wc} (m) is the water storage at the end of the day, $A_{wc,o}$ (m) the water storage at the start of the dry part of the day, fE_{dry} (-) a correction factor for the evaporation

rate during the dry part of the day, and t_d (d) the length of the dry part of the day, which is calculated from the precipitation and average rainfall intensity:

$$t_d = 1 - (P / \bar{R}) \quad (6)$$

Potential transpiration and soil evaporation

Potential transpiration and potential soil evaporation are calculated by partitioning the potential evapotranspiration on the basis of the available energy by a method equivalent to Van Grinsven *et al.* (1987) and Tiktak and Bouten (1992):

$$\begin{aligned} E_{pl}^* &= \max \left[0, \left\{ f_c \cdot sc \cdot E_r - f_i \cdot E_i \right\} \right] \\ E_s^* &= (1 - sc) \cdot E_r \end{aligned} \quad (7)$$

in which E_{pl}^* ($m \, d^{-1}$) is the potential transpiration, E_s^* ($m \, d^{-1}$) is the potential soil evaporation, f_c (-) is an empirical factor that accounts for crop characteristics, sc (-) is the soil cover fraction, E_i ($m \, d^{-1}$) is evaporation of intercepted water, and f_i (-) is the fraction of the daily interception that reduces the potential transpiration. The gap factor is calculated on the basis of the leaf area index.

The actual soil evaporation rate is calculated as a function of time since the last rainfall event according to Black *et al.* (1969):

$$E_s = \varepsilon \cdot \left(\sqrt{t_d + 1} - \sqrt{t_d} \right) E_s^* \quad (8)$$

where E_s ($m \, d^{-1}$) is actual soil evaporation, t_d (d) is time from the start of a drying cycle and ε ($d^{-1/2}$) is an empirical parameter.

Soil water transport

Transport of water through the soil is calculated with a numerical solution of Richard's equation:

$$\frac{\partial \theta}{\partial t} = \frac{\partial}{\partial z} \left[K(h) \cdot \left(\frac{\partial h}{\partial z} + 1 \right) \right] - S(h) \quad (9)$$

where θ ($m^3 \, m^{-3}$) is volumetric water content, t (d) time, z (m) vertical position in the soil, h (m) soil water pressure head, K ($m \, d^{-1}$) hydraulic conductivity and S (d^{-1}) sink term accounting for root water uptake. The model allows for upward water transport.

Actual transpiration

The potential transpiration is distributed among soil layers on the basis of the root length distribution. Reduction of water uptake occurs when soil water pressure heads drop below or exceed a threshold value. The root water uptake fluxes are summed to get the actual transpiration.

2.2.3 Nutrient cycling

Canopy interactions

The solute fluxes to the soil surface by throughfall are calculated in NuCSAM from the total deposition corrected for canopy interactions, i.e. foliar uptake and foliar exudation. Foliar uptake of NH_4^+ , NO_3^- , SO_4^{2-} and H^+ is described as a linear function of the dry deposition of these elements:

$$FX_{fu} = frX_{fu} \cdot FX_{dd} \quad (10)$$

where FX ($\text{mol}_c \text{ ha}^{-1} \text{ a}^{-1}$) refers to the flux of element X , frX_{fu} (-) is the uptake fraction of element X and where the subscript fu refers to foliar uptake and dd to dry deposition.

Foliar uptake of NH_4^+ and H^+ is counterbalanced by exchange with Ca^{2+} , Mg^{2+} and K^+ (Draaijers, 1993):

$$FCa_{fe} + FMg_{fe} + FK_{fe} = FNH_{4,fu} + FH_{fu} \quad (11)$$

where the subscript fe refers to foliar exudation and fu refers to foliar uptake. The foliar exudation flux of each individual cation, FX_{fe} ($\text{mol}_c \text{ ha}^{-1} \text{ a}^{-1}$) is calculated as:

$$FX_{fe} = frX_{fe} \cdot (FNH_{4,fu} + FH_{fu}) \quad (12)$$

where frX_{fe} (-) is the foliar exudation fraction of Ca^{2+} , Mg^{2+} and K^+ . The sum of these fractions equals 1.

Litterfall and root decay

Litterfall and root decay are the input to the organic pools of N, P, Ca, Mg, K and S. Litterfall and root decay are described by first-order rate reactions:

$$FX_{lf} = (1 - frX_{re,lv}) \cdot kX_{lf} \cdot A_{lv} \cdot ctX_{lv} \quad (13)$$

$$FX_{rd} = (1 - frX_{re,rt}) \cdot kX_{rd} \cdot A_{rt} \cdot ctX_{rt} \quad (14)$$

where k_{lf} and k_{rd} (a^{-1}) are the rate constants for litterfall and root decay, A_{lv} and A_{rt} (kg ha^{-1}) are the amounts of leaves and fine roots, ctX_{lv} and ctX_{rt} ($\text{mol}_c \text{ kg}^{-1}$) are the contents of element X in leaves and roots, and $frX_{re,lv}$ and $frX_{re,rt}$ (-) are the reallocation fractions for element X in leaves and fine roots, respectively. The contents of P, Ca,

Mg, K and S in leaves and fine roots are assumed to be constant in time. As high contents of nitrogen are caused by high nitrogen deposition rates, the nitrogen content in stems, branches, leaves and fine roots is calculated as a function of nitrogen deposition by ($FN_{td,min} < FN_{td} < FN_{td,max}$):

$$ctN = ctN_{min} + (ctN_{max} - ctN_{min}) \cdot \left(\frac{FN_{td} - FN_{td,min}}{FN_{td,max} - FN_{td,min}} \right) \quad (15)$$

where ctN_{min} and ctN_{max} ($\text{mol}_c \text{ kg}^{-1}$) are the minimum and the maximum nitrogen content in stems, branches, leaves or fine roots, respectively and $FN_{td,min}$ and $FN_{td,max}$ ($\text{mol}_c \text{ ha}^{-1} \text{ a}^{-1}$) are the minimum and the maximum deposition levels between which the nitrogen content in biomass is affected.

Mineralization

In NuCSAM, both exogenous and endogenous organic matter are distinguished. For the exogenous organic matter, a distinction is made between a litter layer and a fermentation layer. The organic matter in the humus layer is lumped with endogenous organic matter. All equations, except for litter fall fluxes, are first-order rate equations. The mass balances for the litter and fermentation layers ($\text{mol}_c \text{ ha}^{-1} \text{ a}^{-1}$) are described by:

$$\frac{d(A_{lt} \cdot ctX_{lt})}{dt} = (1 - fr_{le}) \cdot FX_{lf} - (k_{mi,lt} + k_{hu,lt}) \cdot A_{lt} \cdot ctX_{lt} \quad (16)$$

$$\frac{d(A_{fe} \cdot ctX_{fe})}{dt} = k_{hu,lt} \cdot A_{lt} \cdot ctX_{lt} - (k_{mi,fe} + k_{hu,fe}) \cdot A_{fe} \cdot ctX_{fe} \quad (17)$$

where fr_{le} (-) is the leaching fraction (see also equation ?), $k_{mi,lt}$ (a^{-1}) is the mineralization constant for the litter layer, $k_{hu,lt}$ (a^{-1}) is the humification constant for the litter layer, $k_{mi,fe}$ (a^{-1}) is the mineralization constant for the fermentation layer and $k_{hu,fe}$ (a^{-1}) is the humification constant for the fermentation layer, ctX_{lt} and ctX_{fe} ($\text{mol}_c \text{ kg}^{-1}$) are the contents of N, P, K, Ca, Mg and S in the litter and fermentation layers, and A_{lt} and A_{fe} (kg ha^{-1}) are the amounts of litter and fermentation, respectively. For each soil layer within NuCSAM, a mass balance ($\text{mol}_c \text{ ha}^{-1} \text{ a}^{-1}$) can be written for endogenous organic matter:

$$\frac{d(A_{hum,i} \cdot ctX_{hum,i})}{dt} = fr_{hum,i} \cdot (k_{hu,fe} \cdot A_{fe} \cdot ctX_{fe} + k_{mi, rn} \cdot A_{rn} \cdot ctX_{rn} - k_{mi,hum} \cdot A_{hum,i} \cdot ctX_{hum,i}) \quad (18)$$

where $fr_{hum,i}$ (-) is fraction of endogenous organic matter in soil layer i , $k_{hu,fe}$ (a^{-1}) is humification constant for the fermentation layer, $k_{mi, rn}$ (a^{-1}) is mineralization constant for the root necromass, and $k_{mi,hum}$ (a^{-1}) is mineralization constant for the humus layer. The amount of produced organic anions by mineralization is calculated from the charge balance including all other ions.

Rate constants are described as maximum values which are reduced for non-optimal water contents and soil temperatures. The mineralization constants for nitrogen are also reduced at low N contents to account for immobilization by microbes according to Janssen (1983) and De Vries (1994).

Uptake of nutrients by roots

Total uptake of NH_4^+ , NO_3^- , Ca^{2+} , Mg^{2+} , K^+ , PO_4^{3-} and SO_4^{2-} ($\text{mol}_c \text{ ha}^{-1} \text{ a}^{-1}$) is described in NuCSAM by a demand function, which consists of maintenance uptake and growth uptake in stems and branches according to:

$$FX_{ru} = FX_{gu} + FX_{lf} + FX_{fe} + FX_{rd} + FX_{fu} \quad (19)$$

where the subscript *ru* refers to root uptake, *lf* to litter fall, *rd* to root decay, *fe* to foliar exudation, *fu* to foliar uptake and *gu* to growth uptake. The growth uptake is directly related to stem growth, which is described by a logistic growth curve:

$$dAm_{st} = \frac{Am_{st,max}}{1.0 + e^{-kr_{gl} \cdot (age + t - t_{50})}} \quad (20)$$

and

$$FX_{gu} = dAm_{st} \cdot (ctX_{st} + fr_{gu,br} \cdot ctX_{br}) \quad (21)$$

where $fr_{gu,br}$ (-) is the fraction of growth uptake for branches, kr_{gl} ($\text{kg ha}^{-1} \text{ a}^{-1}$) is a logistic rate constant, dAm_{st} ($\text{kg ha}^{-1} \text{ a}^{-1}$) is the stem growth, $Am_{st,max}$ (kg ha^{-1}) is the maximum amount of stemwood, ctX_{st} ($\text{mol}_c \text{ kg}^{-1}$) is content of element X in stemwood, ctX_{br} ($\text{mol}_c \text{ kg}^{-1}$) is content of element X in branches, t (a) is time, t_{50} (a) is time at which the amount of stemwood is $0.5 \cdot Am_{st,max}$ and age (a) is the stand age at the start of the simulation. The contents of Ca, Mg, K and S in stemwood are assumed to be constant in time. The concentration of nitrogen in stems is described as a function of the nitrogen deposition according to Equation (15). The nutrient uptake from a given soil layer i is determined by the given root distribution:

$$FX_{ru,i} = FX_{ru} \cdot fr_{rti} \quad (22)$$

where $FX_{ru,i}$ ($\text{mol}_c \text{ ha}^{-1} \text{ a}^{-1}$) is uptake of element X from soil layer i , FX_{ru} ($\text{mol}_c \text{ ha}^{-1} \text{ a}^{-1}$) is total uptake of element X, fr_{rti} is the root fraction in soil layer i . Preferential uptake of NH_4^+ over NO_3^- is calculated according to (Gijsman, 1990):

$$FNH_{4,ru} = \left(\frac{1}{1 + 1/f_p \text{NH}_{4,ru}} \right) \cdot FN_{ru} \quad (23)$$

where $f_p \text{NH}_{4,ru}$ (-) is a preference factor for the uptake of NH_4^+ over NO_3^- . NO_3^- uptake

is calculated as the difference between total nitrogen uptake and NH_4^+ uptake:

$$F\text{NO}_{3ru} = F\text{N}_{ru} - F\text{NH}_{4ru} \quad (24)$$

Nitrogen transformations

Nitrification ($\text{mol}_c \text{ha}^{-1} \text{a}^{-1}$) is described as a first-order reaction by:

$$F\text{NH}_{4ni} = -f_c \cdot \theta \cdot TL \cdot k_{ni} \cdot c\text{NH}_4 \quad (25)$$

where θ ($\text{m}^3 \text{m}^{-3}$) is the volumetric water content, TL (m) is thickness of the soil layer, k_{ni} (a^{-1}) is the nitrification rate constant. As with mineralization, the nitrification rate constant is adjusted on the basis of soil temperature, water content and pH (De Vries, 1988). The nitrification rate constant is reduced at high water contents.

2.2.4 Geochemical process formulations

Rate limited reactions

Protonation of organic anions and weathering are described by rate-limited first-order reactions. Protonation (the association of organic anions with H^+) is described according to:

$$F\text{RCOO}_{pr} = -f_c \cdot \theta \cdot TL \cdot k_{pr} \cdot c\text{RCOO} \quad (26)$$

where k_{pr} (a^{-1}) is a pH dependent protonation rate constant.

Weathering (dissolution) fluxes of Al and base cations from carbonates, silicates (primary minerals) and aluminium hydroxides ($\text{mol}_c \text{ha}^{-1} \text{a}^{-1}$) are described by first-order rate and Elovich reactions. The flux of calcium from dissolution of carbonates is described by:

$$F\text{Ca}_{we,cb} = f_c \cdot \rho \cdot TL \cdot k\text{Ca}_{we,cb} \cdot ct\text{Ca}_{cb} \cdot (c\text{Ca}_e - c\text{Ca}) \quad (27)$$

where ρ (kg m^{-3}) is the bulk density, $k\text{Ca}_{we,cb}$ ($\text{m}^3 \text{mol}_c^{-1} \text{a}^{-1}$) is a weathering rate constant, $ct\text{Ca}_{cb}$ ($\text{mol}_c \text{kg}^{-1}$) is the content of Ca in carbonates, and $c\text{Ca}$ and $c\text{Ca}_e$ ($\text{mol}_c \text{m}^{-3}$) are the concentration and equilibrium concentration of calcium (cf Eqn. (32)), respectively. When the soil solution is supersaturated with respect to calcite, equilibrium is enforced (cf Eqn. (32)) The flux of base cations from silicates (primary minerals) is described by (Van Grinsven, 1988):

$$FX_{we,pm} = f_c \cdot \rho \cdot TL \cdot kX_{we,pm} \cdot ctX_{pm} \cdot c\text{H}^{\alpha(X)} \quad (28)$$

where $kX_{we,pm}$ ($\text{m}^3 \text{mol}_c^{-1} \text{a}^{-1}$) is a weathering rate constant, ctX_{pm} ($\text{mol}_c \text{kg}^{-1}$) is the content of base cation X in primary minerals, $c\text{H}$ ($\text{mol}_c \text{m}^{-3}$) is the H^+ concentration and α (-) is a parameter. The weathering of aluminium from primary minerals is described by:

$$F Al_{we pm} = 3 F Ca_{we pm} + 0.6 F Mg_{we pm} + 3 F K_{we pm} + 3 F Na_{we pm} \quad (29)$$

This equation comes down to congruent weathering of equal amounts of Anorthite (Ca), Chlorite (Mg), Microcline (K) and Albite (Na). When the solution is under saturated with respect to natural gibbsite, the release of aluminium from hydroxides is described by an Elovich equation:

$$F Al_{we ox} = f_c \cdot \rho \cdot TL \cdot kEl_1 \cdot e^{(kEl_2 \cdot ctAl_{ox})} \cdot (cAl_e - cAl) \quad (30)$$

with cAl and cAl_e ($\text{mol}_c \text{ m}^{-3}$) as the actual and equilibrium concentration of aluminium in the soil solution, and $kEl1$ ($\text{m}^3 \text{ mol}_c^{-1} \text{ a}^{-1}$) and $kEl2$ (kg mol_c^{-1}) as Elovich constants. As with calcite, equilibrium is enforced with respect to Al hydroxide when the soil solution is supersaturated (cf Eqn. (34)).

Weathering of P is described by the rate-limited equation:

$$F P_{we} = f_c \cdot \rho \cdot TL \cdot kP_{we} \cdot ctP_t \cdot (cP_e - cP) \quad (31)$$

where ρ (kg m^{-3}) is the bulk density, kP_{we} ($\text{m}^3 \text{ mol}_c^{-1} \text{ a}^{-1}$) is the weathering rate constant for P, ctP_t ($\text{mol}_c \text{ kg}^{-1}$) is the total phosphate content, cP ($\text{mol}_c \text{ m}^{-3}$) is the actual phosphate concentration in the soil solution, and cP_e ($\text{mol}_c \text{ m}^{-3}$) is the equilibrium concentration of phosphate with apatite, variscite or strengite.

Equilibrium reactions

Equilibrium reactions include the dissociation of CO_2 , the calculation of the concentration of Ca^{2+} in equilibrium with Ca carbonate, the concentration of Al^{3+} in equilibrium with Al hydroxide, adsorption/desorption of SO_4^{2-} and cation exchange. The concentration of Ca^{2+} in equilibrium with Ca carbonate is calculated as:

$$cCa_e = KCa_{cb} \cdot \frac{pCO_2}{(cHCO_3^-)^2} \quad (32)$$

where KCa_{cb} ($\text{mol}^3 \text{ L}^{-3} \text{ bar}^{-1}$) is the equilibrium constant for Ca carbonate dissolution and pCO_2 (bar) is the partial CO_2 pressure in the soil. The bicarbonate concentration in the soil solution ($\text{mol}_c \text{ m}^{-3}$) is calculated from:

$$cHCO_3^- = \frac{(KCO_2 \cdot pCO_2)}{cH^+} \quad (33)$$

where KCO_2 ($\text{mol}^2 \text{ L}^{-2} \text{ bar}^{-1}$) is the product of Henry's law constant for the equilibrium between CO_2 in soil water and soil air, and the dissociation constant of H_2CO_3 . The concentration of Al^{3+} in equilibrium with natural gibbsite is calculated by:

$$cAl_e = KAl_{ox} \cdot cH^3 \quad (34)$$

where KAl_{ox} ($\text{mol}^2 \text{ L}^2$) is the equilibrium constant for aluminium hydroxide dissolution.

Cation exchange is described by Gaines-Thomas equations with Ca^{2+} as reference ion according to:

$$\frac{frX_{ac}^2}{frCa_{ac}^{z_x}} = KX_{ex} \cdot \frac{cX^2}{cCa^{z_x}} \quad (35)$$

with z_x (-) as the valence of cation X, KX_{ex} ($(\text{mol L}^{-1})^{z_x-2}$) as the Gaines-Thomas selectivity constant for exchange of cation X against Ca, frX_{ac} (-) is the fraction of cation X on the adsorption complex. X equals H^+ , Al^{3+} , Fe^{3+} , Mg^{2+} , K^+ , Na^+ or NH_4^+ .

frX_{ac} is calculated by:

$$frX_{ac} = \frac{ctX_{ac}}{\text{CEC}} \quad (36)$$

where CEC ($\text{mol}_c \text{kg}^{-1}$) is the cation exchange capacity. The sum of all fractions is equal to 1.

SO_4^{2-} and H_2PO_4^- sorption in each soil layer are described with a Langmuir equilibrium equation according to:

$$ctX_{ad} = \frac{XSC \cdot KX_{ad} \cdot cX}{1 + (KX_{ad} \cdot cX)} \quad (37)$$

where ctX_{ad} ($\text{mol}_c \text{kg}^{-1}$) is the sorbed amount of anion X, XSC ($\text{mol}_c \text{kg}^{-1}$) is the sorption capacity for X (cf Eqn. (46)), and KX_{ad} ($\text{m}^3 \text{mol}_c^{-1}$) is the equilibrium constant for sorption of anion X.

NuCSAM also includes ion speciation, such as the hydrolysis of Al^{3+} and complexation of aluminium with organic anions. All equilibrium reactions are calculated with the chemical equilibrium program EPIDIM (Groenendijk, 1995).

2.2.5 Forest growth

Forest growth is simulated by a logistic growth function (Section 2.2.3) and a nutrient cycling process, in which nutrients are taken up daily by a growing stand, and later returned by means of litter fall and root decay (Section 2.2.3). The vegetation together with the litter layer merely act as a steady state nutrient cycle, with a small part of the nutrients taken up and stored in the accumulating forest biomass. This vegetation cycle is parameterized by root uptake, storage, litter fall and root decay, which are given as time-independent constants for a particular forest type. There is no feedback of nutrient cycling on growth rate. Growth constants are taken from available field and literature

data. Stem growth ($\text{kg ha}^{-1} \text{ a}^{-1}$) is described with a logistic growth function (see equation (20)). Branch growth ($\text{kg ha}^{-1} \text{ a}^{-1}$) is derived from the stem growth using a fixed stem/branch ratio fr_{brst} (-):

$$dAm_{br} = fr_{brst} \cdot dAm_{st} \quad (38)$$

The amounts of leaves and roots (kg ha^{-1}) are described as:

$$Am_{lv} = \frac{Am_{st}}{Am_{st, mx}} \cdot Am_{lv, mx} \quad (39)$$

where Am_{lv} (kg ha^{-1}) is the actual amount of foliage (or roots) and $Am_{lv, mx}$ ($\text{kg ha}^{-1} \text{ a}^{-1}$) is the given maximum amounts of foliage (or roots). The nutrient contents of base cations and sulphur remain constant in all biomass compartments, whereas the nitrogen contents are calculated as a function of the atmospheric deposition.

2.3 Model calibration

Model calibration is defined as the determination of the model parameters, boundary and initial conditions and/or structure on basis of measurements, and of prior knowledge. The applied model contains parameters, initial and boundary conditions, which are incompletely known. More information on these quantities, which are often not measurable, is required to obtain accurate inferences from the model, and to judge its performance adequately. Hence, model calibration is required to determine these values accurately from the available measurements, taking into account the intended model use and available prior knowledge.

Model calibration thus becomes a critical phase in the modelling process. Despite its importance, the required activities for calibration are often given little consideration, and in many cases the model is calibrated using non-structured arbitrary methods. As the model under consideration contain a large number of parameters, a well-structured and systematic calibration approach is needed, supported by useful guidelines.

Strategy

Janssen and Heuberger (1995) present a general outline of the calibration process, and distinguish various important steps:

- (i) identify the characteristics of the data-set.
- (ii) identify the parameters that need calibration, preferably by performing model analyses (sensitivity and uncertainty analyses).
- (iii) specification of model performance criteria, which express the discrepancy between measurements and model results.
- (iv) solution of the calibration problem, which often consists of adjusting the model parameters such that the model results match the measurements adequately (e.g. minimal misfit).

The calibration process is usually completed by assessing the accuracy and quality of the obtained model (validation aspects; see Janssen and Heuberger (1995)).

In the sequel it is briefly addressed how the above mentioned issues apply for the calibration of the NuCSAM model to the Speuld data-set.

The characteristics of the data-set

Measurements were carried out at different spatial scales and at different positions within the stand. Most soil hydrological measurements were carried out at one plot of 30×30 m², although an attempt has been made to scale these measurements to stand average values (Bouten *et al.*, 1992). Soil chemical measurements are 'point' measurements. Samples were taken from three plots and the volume of soil sampled is small. Also the tree physiological measurements were carried out at one point within the forest stand. On the other hand, eddy correlation measurements of deposition and transpiration are representative at a scale which is larger than the stand. Measurements of throughfall amounts, throughfall quality and of forest growth, although point measurements, were scaled to average values. However, all these measurements were carried out at the Eastern half of the stand, possibly leading to a deviation from stand average values.

Due to these different spatial scales it is almost impossible to combine all measurements within one data-set. Consider the following example: If the hydrological part of NuCSAM is calibrated using the average transpiration measured by eddy correlation as a criterion, the hydrological regime will be different from the hydrological regime at the soil chemical sampling points. For this reason, the hydrological part of NuCSAM (i.e. an adapted version of the model SWATRE, cf Section 2.2) was calibrated using data from the soil monitoring plot only. This calibration is not representative for the stand as a whole, but can be used in combination with the soil chemical data-set.

Parameters that need calibration

The choice of the model parameters that need calibration was based on an uncertainty analysis for the model ReSAM (Kros *et al.*, 1993). Table 2.1 summarizes the parameters for which the solute concentrations were most sensitive. These parameters have been chosen for model calibration. To calibrate soil chemistry, simulated soil chemical variables were compared with measured soil chemical variables using statistical measures. For the calibration only concentrations in the soil solution were used since this were the only variables measured in time, soil contents (e.g. oxalate extractable Al) were only measured once. Solute concentrations were measured with cups and plates at different depths for three plots (cf Tiktak *et al.*, 1995b). Because of the large variation in measured concentrations between these three plots (cf Tiktak *et al.*, 1995b) it was decided to choose one plot for calibration (plot 5) because otherwise no trends in soil chemistry would be visible. Model outputs used for calibration are: pH and the concentrations of Al, Ca, Mg, K, NO₃, NH₄, SO₄ and Cl at 10, 20 and 90 cm depth, two depths for the topsoil and one in the subsoil beneath the rooting zone. For comparison with simulated output concentrations in soil water extracted with cups at the same depths were used.

Table 2.1 NuCSAM model parameters that were calibrated

#	Parameter	Description	Effect on concentration of:	Eqn.
1	ff_{SO_2dd}	forest filtering factor SO_2 dd	SO_4^{2-}	-
2	ff_{NO_xdd}	forest filtering factor NO_x dd	NO_3^- and NH_4^+	-
3	ff_{NH_xdd}	forest filtering factor NH_x dd	NO_3^- and NH_4^+	-
4	ff_{dd}	forest filtering dry deposition base cations and Cl^-	Na^+ , K^+ , Ca^{2+} , Mg^{2+} and Cl^-	-
5	kr_{ni}	nitrification rate constant	NO_3^- and NH_4^+	(25)
6	kEl_j	Elovich constant	Al^{3+} and H^+	(30)
7	$ctNlv_{mx}$	Maximum N-content of leaves	NO_3^- and NH_4^+	(15)
8	$krCa_{we}$	rate constant for Ca-weathering	Ca^{2+}	(28)
9	$krMg_{we}$	rate constant for Mg-weathering	Mg^{2+}	(28)

The choice of the hydrological parameters to be calibrated (not shown in Table 2.1) was based on Tiktak and Bouten (1992).

Performance criteria

For the evaluation of model performance in relation to observation data in Speuld, statistical indicators as described by Janssen and Heuberger (1995) have been used. As each of these indicators gives different information about model behaviour, two different performance measurements were use, as described below:

$$NME = \frac{(\bar{P} - \bar{O})}{\bar{O}} \quad (40)$$

$$NMAE = \frac{\sum_{i=1}^n (|P_i - O_i|)}{n \cdot \bar{O}} \quad (41)$$

Here, NME (-) is the Normalized Mean Error, NMAE (-) is the Normalized Mean Absolute Error, P_i is the predicted value, O_i is the observed value, \bar{O} and \bar{P} are the averages for the observed and predicted values, and n is the number of observations. The NME compares predictions and observations on an *average* basis (i.e. over the whole time-span). The NME thus expresses the bias in average values of model predictions and observations and gives a rough indication of overestimation (NME > 0) or underestimation (NME < 0). The NMAE is an absolute indicator for the discrepancy between model predictions and observations. The NMAE does not allow for compensation of positive and negative discrepancies. An NMAE of zero is considered optimal.

These criteria can be defined and evaluated for various model quantities, individually as well as jointly. For a fair comparison between model results and observations, their temporal and spatial scale should be compatible. For model calibration, model results were compared with accumulated throughfall amounts, soil water contents and soil solution composition.

Solution of the calibration problem

The different parameters were calibrated manually after each other by comparing model output and measurements using performance criteria (cf Eqns. (40) and (41)). Table 2.1 gives the order in which parameters were calibrated. Comparison between model output for different parameter values with measured data was done by comparing the statistical measures for the most effected (sensitive) model output (cf Table 2.1). In case of an (almost) equal model performance with respect to the most sensitive variables, differences in model performance for other model outputs were taken into account to choose the most optimal parameter value.

The presented misfit criteria consider only specific aspects of the system under study, and express the agreement between model data and data in a very condensed form, i.e. in one number. Therefore, the use of these quantitative criteria should be supplemented by qualitative techniques (e.g. visual comparison of measurements and model results).

2.3.1 Derivation of input data

2.3.1.1 Site description

Input data was derived mainly from the data set of the Speuld location as described in Tiktak *et al.* (1995b). The Speuld site is located in a 2.5 ha Douglas fir stand. Altitude is 50 m. The stand is surrounded by a large forest of approximately 50 km²; the nearest edge is at a distance of about 1.5 km. The soil is a well-drained Typic Dystochrept (USDA) or Cambic podzol (FAO, 1988) on heterogeneous sandy loam and loamy sand textured ice-pushed river sediments. A full soil profile description is included in Tiktak *et al.* (1988). The water table is at a depth greater than 40 m throughout the year. In 1988, the start of the monitoring period, the stand was 29 years old.

2.3.1.2 Hydrology

Vegetation dependent properties

The most important vegetation dependent hydrologic parameters are presented in Table 2.2.

Table 2.2 Vegetation dependent hydrologic parameter values for the Speulderbos site

Parameter	Symbol	Value	Unit
Soil cover fraction ^a	sc	0.9	(-)
Average precipitation intensity ^d	R	10.0	(mm)
Interception capacity ^b	$A_{wc,max}$	2.1	(mm)
Factor for evaporation ^d			
during dry part of day:	fE_{dry}	1.5	(-)
during wet part of day:	fE_{wet}	0.5 - 9.0	(-)
Reduction point ^a	$h_{r,d}$	-600	(cm)
Wilting point ^a	$h_{r,w}$	-6000	(cm)
Crop factor ^a	f_c	0.85	(-)
Root density distribution ^c :			
litter	R_i	0.05	(-)
00-20 cm	R_i	0.30	(-)
20-40 cm	R_i	0.34	(-)
40-60 cm	R_i	0.15	(-)
60-80 cm	R_i	0.08	(-)
> 80 cm	R_i	0.08	(-)

a) Based on Tiktak and Bouten (1990; 1994).

b) Measured by Bouten (1992).

c) Based on root length distribution measurements by Olsthoorn (1991).

d) Based on the calibration of SWATRE to Speuld.

Soil physical characteristics

Water retention characteristics were obtained from simultaneously measured average water contents and pressure heads at a plot of $30 \times 30 \text{ m}^2$. The physical characteristics are valid for the same plot as the monitoring data. To extrapolate the retention characteristics outside the range of pressure heads that can be measured with tensiometers, and to obtain conductivity characteristics, the measured data were fitted to the Mualem-Van Genuchten functions (Van Genuchten, 1980):

$$\theta(h) = \theta_r + \frac{(\theta_s - \theta_r)}{[1 + (\alpha|h|)^n]^m} \quad (42)$$

and:

$$K(h) = K_s \cdot \frac{(1 - (\alpha|h|)^{n-1}) \cdot [1 + (\alpha|h|)^n]^{-m/2}}{[1 + (\alpha|h|)^n]^{m/2}} \quad (43)$$

where θ_s ($\text{m}^3 \text{ m}^{-3}$) is saturated volumetric water content, θ_r ($\text{m}^3 \text{ m}^{-3}$) residual water content, h (m) pressure head, α (m^{-1}) reciprocal of the air entry value, K (m d^{-1}) hydraulic conductivity, n (-) a fitting parameter and $m = 1 - 1/n$. Table 2.3 summarizes the results of the fitting.

Table 2.3 Parameters of the Mualem-Van Genuchten functions to describe the soil physical properties. Source: Tiktak and Bouten (1992)

Depth	θ_s ($\text{m}^3 \text{m}^{-3}$)	θ_r ($\text{m}^3 \text{m}^{-3}$)	α (cm^{-1})	n (-)	K_s (cm d^{-1})
litter	0.500	0.00	0.10	1.25	800
0-60 cm	0.330	0.00	0.10	1.25	800
> 60 cm	0.210	0.00	0.04	1.40	100

2.3.1.3 Soil chemistry

For the derivation of the geo-chemical input parameters of NuCSAM, the data-set for plot B was used (see Tiktak *et al.* 1995b). However, parameters were often available for different depths in the soil profile. In order to obtain a coherent set of input parameters, all state variables used in the derivation of input parameters were estimated for the same depths according to:

$$\hat{X}_z = \frac{\Delta z_2 X_1 + \Delta z_1 X_2}{\Delta z_1 + \Delta z_2} \quad (44)$$

with X_z as the estimated value of state variable X at depth z , $X_{1/2}$ as the measured value of state variable X at depth $z_{1/2}$, and $z_{1/2}$ as the nearest depth with measurement $z_1 < z < z_2$. For state variables related to a soil layer with thickness Δz , z is the depth in the middle of that layer.

Exchange constants

Gaines-Thomas exchange coefficients were calculated from the long-term average soil solution concentrations extracted with cups (plot B; Tiktak *et al.*, 1995b) and the amount of exchangeable cations as measured with Bascomb (Tiktak *et al.*, 1995b)) and Li-EDTA. Fractions of exchangeable cations and total CEC were calculated as the mean of both methods. From the concentrations, activities were calculated with the chemical equilibrium program EPIDIM (Groenendijk, 1995). Coefficients were calculated with equation (35) using Ca^{2+} as the reference ion. As the content of exchangeable base cations was below the detection limit, the exchangeable fractions (fraction of total CEC) of all base cations were set to 0.01 to calculate Gaines-Thomas exchange coefficients and to initialize the model. Results are shown in Table 2.4.

Weathering rate parameters

Parameters for weathering of silicates (equation (28)) were calculated from results of batch experiments (De Vries *et al.*, 1995b) for a generic Cambic Podzol. They estimated the total weathering flux for a 70 cm profile by dividing the fluxes derived from the batch experiments by 50. This factor was introduced to account for differences between field and laboratory conditions. The fluxes presented by De Vries *et al.* (1995b) were multiplied by a factor 10/7 to calculate the weathering fluxes for a 1 m profile. The weathering rate constant for the Speuld profile, $kX_{we,pm}$, is calculated as follows. The

coefficients α and $kX_{we,pm}$ are assumed to be layer independent. Parameter α was taken directly from De Vries *et al.* (1995b). The average pH value as measured for plot B by Van der Maas and Pape (1990) was substituted. Total contents of primary minerals and the bulk density were taken from Tiktak *et al.* (1988). Equation (28) can be written down for each soil layer. By substituting all parameters into equation (28), and by assuming that the total weathering fluxes calculated by this equation equals the weathering flux by De Vries *et al.* (1995b), the weathering rate constant can be calculated. The results of the calculations are presented in Table 2.5.

Table 2.4 Gaines Thomas exchange coefficients ($\text{mol l}^{-1}\text{c}^{-2}$ and cation exchange capacity ($\text{mmol}_c \text{kg}^{-1}$)

Depth (cm)	Gaines Thomas exchange coefficient relative to Ca^{2+} ($\text{mol L}^{-1}\text{c}^{-2}$)						CEC ($\text{mmol}_c \text{kg}^{-1}$)
	H^+	Na^+	K^+	NH_4^+	Mg^{2+}	$\text{Al}^{3+}+\text{Fe}^{3+}$	
-9-0	4.00×10^4	42.9	151.9	1890.9	3.4	561.7	245.67
0-5	1.70×10^4	22.3	128.3	289.1	2.5	813.7	96.94
5-10	0.57×10^4	6.7	80.6	13.6	1.2	127.5	58.33
10-20	0.13×10^4	6.0	120.8	6.7	1.1	73.0	57.08
20-30	0.87×10^4	8.6	267.0	11085.1	1.4	32.2	42.83
30-40	6.66×10^4	5.1	162.5	2136.4	0.9	1.8	29.00
40-50	2.50×10^5	3.3	93.7	1624.7	0.7	0.4	26.92
50-60	2.95×10^5	3.1	69.6	10526.7	0.7	0.4	25.67
60-70	2.43×10^5	3.5	59.2	19454.1	0.8	0.7	27.65
70-80	2.33×10^5	4.5	56.5	3625.4	1.0	1.4	28.83
80-100	2.83×10^5	6.6	52.5	0.0	1.2	2.5	39.67

Parameters for weathering of secondary Al compounds (Table 2.6) were taken from batch experiments as described by De Vries *et al.* (1995). They investigated a total number of 15 sites throughout the Netherlands. For the model applications, we selected the soil horizons that showed most resemblance to Speuld site. These included the Ah, Bhs, BCs and C horizons. The rate constant, $kEll$, as determined by De Vries *et al.* (1995b) was divided by an empirical value 100 to account for differences between field and laboratory conditions (Van Grinsven, 1988; Wesselink, 1994).

Table 2.5 Parameters for weathering of silicates (Eqn. (28))

Cation	Total weathering flux ^{a)}	pH dependent		pH independent
	($\text{mol}_c \text{ha}^{-1} \text{a}^{-1}$)	$kX_{we,pm}$	α	$kX_{we,pm}$
		(a^{-1})	(-)	(a^{-1})
Na^+	80	8.43×10^{-2}	0.87	4.19×10^{-5}
K^+	75	2.33×10^{-1}	1.02	4.87×10^{-2}
Ca^{2+}	45	2.26×10^{-1}	0.85	7.11×10^{-3}
Mg^{2+}	20	1.92×10^{-1}	1.54	8.81×10^{-1}

a) source: De Vries *et al.*, 1995b.

Table 2.6 Parameters for the calculation of weathering of oxalate extractable Al (De Vries et al., 1995b)

Depth (cm)	$kEI1$ ($\text{kg}^{-1} \text{a}^{-1}$)	$kEI2$ ($\text{m}^3 \text{mol}_c^{-1}$)	Horizon in De Vries et al.
0- 10	1.13×10^{-6}	11.4	Ah
10- 40	2.04×10^{-4}	9.1	Bhs
40- 80	7.49×10^{-4}	7.3	Bcs
80- 100	1.67×10^{-4}	9.8	C

Sulphate and phosphate sorption parameters

The sulphate sorption capacity, SSC ($\text{mmol}_c \text{kg}^{-1}$), was calculated from the oxalate extractable amount of secondary Al according to (Johnson and Todd, 1983):

$$SSC = 0.02 \cdot ct \text{ Al}_{\text{ox}} \quad (45)$$

The phosphate sorption capacity, PSC ($\text{mol}_c \text{kg}^{-1}$), was calculated from the equation (Van der Zee, 1988):

$$PSC = 0.2 \cdot (ct \text{ Al}_{\text{ox}} + ct \text{ Fe}_{\text{ox}}) \quad (46)$$

Contents of oxalate extractable Al are from Tiktak et al. (1988), contents of oxalate extractable Fe are from measurements on comparable Cambic podzols (De Vries, unpublished results). The Langmuir adsorption constant for SO_4 , $Ke\text{SO}_4 \text{ ad}$, is set to $0.5 \text{ m}^{-3} \text{mol}^{-1}$ and is extracted from the ReSAM database (De Vries et al., 1994). The Langmuir adsorption constant for phosphate, $Ke\text{H}_2\text{PO}_4 \text{ ad}$ is determined from P_w (phosphate in water) and P_{ox} (oxalate extractable phosphate) as determined in 150 forest stands in the Netherlands. Results are shown in Table 2.7.

Table 2.7 Sulphate and phosphate sorption capacities as a function of depth, calculated according to Eqn. (45) and (46)

Depth (cm)	SSC ($\text{mmol}_c \text{kg}^{-1}$)	PSC^a ($\text{mmol}_c \text{kg}^{-1}$)
0-5	3.3	59
5-10	3.4	60
10-20	5.7	99
20-30	8.1	123
30-40	9.8	140
40-50	7.6	118
50-60	6.3	106
60-70	5.6	98
70-80	5.2	94
80-100	5.4	66

^{a)} derived from generic data for a Cambic Podzol

Soil layer independent parameters

The Al equilibrium constant and parameters for nutrient cycling are presented in Table 2.8.

Table 2.8 Values for soil-layer independent model parameters

Process	Parameter	Unit	Value	Eqn.
Foliar uptake ^a	$frNH_{4, fu}$	(-)	0.21	(10)
	frH_{fu}	(-)	0.58	(10)
Foliar exudation ^a	$frCa_{fe}$	(-)	0.18	(12)
	$frMg_{fe}$	(-)	0.11	(12)
	frK_{fe}	(-)	0.71	(12)
Nitrification ^b	k_{ni}	(a ⁻¹)	100.0	(25)
Al dissolution ^c	KAl_{ox}	(L ² mol ⁻²)	5.0x10 ⁸	(34)

^a Based on throughfall data over the period 1987-1990 (Van der Maas and Pape, 1990).

^b Obtained by calibration. The generic value for k_{ni} is 40 a⁻¹.

^c Average IAP for Al(OH)₃ at 90 cm over the period 1987-1990, activities calculated from measured concentrations (Van der Maas and Pape, 1990).

2.3.1.4 Forest growth

The main ecophysiological research and growth analysis was carried out from 1987 until 1989 (Evers *et al.*, 1991) in a plot adjacent to the plot where most of the soil research was done. The soil subplot had a somewhat higher stand density compared to the ecophysiological plot (812 vs. 765 trees ha⁻¹). After 1989, the biomass analysis was moved to the soil research plot, causing a discontinuity in the data series. Table 2.9 gives an overview of basic stand data for the soil plot and for the tree physiological plot as measured in December 1988.

Table 2.9 Tree growth parameters as derived from data for plot 1 measured by Jans *et al.* (1994) and data for the soil plot (Olsthoorn, 1991)

Parameter	Symbol	Unit	Value
Stand age	age_{it}	(a)	30
Logistic growth constant	kr_{grl}	(a ⁻¹)	0.094
Maximum amount of stems	$Amsl_{mx}$	(Mg ha ⁻¹)	543.8
Amount of foliage	Am_{lv}	(Mg ha ⁻¹)	19.5
Half life time growth function	$t05$	(a ⁻¹)	38
Branch stem ratio	fr_{brst}	(-)	0.11
Litter fall rate ^a	klf	(a ⁻¹)	0.15

^a) Litterfall was measured directly using 12 litter traps with a surface area of 1 m² (Van der Maas and Pape, 1990).

State variables that must be known at the beginning of the simulation include the element contents in needles, stems, branches, roots and litter. Data related to these compartments are given in Table 2.10. Data are given for the end of the year 1988.

Table 2.10 Data on biomass and element contents of needles, roots and stems of Speuld stand

Compartment	Biomass (Mg ha ⁻¹)	Element content (% of dry weight)				
		N	K	Ca	Mg	S
Foliage (Am_{lv}) ^a	18.5	1.84	0.58	0.33	0.09	0.14
Branches (Am_{br}) ^b	14.0	0.30	0.10	0.05	0.03	0.05
Stems (Am_{st}) ^b	60.0	0.20	0.10	0.05	0.01	0.05
Fine roots (Am_r) ^c	3.2	1.00	0.08	0.16	0.04	0.10
Litter (Am_{li}) ^d	35.0	-	-	-	-	-

a) measured in the ecophysiological research (Evers *et al.*, 1991).

b) nutrient contents in branches, wood and roots inferred from general data (Berdowski *et al.*, 1991).

c) measured in the soil research plot by Olsthoorn (1991).

d) Measured by Tiktak and Bouten (1992). The litter mass is an average value for 485 samples. Element contents in litter are calculated by the model using the foliage contents as initial values.

2.3.2 Results

2.3.2.1 Hydrology

Interception and throughfall

The hydrological submodel was calibrated in two steps: (i) calibrating the interception losses using measured throughfall values and (ii) calibrating the transpiration and soil evaporation fluxes using measured water contents. The interception fluxes were calibrated using data for the year 1988 only, because for this year the differences between the daily precipitation at station Drie and the weekly site measurements were smallest. The transpiration and soil evaporation fluxes were calibrated by using data for the year 1989, because frequent measurements on water content were available for that year only.

Simulated throughfall amounts for the years 1988 and 1989 are presented in Fig. 2.1. Table 2.11 presents the annual water balances for the period 1987-1989. The calibrated NuCSAM model overestimated the accumulated throughfall amount for 1989 and underestimated the throughfall amount for 1987. For 1988, throughfall amounts are in close agreement with measured throughfall values (maximum deviation < 10% of observed value). The overestimation of throughfall for 1987 and 1989 are partly caused by deviations between measured precipitation at station Drie and on-site measured precipitation (see footnote in Table 2.11). Whereas in 1989, rainfall mainly occurred as large storms. After such storms, a large part of the total precipitation drains instantaneously from the canopy and evaporation loss is relatively small. In 1987, however, a large part of the annual precipitation was in the form of small storms and evaporation losses were high. In addition NuCSAM uses an average rainfall intensity (R), which may also lead to deviations.

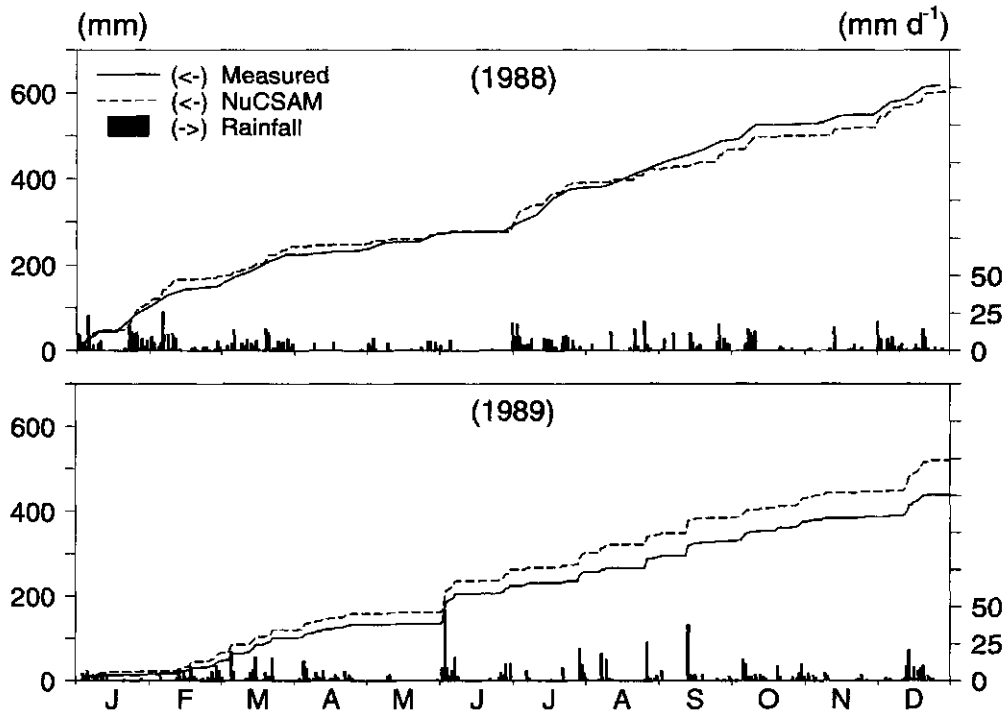


Fig. 2.1 Accumulated simulated throughfall for the years 1988 and 1989

Table 2.11 Simulated water balance terms for the Speuld experimental forest

	1987		1988		1989	
	Observed	NuCSAM	Observed	NuCSAM	Observed	NuCSAM
	Fluxes (mm a^{-1})					
Precipitation	950 ^{a)}	976 ^{b)}	935 ^{a)}	933 ^{b)}	710 ^{a)}	806 ^{b)}
Interception	-	357	-	331	-	285
Throughfall	660	619	618	602	449	521
Evaporation	-	55	-	56	-	66
Transpiration	-	365	-	323	-	371
Drainage	-	199	-	221	-	84
Transpiration reduction (%)	-	0.8	-	13	-	16

a) On-site measured precipitation. These values were not used by NuCSAM, because on-site measurements were not carried out daily.

b) Precipitation measured at station Drie was used as input to NuCSAM.

Soil water contents

Simulated soil water contents for 1989 are shown in Fig. 2.2. Table 2.12 gives an overview of performance criteria for the discrepancy between the observed and measured soil water contents. The performance for the 0-50 cm soil layer appeared to be reasonably good, whereas for the 50-100 cm soil layer, soil water contents are underestimated. However, differences mainly occur in autumn, indicating that rewetting of the soil occurs too late. NuCSAM was not able to predict the dynamic behaviour of measured soil water contents correctly, probably indicating that fingered flow is a relevant hydrological process for Speuld.

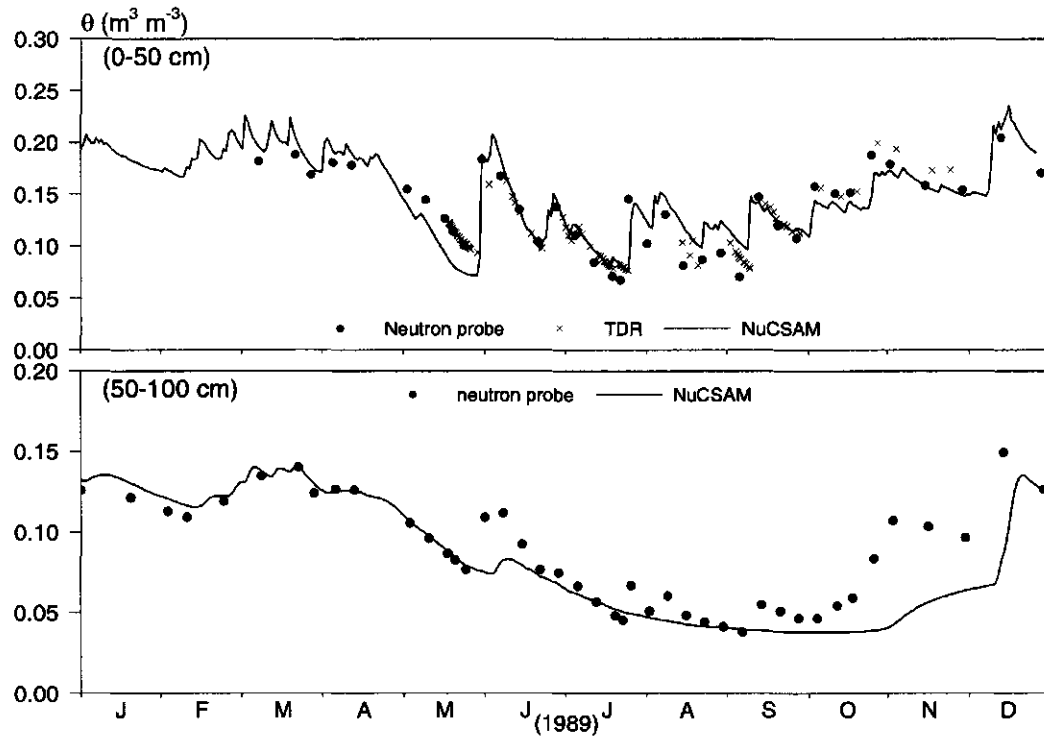


Fig. 2.2 Comparison of observed and simulated water contents in the 0-50 and 50-100 cm soil layers for the year 1989

Table 2.12 NuCSAM Performance criteria for the discrepancy between observed and measured soil water contents

Layer	NME	NMAE
0-50 cm ^a	0.097	0.248
50-100 cm ^b	-0.130	0.174

a) Model output compared with TDR measurements ($n = 88$).

b) Model output compared with neutron probe measurements (plot B; $n = 43$).

2.3.2.2 Soil chemistry

Soil solution concentrations

Results of the calibration are shown for 20 cm depth in Fig. 2.3 and 90 cm depth in Fig. 2.4. Table 2.13 shows the NME and NMAE (Eqn. (41)) for the major components for 10, 20 and 90 cm depth.

pH

Simulated pH values are calculated from the charge balance in NuCSAM. Thus, pH values are affected by virtually all biogeochemical processes. Simulated pH values showed to be over estimated for 20 cm and slightly under estimated for 90 cm. At 10 cm depth the agreement was good (figure not shown). This is also reflected by the performance criteria, i.e. the Normalized Mean Absolute Error (NMAE) for H⁺ concentration at these depths (Table 2.13).

Aluminium

The Al³⁺ concentration was simulated fairly good at both depths. Regarding the calibration results for both the pH and the Al³⁺ concentration, it can be concluded that the pH and Al behaviour in Speuld can be described reasonably good with a combination of the Al-hydroxide equilibrium model (Eqn. (34)) and rate limited dissolution of Al-hydroxides (Eqn. 42). This contrasts with the results from the model comparison study for the Solling site in Germany (Kros and Warfvinge, 1995).

Calcium

The Ca²⁺ concentration at 20 cm depth was under estimated. This is also reflected by the NME, which is ≤ -0.50 . At 90 cm depth, NuCSAM gives a slight underestimation. The underestimation of the Ca²⁺ concentration at 20 cm depth is probably due to either an overestimation of the calcium root uptake in the topsoil or an underestimation of the calcium cycling through the vegetation. Changing the internal cycling of base cations within the system will lead to higher calcium concentrations in the topsoil, without affecting the calcium concentrations below the root zone (i.e. > 90 cm). Because of the moderate fit for 90 cm (i.e. below the root zone), it is presumable that the calcium input by weathering and deposition is correct.

Nitrate

NO₃⁻ concentrations were reasonably reproduced by NucSAM (NMAE = 0.41 - 0.54). Comparing these results with the results of a model comparison study for the Solling site (Kros and Warfvinge, 1995), it is notable that the nitrogen behaviour can be simulated reasonably with NucSAM for Speuld, whereas for Solling this was not possible.

Sulphate and chloride

For 90 cm, the SO₄²⁻ and Cl⁻ concentrations were predicted rather poor (MNAE = 0.40 - 0.58). This is striking because Cl⁻ and SO₄²⁻ are rather conservative anions in Dutch forest soils. The poor performance for these anions is most likely caused by the strong spatial variability of throughfall fluxes and spatial patterns of water uptake by roots. Consequently, the hydrological calibration is not valid for the soil chemical monitoring pit.

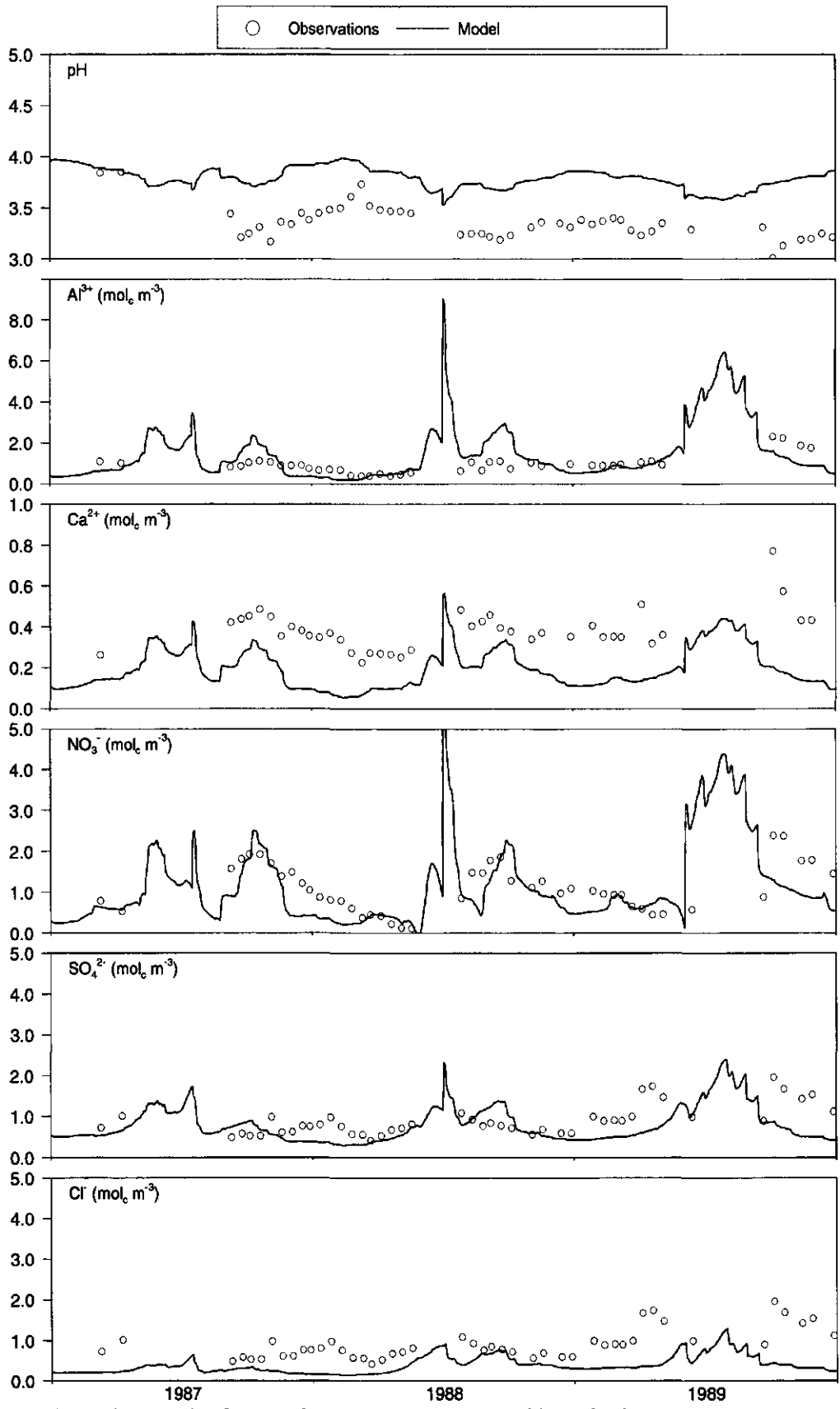


Fig. 2.3 Simulations of soil water chemistry by NuCSAM for 20 cm depth

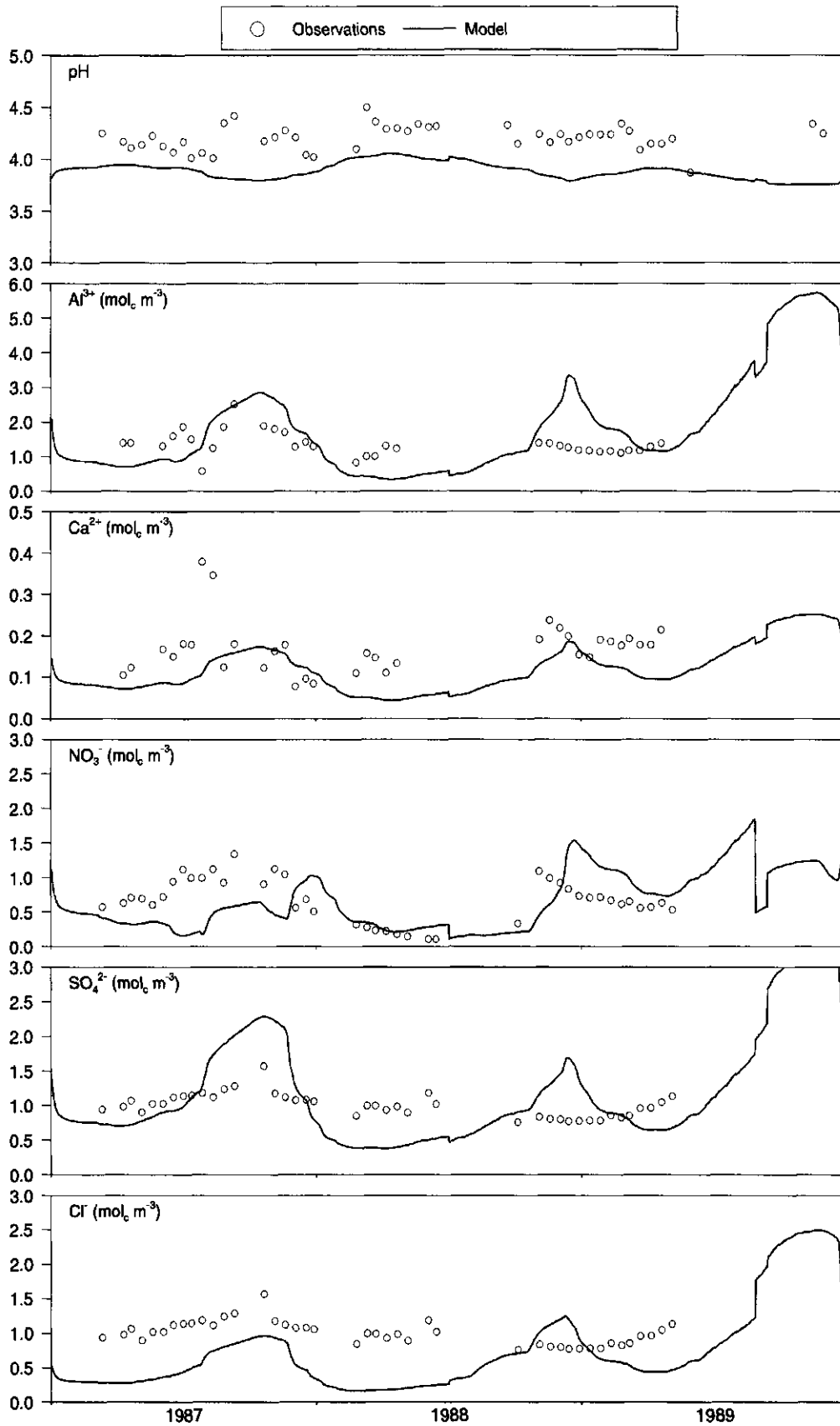


Fig. 2.4 Simulations of soil water chemistry by NuCSAM for 90 cm depth

Table 2.13 Performance of NucSAM during the observation period

Parameter	Performance measurement (-) and number of observations (-)								
	H ⁺	Al ³⁺	Ca ²⁺	Mg ²⁺	K ⁺	NO ₃ ⁻	NH ₄ ⁺	SO ₄ ²⁻	Cl ⁻
Depth 10 cm.									
n ^a	48	37	37	37	37	41	44	41	41
NMAE ^b	0.39	0.60	0.52	0.86	0.83	0.54	0.84	0.62	0.65
NME ^b	-0.37	-0.30	-0.45	-0.86	0.80	-0.37	-0.82	-0.60	-0.65
Depth 20 cm.									
n	48	41	40	40	40	46	44	46	46
NMAE	0.81	0.49	0.63	0.86	2.16	0.41	4.70	0.44	0.47
NME	-0.81	0.10	-0.63	-0.86	2.16	-0.24	3.94	-0.33	-0.40
Depth 90 cm.									
n	48	35	35	35	35	43	34	43	43
NMAE	0.32	0.57	0.40	0.54	0.84	0.53	0.97	0.40	0.52
NME	0.20	0.28	-0.34	-0.54	-0.84	0.02	-0.90	0.02	0.04

a) n is number of observations

b) NMAE is Normalized Mean Absolute Error and NME is Normalized Mean Error (see Eqn. (41)).

Element budgets

Element budgets are presented in Table 2.14. In spite of preferential uptake of NH₄⁺ (Eqn. (23)), the uptake of nitrogen occurs almost completely in the form of NO₃⁻. Due to the fast response of both Al-exchange and dissolution of secondary Al-oxides to a change in pH, the contribution of both processes to net Al-mobilization remains unpredictable for short time periods (Van Grinsven *et al.*, 1989). The Al transfer from the oxide pool to the adsorption complex or vice versa within specific years can be much higher than the net Al-mobilization.

Table 2.14 Major element fluxes of the simulated element budgets for NO₃⁻, NH₄⁺, Al³⁺ and Ca²⁺ for the soil component. Element budgets are averages for the period 1988-1991. Positive fluxes indicate an increase in the soil solution concentration

Process	Fluxes (kmol _c ha ⁻¹ a ⁻¹)			
	NO ₃ ⁻	NH ₄ ⁺	Al ³⁺	Ca ²⁺
throughfall	0.84	2.09	0.01	0.38
uptake	-6.96	-0.40	0.00	-1.38
mineralization	0.00	5.79	0.00	1.11
nitrification	7.40	-7.40	0.00	0.00
weathering ^a	0.00	0.00	-5.43	0.15
exchange	0.00	-0.09	8.71	0.09
leaching	-1.23	-0.00	-2.14	-0.29

a) including dissolution/precipitation of secondary aluminium compounds.

2.4 Scenario analyses

NuCSAM was also used to assess the long-term development of soil solution chemistry, in particular Al concentration in the soil solution, Al/Ca ratio, the content of secondary aluminium compounds and nutrient status. This goal was achieved by performing scenario analyses for the following two generic forest-soil combinations:

- (i) Douglas fir on a Cambic podzol¹;
- (ii) Scots pine on a Haplic arenosol¹.

For both combinations, model simulations were carried out with deposition scenarios that are representative for Dutch regions with low, average and high deposition rates, respectively. It was assumed that in a clean region, the target acid deposition load of $1400 \text{ mol}_c \text{ ha}^{-1} \text{ a}^{-1}$ (NMP+) is reached in 2010, whereas in average and polluted regions these loads are reached in 2050 and 2100, respectively (Keizer, 1994). This scenario is a rather optimistic one with respect to the reduction of deposition. Weather data were randomly selected by a statistical model of historically observed weather data (Richardson and Wright, 1984). The results of these scenario analyses were primarily meant as an example of model use for predictive purposes, as only one deposition scenario and one realization of weather data was evaluated.

2.4.1 Derivation of input data

2.4.1.1 Deposition scenarios

Table 2.15 presents the deposition scenarios for the six combinations evaluated

Table 2.15 Total acid deposition ($\text{mol}_c \text{ ha}^{-1} \text{ a}^{-1}$) for generic Scots pine (SP) and Douglas fir (DF) stands in Drenthe (situated in the Northern Netherlands), Veluwe (Central Netherlands) and North Limburg (Southern Netherlands).

Year	Total acid deposition ($\text{mol}_c \text{ ha}^{-1} \text{ a}^{-1}$)					
	Drenthe		Veluwe		North Limburg	
	SP	DF	DF	SP	DF	SPDF
1980 ^a	5800	6700	8300	8700	8900	10400
1990 ^a	4300	4900	5400	6400	6800	7900
2000 ^b	2400	2800	2600	3000	4000	4600
2010 ^b	1400	1600	2000	2300	3000	3500
2050 ^b	1400	1600	1400	1600	2000	2300

a) inferred from DEADM calculations (see further text).

b) deposition target (Keizer, 1994).

For the period between 1980 and 1991, the deposition of acidifying components was estimated with the DEADM model (Erisman, 1993). The DEADM model was used to generate data for an average stand, based on meteorological measurements and

¹ Soil classification according to FAO (1988). According to the American Soil Taxonomy, these soils can be classified as Typic Dystochrepts and Typic Udipsamments, respectively.

measurements of concentrations in the atmosphere and precipitation. For the period before 1980, concentration measurements were not available and the deposition was inferred from historical deposition data which were based on emissions in those years (De Boer and Thomas, 1991). The historical deposition was scaled to the DEADM deposition, using the following equation:

$$Ac_{id} = Ac_{id,hist} \cdot \left(\frac{\overline{Ac_{id,DEADM}}}{\overline{Ac_{id,hist}}} \right) \quad (47)$$

where Ac_{id} ($\text{mol}_c \text{ ha}^{-1} \text{ a}^{-1}$) is the total deposition of acidity, $Ac_{id,hist}$ ($\text{mol}_c \text{ ha}^{-1} \text{ a}^{-1}$) is the deposition based on emissions, $\overline{Ac_{id,DEADM}}$ ($\text{mol}_c \text{ ha}^{-1} \text{ a}^{-1}$) is the average deposition of

acidity calculated with DEADM for the period 1980-1991 and $\overline{Ac_{id,hist}}$ ($\text{mol}_c \text{ ha}^{-1} \text{ a}^{-1}$) is the average deposition of acidity based on emission data for 1980-1991. Future deposition data of acidity (1992-2050) were inferred from average DEADM results for 1989-1991 and the deposition targets (Table 2.15) by linear interpolation. Moreover, it was assumed that the relative contributions of SO_x , NO_x and NH_x were constant and equal to the contributions for 1991. The average deposition figures were converted to deposition figures for Douglas fir and Scots pine by applying filter factors (De Vries, 1991). Scots pine was assumed to behave as an average tree with respect to dry deposition, so the calculated deposition figures directly apply to Scots pine. Dry deposition for generic Douglas fir was inferred from the DEADM results using a dry deposition filter factor of 1.2. Finally, the deposition of base cations was calculated using a filter factor of 2.5 for Scots pine, and 3.0 for Douglas fir.

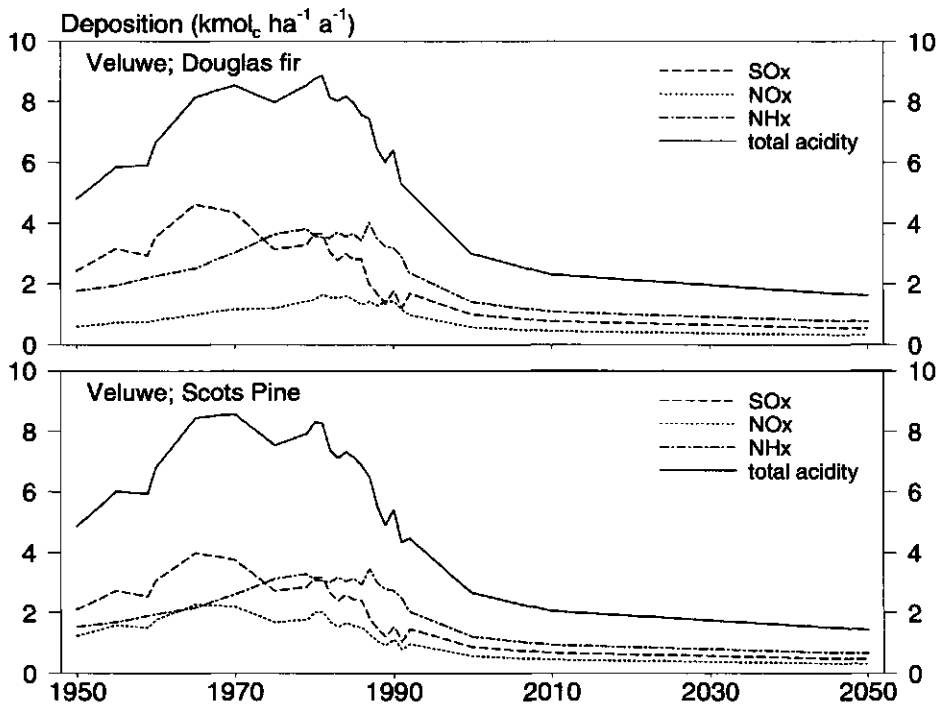


Fig. 2.5 Deposition scenarios for Scots Pine and Douglas fir stands in the Veluwe

The results for region 'Veluwe' are shown in Fig. 2.5. It is obvious that the DPPA-3 scenario is a rather optimistic one. Deposition targets for 2010 are lower than the deposition calculated on the basis of future emissions. These emission data were based on an evaluation of the current environmental policy (RIVM, 1993). On the other hand, the deposition for a generic Douglas fir stand is higher than the deposition for the Speuld site, due to the large distance of Speuld from forest edges.

2.4.1.2 Hydrology

Soil physical characteristics

The retention and conductivity characteristics were taken from the new 'Staring soil series' (Wösten *et al.*, 1994). A drawback from using the Staring Soil Series is that they particularly apply to agricultural soils, and not to forest soils. Therefore, the saturated conductivities are underestimated, and retention and conductivity characteristics derived from the Staring series are steeper (larger values for n ; see equations (42) and (43)), particularly for the sub soil. Results are shown in Table 2.16.

Table 2.16 Parameters of the Mualem-Van Genuchten functions to describe the soil physical properties for a Cambic podzol and a Haplic arenosol

Depth	Code ^a	θ_s (m ³ m ⁻³)	θ_r (m ³ m ⁻³)	α (cm ⁻¹)	nK_s ^b (cm d ⁻¹)	
<u>Cambic podzol</u>						
litter	(B3)	0.500	0.010	0.0152	1.41	17.8
0-50 cm	(B3)	0.450	0.010	0.0152	1.41	17.8
50-70 cm	(B2)	0.430	0.020	0.0227	1.55	9.7
> 70 cm	(O2)	0.380	0.020	0.0214	2.08	15.6
<u>Haplic arenosol</u>						
litter	(B1)	0.500	0.010	0.0249	1.51	17.4
0-80 cm	(B1)	0.430	0.010	0.0249	1.51	17.4
> 80 cm	(O1)	0.360	0.010	0.0224	2.17	13.2

a) Codes refer to the Staring series.

b) See Section 2.3.2 for an explanation of symbols.

Crop dependent properties

Parameters for generic Scots pine and Douglas fir are given in Table 2.17.

Table 2.17 Hydrological parameter values for generic Douglas fir on a Cambic podzol and Scots pine on a Haplic arenosol

Parameter	Symbol	Douglas fir	Scots pine	Unit
Canopy gap fraction ^a	G	0.1	0.3	(-)
Average precipitation intensity	R	10.0	10.0	(mm)
Interception efficiency ^b	f_i	0.141	0.141	(-)
Interception capacity ^c	$A_{wc,max}$	2.1	1.6	(mm)
Factor for evaporation				
during dry part of day:	fE_{dry}	1.5	1.5	(-)
during wet part of day:	fE_{wet}	0.5 (summer) - 9.0 (winter)	0.5 (summer) - 9.0 (winter)	(-)
Reduction point ^d	h_r	-600	-600	(cm)
Wilting point ^d	h_w	-6000	-6000	(cm)
Crop factor ^d	f_c	0.85	0.70	(-)
Root length distribution ^e :	R_i	cf Table 2.1	cf Table 2.1	(-)

a) Based on Tiktak and Bouten (1990; 1994) for Douglas fir and De Visser and De Vries (1989).

b) Measured by Bouten (1992) for Douglas fir.

c) Measured by Mitscherlich and Moll (1970) for Scots pine and Bouten (1992) for Douglas fir.

d) Obtained by Tiktak and Bouten (1990; 1994) for the Speuld site.

e) Based on root length distribution measurements for Douglas fir by Olsthoorn (1991).

Generally, the hydrological parameters used for generic Douglas fir were identical to those used for Speulderbos. Parameters for Scots pine were assumed identical to Douglas fir when no better alternatives were available. Important differences between Scots pine and Douglas fir are present for the gap factor (larger for Scots pine) and for the interception storage capacity (smaller for Scots pine). Parameters with no source indication were derived by calibration.

2.4.1.3 Soil chemistry

Initial values of state variables that must be known at the beginning of the simulation include the amount of elements in all soil compartments, i.e. primary minerals, secondary Al-oxides, the adsorption complex and the soil solution.

Data used for the element amounts in primary minerals, secondary Al-oxides and the adsorption complex are given in Table 2.18.

Table 2.18 Element contents in primary minerals, hydroxides and the adsorption complex for the generic Cambic podzol and the Haplic arenosol

# ^f	Horizon	Depth (cm)	Density ^{a)} (kg m ⁻³)	Total contents ^b (mmol _c kg ⁻¹)				ctAl _{ox} ^{c)} (mmol _c kg ⁻¹)	CEC ^a (mmol _c kg ⁻¹)	Exchangeable fraction ^a (-)			
				Ca ²⁺	Mg ²⁺	K ⁺	Na ⁺			H ⁺	Al ³⁺	BC ^{e)}	NH ₄ ⁺
<u>Cambic podzol</u>													
0	O	3.5-0 ^{d)}	140	-	-	-	-	-	275	0.30	0.08	0.54	0.08
1	Ah	0-10	1345	35	40	230	155	95	42	0.33	0.50	0.12	0.05
2	Ah	10-20	1345	35	40	230	155	95	42	0.33	0.50	0.12	0.05
3	Bhs	20-30	1460	25	45	225	150	185	18	0.10	0.77	0.08	0.05
4	BC	30-50	1535	30	45	240	140	175	18	0.05	0.77	0.08	0.10
5	C	50-70	1535	30	45	240	140	175	18	0.05	0.77	0.08	0.10
6	C	70-110	1555	30	50	240	160	94	4	0.06	0.75	0.07	0.12
<u>Haplic arenosol</u>													
0	O	3.5-0 ^{d)}	140	-	-	-	-	-	275	0.30	0.08	0.54	0.08
1	Ah	0-10	1375	75	60	480	430	55	42	0.20	0.63	0.09	0.10
2	C	10-20	1455	40	35	225	175	70	42	0.22	0.49	0.38	0.09
3	C	20-40	1455	40	35	225	175	70	42	0.22	0.49	0.38	0.09
4	C	40-60	1455	40	35	225	175	70	42	0.22	0.49	0.38	0.09
5	C	60-80	1455	40	35	225	175	70	42	0.22	0.49	0.38	0.09
6	C	80-100	1455	40	35	225	175	70	42	0.22	0.49	0.38	0.09

a) Derived from a field survey (Kleijn *et al.*, 1989). The CEC was measured in an unbuffered solution of silverthioureum. In a buffered solution, both the CEC and the exchangeable H content would have been higher.

b) Derived from laboratory analyses.

c) Derived from a soil information system (Bregt *et al.*, 1986).

d) Thickness calculated for the beginning of the simulation period in 1980.

e) BC is the sum of Ca²⁺, Mg²⁺, K⁺ and Na⁺.

f) Horizon numbers used in NuCSAM.

The initial content of sorbed sulphate was calculated from the equilibrium with the soil solution SO₄²⁻ concentration, using a sulphate sorption capacity (SSC) equal to 2% of the Al-oxalate content (Johnson and Todd, 1983). The initial (i.e. 1980) ion concentrations in each soil layer were derived by running the model during 25 years (1955-1990) using historical emission-deposition data for the corresponding region. Anion concentrations in 1955 were estimated from the annual atmospheric input at that time and the annual average water flux per layer. Cation concentrations in 1955 were derived by combining the charge balance equation with the various cation exchange equations, using given initial exchangeable cation fractions (cf Table 2.18), and cation exchange constants (cf Table 2.20). During the initialization period (1955-1990), the cation contents in primary minerals and hydroxides were kept constant, while the contents of sorbed sulphate and cation contents were continuously updated.

An overview of various overall parameters for Douglas fir on a Cambic podzol and Scots pine on a Haplic arenosol are given in Table 2.19. Most data were derived indirectly from available literature. For example, foliar uptake and foliar exudation fractions were derived from throughfall and bulk deposition data of more than 20 Douglas stands as summarized in Erisman (1990) while using a derivation procedure described in Van der Maas and Pape (1990). Maximum values for the nitrification and protonation rate constants were derived by calibration of model results on measured

$\text{NH}_4^+/\text{NO}_3^-$ ratios and RCOO^- concentrations as given in Van Breemen and Verstraten (1991). An overview of soil-layer dependent parameters is given in Table 2.19.

Table 2.19 Values used for overall model parameters for Douglas fir on a Cambic podzol and Scots pine on a Haplic arenosol

Process	Parameter	Unit	Value	Derivation
Foliar uptake	$f_r\text{NH}_{4, fu}^a$	-	0.30	Erismán (1990)
	$f_r\text{NO}_{3, fu}$	-	0.05	Erismán (1990)
	$f_r\text{SO}_{4, fu}$	-	0.10	Erismán (1990)
Foliar exudation	$f_r\text{Ca}_{fe}$	-	0.24	Erismán (1990)
	$f_r\text{Mg}_{fe}$	-	0.13	Erismán (1990)
	$f_r\text{K}_{fe}$	-	0.63	Erismán (1990)
Litterfall	k_{lf}	a^{-1}	0.28	De Vries <i>et al.</i> (1990)
Root decay	k_{rd}	a^{-1}	1.40	De Vries <i>et al.</i> (1990)
Reallocation	$f_{re, max}$	-	0.36	Berdowski <i>et al.</i> (1991)
Mineralization	$f_{mi, lt, max}$	-	0.40	De Vries <i>et al.</i> (1990)
	$k_{mi, lt, max}$	a^{-1}	0.05	De Vries <i>et al.</i> (1990)
	RDA_{mo}	-	1.5	Janssen (1983)
	C/N_{mo}	-	15	Janssen (1983)
Root uptake	$f_p\text{NH}_{4, ru}$	-	1.5	Gijsman (1990)
Nitrification	$k_{ni, max}$	a^{-1}	40	De Vries <i>et al.</i> (1994)
Denitrification	$k_{de, max}$	a^{-1}	10	Reddy <i>et al.</i> (1982)
Protonation	$k_{pr, max}$	a^{-1}	40	De Vries <i>et al.</i> (1994)
Al dissolution	KAl_{ox}	$\text{mol}^{-2} \text{L}^2$	$4 \cdot 10^7$	Kleijn <i>et al.</i> (1989)
SO_4 adsorption	$KSO_{4, ad}$	$\text{mol}^{-1} \text{L}$	5.10^{-4}	Foster <i>et al.</i> (1986)

a) The foliar uptake fractions for H^+ and NH_4^+ were taken equal. This implies that a decrease in NH_4^+ deposition which is compensated by an increase in H^+ deposition does not affect the foliar exudation flux of base cations.

Table 2.20 Elovich constants for Al dissolution, base cation weathering rate constants and Gaines Thomas exchange constants of the Cambic podzol and the Haplic arenosol used in the simulation

Soil horizon	kEL_1^a ($10^{-7} \text{ m}^3 \text{ kg}^{-1} \text{ a}^{-1}$)	kEL_2^a ($10^{-2} \text{ kg mol}_c^{-1}$)	Weathering rate constants (10^{-5} a^{-1}) ^a				Exchange constants ^b (mol L^{-1}) ^z x ⁻²					
			Ca	Mg	K	Na	H	Al	Mg	K	Na	NH_4
Cambic podzol												
Ah	5.7	9.3	25	11	2.3	2.9	1870	0.62	0.35	0.21	0.77	1.05
Bhs	6.4	6.3	9.1	1.8	5.3	8.5	7830	1.77	0.30	1.31	3.35	6.53
BC	42	4.4	2.9	0.16	3.1	5.9	11470	1.91	0.33	6.14	5.00	30.7
C	87	9.1	17.0	1.5	1.5	2.0	2454	4.41	0.85	8.05	4.04	40.2
Haplic arenosol												
Ah	3.7	9.4	8.3	115	1.0	2.4	6439	1.06	0.30	0.31	0.33	1.53
C	360.0	7.9	16.7	1.6	1.5	2.0	2445	4.41	0.85	8.05	4.04	40.2

a) Derived from batch experiments that were conducted during one year for two Cambic podzols and Haplic arenosols (De Vries, 1994). Base cation weathering rate constants thus derived were divided by 50 to scale results to field weathering rates, that were estimated by the depletion of base cations in these two soil profiles (De Vries and Breeuwsma, 1986). In this model application we assume a negligible pH influence on the weathering rate.

b) Derived from simultaneous measurements of chemical components at the adsorption complex and in the soil solution of two Cambic Podzols at five locations and at four soil depths (Kleijn *et al.*, 1989).

Forest growth and nutrient cycling

Table 2.21 presents the initial basic stand data for Douglas fir on a Cambic podzol and Scots pine on a Haplic arenosol. The biomass of stems was derived from a logistic growth function for Douglas fir (La Bastide and Faber, 1972, De Vries *et al.*, 1990) using a tree age of 30 years. At this age, the amount of needles and fine roots is assumed at it's maximum. The initial litter amount was calculated by integrating the various mineralization equations, using a stand age of 30 years. Initial element contents in litter were taken equal to needle contents.

Table 2.21 Initial stand structure conditions for generic Douglas fir and Scots pine

Parameter	Unit	Douglas fir on Cambic podzol	Scots pine on Haplic arenosol
Stand age	(a)	30	30
Logistic growth constant	(a ⁻¹)	0.077	0.085
Maximum amount of stems	(Mg ha ⁻¹)	543.8	105.1
Amount of foliage	(Mg ha ⁻¹)	10.9	7.5
Half life time growth function	(a ⁻¹)	37	34
Branch stem ratio	(-)	0.1	0.1
Litter fall rate	(a ⁻¹)	0.28	0.55
Soil organic matter	(Mg ha ⁻¹)		
L		15	10
F		45	20
H		350	100
Dead roots		15	10

Data related to various tree compartments are given in Table 2.22. Biomass data of needles and fine roots, and element contents in fine roots and stems were based on literature surveys (Janssen and Sevenster, 1995; Scherfose, 1990; De Vries *et al.*, 1990), whereas the element contents in needles were based on a field survey in 1987 in eight Douglas stands (Oterdoom *et al.*, 1987), and 150 stands (Hendriks *et al.*, 1994).

Table 2.22 Data on biomass and element contents of leaves, fine roots and stems for the generic Douglas fir and Scots pine (see text for data sources)

Compartment	Biomass (kg ha ⁻¹)	Element content (%)				
		N	Ca	Mg	K	S
<u>Douglas fir</u>						
Needles	15000	1.75	0.35	0.12	0.65	0.20
Fine roots	3500	1.00	0.30	0.05	0.20	0.10
Stems	120000	0.20	0.05	0.03	0.06	0.03
Branches	15000	0.30	0.05	0.03	0.10	0.05
<u>Scots pine</u>						
Needles	6000	1.85	0.20	0.13	0.50	0.20
Fine roots	2500	1.00	0.15	0.05	0.15	0.10
Stems	50000	0.15	0.04	0.01	0.05	0.03
Branches	10000	0.40	0.04	0.03	0.08	0.05

2.4.2 Results

2.4.2.1 Hydrology for the 'Veluwe' region

Table 2.23 shows the long-term average simulated water balance for Douglas fir on a Cambic podzol and Scots pine on a Haplic arenosol in the 'Veluwe' region. Some general conclusions can be drawn from the table:

- (i) NuCSAM simulates a lower average interception evaporation for Scots pine than for Douglas fir.
- (ii) Potential transpiration for Douglas fir is higher than for Scots pine, mainly because of the higher crop factor and the lower canopy gap factor for Douglas fir. This demonstrates that feed-backs between the hydrological submodel and the forest-growth submodel may not be ignored in the long run.
- (iii) Actual transpiration for Scots pine is much lower than for Douglas fir due to a lower potential transpiration.
- (iv) Soil evaporation is lower under Douglas fir than under Scots pine. This is mainly caused by the lower Leaf Area Index and higher canopy gap fraction for Scots pine.
- (v) Variation in time of potential transpiration, interception evaporation, actual transpiration and soil evaporation is much smaller than variation in time of precipitation.
- (vi) There is hardly any reduction of soil evaporation calculated by NuCSAM. This is the consequence of using the approach by Black *et al.* (1969), which is only sensitive to the length of the period with a daily precipitation less than 0.3 mm. The generated meteorological dataset contains correct drought intervals but apparently underestimates the length of periods without precipitation.
- (vii) The average precipitation surplus for Douglas fir is very small.

Table 2.23 Average simulated water balance for Douglas fir on a Cambic podzol (DFCP) and Scots pine on a Haplic arenosol (SPHA) in the 'Veluwe' region for the period 1980-2050

Tree/Soil combination	Fluxes and standard deviation (mm a^{-1}) ^a							α (-) ^b
	<i>P</i>	<i>I</i>	E_{pl}	E_s	E_{pl}^*	E_s^*	<i>PS</i>	
DFCP	804 ±98	304 ±35	371 ±20	59 ±3	389 ±17	60 ±2	74 ±40	0.96 ±0.06
SPHA	804 ±98	288 ±34	268 ±11	95 ±4	272 ±12	97 ±5	188 ±38	0.99 ±0.03

^a *P* (mm a^{-1}) is precipitation, *I* (mm a^{-1}) is interception loss, E_{pl} (mm a^{-1}) is transpiration, E_s is soil evaporation, E_{pl}^* (mm a^{-1}) is potential transpiration, E_s^* (mm a^{-1}) is potential soil evaporation, and *PS* (mm a^{-1}) is precipitation surplus.

^b α (-) is ratio of actual transpiration over potential transpiration (E_{pl} / E_{pl}^*)

Compared to transpiration values given by Roberts (1983) for an average forest in Europe (330 mm a^{-1}), values for Douglas fir are higher and for Scots pine lower. The actual transpiration for Douglas fir is almost similar to that for Speuld. The actual transpiration simulated by NuCSAM for Scots pine (268 mm a^{-1}) compares well with that from previous SWATRE simulations by De Visser and De Vries (1989) (281 mm a^{-1}), but are substantially higher than for Douglas fir (371 mm a^{-1} by NuCSAM and 328 mm a^{-1} by De Visser and De Vries, 1989).

2.4.2.2 Soil chemistry for region ‘Veluwe’

Fig. 2.6 shows the simulated yearly average soil solution concentrations for the ‘Veluwe’ region.

Sulphate, aluminium and pH

Concentrations of sulphate and Al are higher and the pH is lower in the soil under Douglas fir than under Scots pine due to higher filtering of air pollutants by Douglas fir, and a lower precipitation surplus. NuCSAM simulates a fast response of the sulphate concentration after a reduction in SO_x deposition, whereas the response of Al shows a considerable time delay. The pH increase under Douglas fir is clearly higher than the increase under Scots pine. This difference is mainly due to the use of a log scale. When inspecting the H^+ concentration (not shown), the decrease in H^+ concentration was more or less comparable.

Nitrate

Results showed a higher concentration of NO_3^- under Douglas fir than under Scots pine. As with sulphate, this is caused by higher filtering of NO_x and NH_x by Douglas. NuCSAM also simulates a time delay for the decrease of the NO_3^- concentration in the soil solution after a decrease in NH_x and NO_y deposition, caused by the release of nitrogen previously stored in living biomass and litter. The NO_3^- leaching fluxes at 90 cm depth show the same behaviour as the NO_3^- concentrations at 90 cm depth.

Table 2.24 Annual simulated fluxes of NO_3^- and NH_4^+ for generic Douglas fir on a Cambic Podzol for region ‘Veluwe’, and for 1990 and 2010. As these results apply to two individual years, conclusions with respect to time-trends must be drawn carefully (e.g. with respect to mineralization). Positive fluxes indicate an increase in the soil solution concentration

Parameter	Fluxes ($\text{mol}_c \text{ ha}^{-1} \text{ a}^{-1}$)			
	NH_4^+		NO_3^-	
	1990	2010	1990	2010
throughfall	3.20	1.09	1.42	0.54
mineralization	6.57	3.05	0.00	0.00
root uptake	-3.92	-1.68	-2.61	-1.12
leaching ^a	-0.15	-0.49	-2.92	-2.53

^a) Refers to 1 m depth

Table 2.24 shows that root uptake of NH_4^+ and NO_3^- in 2010 is approximately 66% of the uptake in 1990. There is a clear reduction in N root uptake flux in 2010. This is caused by a fast decrease of the nitrogen content in needles simulated by this model, which in turn is a result of the assumed empirical relationship between the nitrogen content in needles and the nitrogen deposition (eqn. (15)).

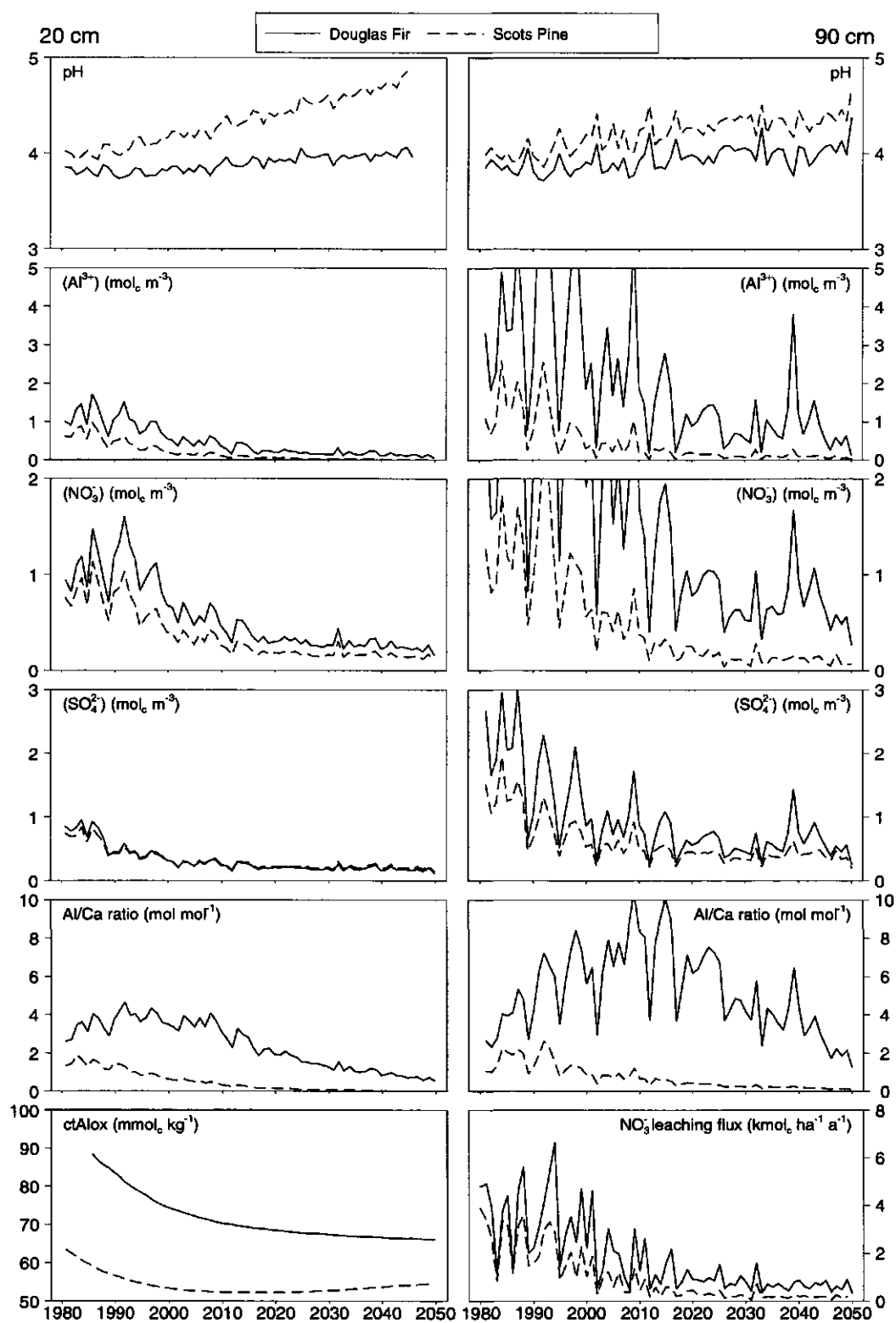


Fig. 2.6 Simulated soil water chemistry for Douglas fir on a Cambic podzol and for Scots pine on a Haplic arenosol (right) in the 'Veluwe' region at 20 cm (left) and at 90 cm (right)

Al/Ca ratio

Differences between Douglas and Scots pine showed again to be large. A considerable time delay was found for the Al/Ca ratio, which continues to rise for a short time after deposition reduction. This phenomenon was also observed in an application on a Norway Spruce stand at Solling, Germany (Groenenberg *et al.*, 1995; Chapter 3). It can be explained by exchange of Ca^{2+} from the soil solution against sorbed Al^{3+} . This is less pronounced in this study than in Solling, due to the smaller CEC of the soils used in this study. Both the Al/Ca ratio and the time-delay for decrease of this ratio is larger for Douglas compared to Scots pine, which is caused by the higher acid load for a soil under Douglas.

Critical values

Regarding the criteria for indirect effects on forest stress (Al/Ca ratio < 1 and no depletion of the pool of secondary aluminium compounds), the results show that an Al/Ca ratio < 1 at 20 cm depth for both forest-soil combinations in 2050 in the 'Veluwe' region. NuCSAM simulates an initial decrease of the pool of secondary aluminium compounds. However, a faster decrease of this pool was simulated for the soil under Douglas fir, whereas for Scots pine a slight increase of this pool was simulated.

Conclusions

Results show a fast response of the sulphate and aluminium concentrations after a decrease in SO_x deposition, a time-delay for the NO_3^- concentration following a decrease in deposition, and higher soil solution concentrations for Douglas.

2.4.3 Comparison of results for the three deposition scenarios

Fig. 2.7 shows the simulated pH at 20 cm depth for all six forest-soil-deposition combinations considered, whereas Table 2.25 show some important averaged model outputs for the periods 1990-2000 and 2040-2050. All soil parameters in Table 2.25 are shown for 20 cm depth.

Fig. 2.7 shows that for both forest-soil combinations the difference in pH of the topsoil (20 cm) is very small for the regions Drenthe and Veluwe. Only region Northern-Limburg, the region with the highest deposition level, can be distinguished with a lower pH and higher NO_3^- , SO_4^{2-} and Al^{3+} concentrations (Table 2.25).

For the subsoil (90 cm), NO_3^- and SO_4^{2-} concentrations differ for the three regions, which is also reflected in the difference in nitrate leaching at 90 cm (Table 2.25). However, effects on the pH and Al concentration at 90 cm are limited. There is quite a large difference in the fate of the pool of secondary aluminium compounds (oxalate extractable Al). For region Drenthe and Veluwe this amounts stabilizes or even increases, as for region Northern-Limburg there is an ongoing decrease of this pool, which can lead to an exhaustion of this pool and pH drop in the long run (figure not shown).

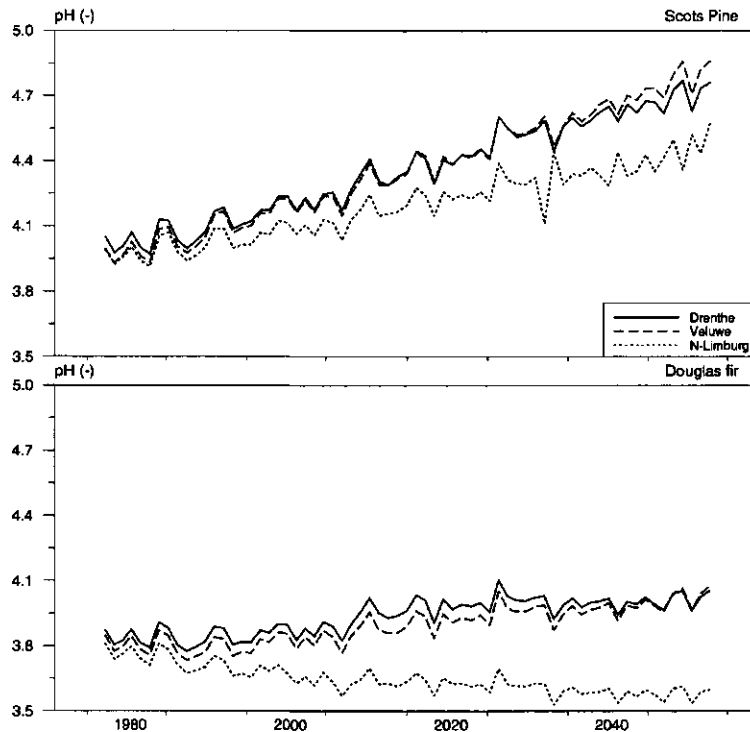


Fig. 2.7 Simulated pH at 20 cm depth for Scots pine on a Haplic arenosol (top) and Douglas fir on a Cambic podzol (bottom) for scenario 'Drenthe', 'Veluwe' and 'N-Limburg'

Regarding the criteria for indirect effects on forest stress, results show that the scenarios for Drenthe and Veluwe for both Douglas fir and Scots pine will cause a reduction in the Al/Ca ratio down to or even below the defined critical values in the year 2050. The same is true for Scots pine in region N-Limburg, but for Douglas fir in this region the Al/Ca ratio remains above the critical values up to 2050.

Table 2.25 Mean predicted soil parameters at 20 cm depth simulated by NuCSAM between 1990 and 2000, and between 2040 and 2050 for generic Douglas fir on a Cambic podzol and generic Scots pine on a Haplic arenosol

Model variable	Unit	Douglas fir on a Cambic podzol		Scots pine on a Haplic arenosol	
		Period		1990-2000	2040-2050
		1990-2000	2040-2050	1990-2000	2040-2050
Drenthe					
pH	(-)	3.8	4.0	4.1	4.7
Al-concentration	(mol _c m ⁻³)	0.8	0.2	0.3	0.1
ctAlox ^a	(mmol _c kg ⁻¹)	81	70	57	57
Al/Ca	(mol mol ⁻¹)	4.4	1.0	0.9	0.0
NO ₃ leaching	(kg ha ⁻¹)	16	3	8	0
N content leaves	(%)	1.5	1.0	1.2	1.0
Veluwe					
pH	(-)	3.8	4.0	4.0	4.8
Al-concentration	(mol _c m ⁻³)	1.0	0.1	0.4	0.0
ctAlox ^a	(mmol _c kg ⁻¹)	78	66	54	54
Al/Ca	(mol mol ⁻¹)	4.0	0.8	1.0	0.0
NO ₃ leaching	(kg ha ⁻¹)	25	5	13	1
N content leaves	(%)	1.9	1.0	1.7	1.0
N-Limburg					
pH	(-)	3.7	3.6	4.0	-
Al-concentration	(mol _c m ⁻³)	1.5	0.5	0.6	-
ctAlox ^a	(mmol _c kg ⁻¹)	81	70	57	-
Al/Ca	(mol mol ⁻¹)	4.4	1.0	0.9	-
NO ₃ leaching	(kg ha ⁻¹)	36	10	20	-
N content leaves	(%)	2.5	1.8	2.2	-

c) ctAlox refers to content of secondary aluminium compounds at 20 cm depth.

2.5 General discussion and conclusions

The application of NuCSAM to detailed observation data-sets, like the one for Speuld, was a challenge. However, a first remark should be that both the Speuld data-set and the models were not really ready for this exercise to be carried out efficiently. Too much technical and practical questions arose when compiling the Speuld data-set and preparing it for the model application. We feel that in the past not enough attention was paid to quality control, compilation, maintenance and distribution of the data-set *as a whole*. In future research programs, more attention should be paid to quality control and to bridging the gap between models and data.

2.5.1 Model validation

A major conclusion arising from this exercise should be that the detailed NuCSAM model is now thoroughly tested against a common data-sets (Speuld), and that it provide a wealth of opportunities to test hypotheses about the interactions between forest, soil

and atmosphere. However, it is not yet clear whether the models are suitable instruments for long-term predictions and scenario analyses. It is obvious that the Speuld data-set was too short for true model-validation. Moreover, due to the large spatial variability of throughfall, soil solution chemistry and stand structure, it was almost impossible to build a meaningful and representative data-set. A major reason for this was that the monitoring at Speuld followed a disciplinary approach, with separate subplots for hydrology, soil chemistry and forest growth. Either was the number of sampling replicates too small to calculate stand averages (soil chemistry), or it was impossible to select more or less homogeneous subplots (hydrology and biomass inventory). Furthermore, individual monitoring groups came with different data for some model parameters. Nevertheless, NuCSAM could reproduce the general magnitude of measured quantities, such as soil water contents and soil solution chemistry. However, NuCSAM was not always successful in simulating measured seasonal dynamics.

2.5.2 Scenario analyses

Scenario analyses were carried out for Douglas fir on a Cambic podzol and Scots pine on an Haplic arenosol in areas with low, intermediate and high atmospheric deposition. The most important trends were a fast response of the sulphate and aluminium concentrations after a decrease in SO_x deposition, time-delay for the NO_3^- concentration following a decrease in nitrogen deposition, higher soil solution concentrations in the soil below Douglas fir, and depletion of the pool of secondary aluminium compounds.

2.5.3 Uncertainties

One of the problems with calibrating a complicated model is that it is difficult, if not impossible, to find a unique set of model parameters. One way to improve the uniqueness of the obtained calibration is using automated and objective calibration procedures. In view of the large number of model parameters that need calibration, such a calibration procedure is very time-consuming. For this reason, automated calibration procedures have not been applied to NuCSAM, but strict (manual) calibration procedures have been postulated. However, if the uniqueness of the calibration remains questionable, results of scenario analyses are also uncertain. Model uncertainty can be assessed by performing thorough and systematic uncertainty analyses. Confidence in predictions from an individual model will also increase when other models predict the same magnitude and trends of model outputs. Therefore, NuCSAM was used in two model comparison studies (Van Grinsven *et al.*, 1995 and Tiktak *et al.* 1995b). Results showed that the compared models were able to identify the general trends and levels of ion concentrations and fluxes. Arguably, stress factors (cf pH, Al, Al/Ca ratios etc.) may be modelled with a level of detail corresponding to the uncertainties in how the trees react to chemical stress in the rhizosphere (Sverdrup *et al.*, 1994). Problems remain, however, when inspecting the details (e.g. seasonality) especially for modelling of Al, pH and N behaviour.

2.5.4 Recommendations for future research

After application of the integrated model NuCSAM at the stand-level, some uncertainties still remain, and new uncertainties arose. However, despite these uncertainties progress was made. This exercise clearly shows that for further hypothesis testing and validation of the model NuCSAM, there is a need to continue intensive monitoring programs, but the balance between data acquisition in the various compartments of the ecosystem should be emphasized. Moreover, much more attention should be paid to bridging the gap between models and experimental data. NuCSAM should be used to select the most important parameters to be monitored. Furthermore, NuCSAM can be used to set-up sampling strategies (in particular sampling frequencies). Another major point of concern should be the issue of *quality control*. The current exercise shows that both the model and the dataset were poorly adjusted. Perhaps the only way to guarantee that integrated data-sets become available is by building databases, which are maintained by a small group of researchers. Besides long-term monitoring of important model parameters, there is a need for measurement campaigns aimed at reducing the uncertainty in the model results. However, such campaigns should be directed by the requirements of integrated models, and not follow a disciplinary line. Besides intensive monitoring programs there is a need for extensive monitoring on a larger number of locations. Such extensive monitoring programs are mandatory for calibration of regional models. However, as with the intensive monitoring programs, much more attention should be paid to bridging the gap between models and measurements. In extensive monitoring, the need for using models to set-up measurements campaigns is even more evident than in intensive monitoring programs.

In the near future, NuCSAM should be used to further explore available manipulation experiments, and present site calibrations could be used to assess the uncertainty of predictions for Speuld, and the deposition scenarios.

2.5.5 Major conclusions

- (i) NuCSAM could reproduce the general magnitude of measured quantities.
- (ii) The scenario analyses showed a fast response of the sulphate and aluminium concentrations in the soil solution after a decrease of the SO_x deposition, time-delay for the NO_3^- concentration following a decrease in nitrogen deposition, and depletion of the pool of secondary aluminium compounds in regions with high deposition.
- (iii) This research clearly shows that for further hypothesis testing and validation of NuCSAM. There is a need to continue intensive monitoring programs, but the balance between data acquisition in the various compartments should be emphasized. For further validation, NuCSAM should be applied to experimental manipulation sites.

References

- Belmans, C., J.G. Wesseling and F.E. Feddes, 1983. Simulation model of the water balance of a cropped soil: SWATRE. *J. Hydrology* 63:271-286.
- Berdowski, J.J.M., C. van Heerden, J.J.M. van Grinsven, J.G. van Minnen and W. de Vries, 1991. *SoilVeg: A model to evaluate effects of acid atmospheric deposition on soil and forest. Volume 1: Model principles and application procedures.* Dutch Priority Programme on Acidification, rep. no. 114.1-02, RIVM, Bilthoven, Netherlands, 93 pp.
- Black, T.A., W.R. Gardner and G.W. Thurtell, 1969. The prediction of evaporation, drainage and soil water storage for a bare soil. *Soil Sci. Soc. Am. Proc.* 33:655-660.
- Bouten, 1992. Monitoring and modelling forest hydrological processes in support of acidification research. Ph.D. thesis, University of Amsterdam, Amsterdam, Netherlands, pp. 218.
- Bouten, W., T.J. Heimovaara and A. Tiktak, 1992. Spatial patterns of throughfall and soil water dynamics in a Douglas fir stand. *Water Res. Res.* 28:3227-3233.
- Bredemeier, M, A. Tiktak and C. van Heerden, 1995. The Solling spruce site: Background information on the data set. *Ecol. Model.* 83:7-15.
- Cannell, M.G.R. 1982. World forest biomass and primary production data. London, Academic Press, 391 pp.
- De Visser, P.H.B. and W. De Vries, 1989. De gemiddelde jaarlijkse waterbalans van bos-, heide- en graslandvegetaties (The yearly average water balance of forest, heathland and grassland vegetations). STIBOKA rapport nr. 2085, Wageningen, Netherlands, 136 pp.
- De Vries, W., 1988. Critical deposition levels for nitrogen and sulphur on Dutch forest ecosystems. *Water Air and Soil Pollut.* 42:221-239.
- De Vries, W., 1991. Methodologies for the assessment and mapping of critical loads and of the impact of the abatement strategies on forest soils. Winand Staring Centre, report 46, Wageningen, Netherlands, pp. 152.
- De Vries, W., 1994. Soil response to acid deposition at different regional scales. Field and laboratory data, critical loads and model predictions. Ph.D. thesis, Agricultural University, Wageningen, Netherlands, pp. 487.
- De Vries, W. and A. Breeuwsma, 1986. Relative importance of natural and anthropogenic proton sources in soils in the Netherlands. *Water Air and Soil pollut.* 35:293-310.
- De Vries, W., A. Hol, S. Tjalma en J.C. Voogd, 1990. Literatuurstudie naar voorraden en verblijftijden van elementen in een boscysteem. DLO-Staring Centrum, Rapport nr. 94, Wageningen, Netherlands, pp. 205 (In Dutch).
- De Vries, W., J. Kros and C. van der Salm, 1994. The long-term impact of three emission-deposition scenarios on Dutch forest soils. *Water Air and Soil Pollut.* 75:1-35.
- De Vries, W., J. Kros and C. van der Salm, 1995a. Modelling the impact of nutrient cycling and acid deposition on forest soils. *Ecol. Model.*, 79:231-254.
- De Vries, W., M.M.T. Meulenbrugge, W. Balkema, J.C.H. Voogd and R.C. Sjardijn, 1995b. Rates and mechanisms of cation and silica release in acid sandy soils: 3. Differences between soil horizons and soil types. Submitted to *Geoderma*.

- Draaijers, G.P.J., 1993. The variability of atmospheric deposition to forests. The effects of canopy structure and forest edges. Ph.D. thesis, Univ. Utrecht, Utrecht, Netherlands, pp. 156.
- Erismann, J.W., 1990. Atmospheric deposition of acidifying compounds onto forests in the Netherlands. Throughfall measurements compared to deposition estimates from inference. National Institute of Public Health and Environmental Protection report no. 723001001, Bilthoven, Netherlands, pp. 29.
- Erismann, J.W., 1993. Acid deposition onto nature areas in the Netherlands. Part I. Methods and results. *Water, Air and Soil pollut.* 71:51-80.
- Evers, P.W., C.J.M. Konsten and A.W.M. Vermetten, 1987. Acidification research on Douglas fir forests in the Netherlands (ACIFORN project). *Proc. Symp. Effects of Air Pollution on Terrestrial and Aquatic Ecosystems. Grenoble*, 887-909.
- Evers, P.W., W.W.P. Jans and E.G. Steingröver, 1991. Impact of air pollution on ecophysiological relations in two Douglas fir stands in the Netherlands. De Dorschkamp Research Institute for Forestry and Urban Ecology, Report no. 637, Wageningen, Netherlands, pp. 306.
- FAO, 1988. Soil map of the World, revised legend. World soil resources report 60, FAO, Rome, pp. 138.
- Foster, N.W., I.K. Morrison and J.A. Nicolson, 1986. Acid deposition and ion leaching from a podzolic soil under hardwood forest. *Water Air and Soil pollut.* 31:879-889.
- Gash, J.H.C., 1979. An analytical model of rainfall interception by forests. *Quart. J. R. Met. Soc.* 105:43-55.
- Gijsman, A.J. 1990. Nitrogen nutrition and rhizosphere pH of Douglas-fir. Ph.D. Thesis, State University Groningen, Netherlands, 132 pp.
- Groenenberg, J.E., J. Kros, C. van der Salm and W. de Vries, 1995. Application of the model NuCSAM to the Solling spruce site. *Ecol. Model.* 83:97-107.
- Groenendijk, P., 1995. The calculation of complexation, adsorption, precipitation and weathering reactions in a soil water system with the geochemical model EPIDIM. DLO Winand Staring Centre Report no. 70, Wageningen, Netherlands (in prep).
- Heij, G.J. and T. Schneider, 1991. Acidification research in the Netherlands. Final report of the Dutch Priority Programme on Acidification. *Studies in Environmental Science* 46, Elsevier, Amsterdam, 771 pp.
- Hendriks, C.M.A., W. de Vries and J. van den Burg, 1994. Effects of acid deposition on 150 forest stands in the Netherlands. 2. Relationship between forest vitality and the chemical composition of the foliage, humus layer and the soil solution. DLO Winand Staring Centre report no. 69.2, Wageningen, the Netherlands, pp. 55.
- Jans, W.W.P., G.M. van Roekel, W.H. van Orden and E.G. Steingröver, 1991. Above ground biomass of adult Douglas fir. A data set collected in Garderen and Kootwijk from 1986 onwards. IBN Research Report 94/1. Institute for Forestry and Nature Research, Wageningen, Netherlands.
- Janssen, B.H., 1983. Organische stof en bodemvruchtbaarheid. Landbouwniversiteit Wageningen, intern rapport, Wageningen, Netherlands, 215 pp (in Dutch).
- Janssen, P.H.M. and P.S.C. Heuberger, 1995. Calibration of process-oriented models. *Ecol. Model.* 83:55-66.
- Janssen, J.J. and J. Sevenster (Eds.), 1995. Opbrengsttabellen voor belangrijke boomsoorten in Nederland. Instituut voor Bos- en Natuuronderzoek, rapport in voorbereiding, Wageningen, The Netherlands (in Dutch).

- Johnson, D.W. and D.E. Todd, 1983. Relationships among iron, aluminum, carbon, and sulfate in a variety of forest soils. *Soil Sci. Soc. Am. J.* 47:792-800.
- Keizer, V.G. 1994. Facsimile (June 23 1994) to the Steering Committee. DGM/LE, The Hague, Netherlands.
- Kleijn, C.E., G. Zuidema en W. de Vries, 1989. De indirecte effecten van atmosferische depositie op de vitaliteit van Nederlandse bossen. 2. Depositie, bodemeigenschappen en bodemvocht-samenstelling van acht Douglas opstanden. Stichting voor Bodemkartering rapport nr. 2050, Wageningen, Netherlands, pp. 96 (In Dutch).
- Kros, J., W. de Vries, P.H.M. Janssen and C.I. Bak, 1993. The uncertainty in forecasting trends of forest soil acidification. *Water Air and Soil Pollut.* 66:29-58.
- Kros J. and P. Warfvinge, 1995. Evaluation of model behaviour with respect to biogeochemistry at the Solling Spruce site. *Ecol. Model.* 83, 255-262.
- La Bastide, J.G.A. and P.J. Faber, 1972. Revised yield tables for six tree species in the Netherlands. Research Institute for Forestry and Urban Ecology, Report no. 11(1), Wageningen, Netherlands, pp. 64.
- Makkink, G.F., 1957. Testing the Penman formula by means of lysimeters. *Journ. Inst. of Water Eng.* 11:277-288.
- Mälkönen, E. 1974. Annual primary production and nutrient cycling in some Scots pine stands. *Communicationes Instituti Forestalis Fenniae*, Helsinki, 84.5, 87 pp.
- Mitscherlich, G. and W. Moll, 1970. Untersuchungen über die Niederschlags- und Bodenfeuchtigkeitsverhältnisse in einigen Nadel- und Laubholzbeständen in der Nähe von Freiburg. *A.F.J.Z.* 141:49-60.
- Mohren, G.M.J., 1987. Simulation of forest growth applied to Douglas fir stands in the Netherlands. Ph.D. thesis, Wageningen Agricultural University, Wageningen, Netherlands, 184 pp.
- Mohren, G.M.J., H.H. Bartelink, I.T.M. Jorritsma and K. Kramer, 1993. A process-base growth model (ForGro) for analysis of forest dynamics in relation to environmental factors. In: M.E.A. Broekmeyer, W. Vos and H. Koop (eds.): *European Forest Reserves. Proc. of the European Forest Reserves Workshop, 6-8 May 1992, The Netherlands, PUDOC, Wageningen, Netherlands*, p. 273-280.
- Olsthoorn, A.F.M., 1991. Fine root density and biomass of two Douglas fir stands on sandy soils in the Netherlands. I. Root biomass in early summer. *Neth. J. Agric. Sci.*, (39): 49-60.
- Oterdoom, J.H., J. van den Burg and W. de Vries, 1987. Resultaten van een oriënterend onderzoek naar de minerale voedingstoestand en bodem-chemische eigenschappen van acht douglasopstanden met vitale en minder vitale bomen in Midden-Nederland, winter 1984/1985. De Dorschkamp, Rapport nr. 470, Wageningen, Netherlands, pp. 47 (In Dutch).
- Reddy, K.R., P.S.C. Rao and R.E. Jessup, 1982. The effect of carbon mineralization on denitrification kinetics in mineral and organic soils. *Soil Sci. Soc. Am. J.* 46:62-68.
- Richardson, C.W. and D.A. Wright, 1984. WGEN: A model for generating daily weather variables. U.S. Dept. for Agriculture, Agric. Science, ARS-8, p.5-15.
- RIVM, 1993. Nationale Milieuverkenning 3. 1993-2015. Samson H.D. Tjeenk Willink, Alphen aan den Rijn, Netherlands, pp. 167 (In Dutch).
- Roberts, J., 1983. Forest transpiration: A conservative hydrological process? *J. Hydrology* (66):133-141.

- Scherfose, V. 1990. Feinwurzelverteilung und Mykorrhizatypen von *Pinus sylvestris* in verschiedenen Bodentypen. Berichte Forschungszentrum WaldÖkosystemen, Univ. Göttingen, Reihe A, Band 62, 169 pp.
- Skeffington, 1988. Excess nitrogen deposition. *Environmental Pollution* 54:159-296.
- Sverdrup, H., P. Warfvinge and B. Nihlgård, 1994. Assessment of soil acidification effects on forest growth in Sweden. *Water, Air, and Soil Pollut.* 78: 1-36.
- Tiktak, A. and W. Bouten, 1990. Soil hydrological system characterization of the two ACIFORN stands using monitoring data and soil hydrological model 'SWIF'. Dutch Priority Programme on Acidification report no. 102.2-01, RIVM, Bilthoven, Netherlands, pp. 62.
- Tiktak, A. and W. Bouten, 1992. Modelling soil water dynamics in a forested ecosystem. III: Model description and evaluation of discretization. *Hydrol. Proc.* 6:455-465.
- Tiktak, A. and W. Bouten, 1994. Soil water dynamics and long-term water balances of a Douglas fir stand in the Netherlands. *J. Hydrology* 156:265-283.
- Tiktak, A., C.J.M. Konsten, M.P. Van der Maas and W. Bouten, 1988. Soil chemistry and physics of two Douglas-fir stands affected by acid atmospheric deposition on the Veluwe, the Netherlands. Dutch Priority Programme on Acidification, report no. 03-01, RIVM, Bilthoven, Netherlands, pp. 93.
- Tiktak, A., M. Bredemeier and C. van Heerden, 1995a. The Solling data-set: Site characteristics and deposition scenarios. *Ecol. Model.* 83:17-34.
- Tiktak, A., J.J.M. van Grinsven, J.E. Groenenberg, C. van Heerden, P.H.M. Janssen, J. Kros, G.J.M. Mohren, C. van der Salm, J.R. van der Veen and W. de Vries, 1995b. Application of three Forest-Soil-Atmosphere models to the Speuld experimental forest. RIVM report 792310002.
- Ulrich, B., 1983. Interaction of forest canopies with atmospheric constituents: SO₂, alkali and earth alkali cations and chloride. In: B. Ulrich and J. Pankrath (eds.). *Effects of accumulation of air pollutants in forest ecosystems*. Reidel, Dordrecht, Netherlands, 33-45.
- Van Breemen, N. and J.M. Verstraten, 1991. Soil acidification and N cycling. In: T. Schneider and G.J. Heij (Eds.). *Acidification Research in the Netherlands*. Final report of the Dutch Priority Programme on Acidification. *Studies in Environmental Science* 46, Elsevier, Amsterdam, 289-352.
- Van der Maas, M.P. and Th. Pape, 1990. Hydrochemistry of two Douglas fir ecosystems and a heather ecosystem in the Veluwe. Dutch Priority Programme on Acidification 102.1.01, RIVM, Bilthoven, Netherlands, pp. 28 and appendixes.
- Van der Zee, S.E.A.T.M., 1988. Transport of reactive contaminants in heterogeneous soil systems. Ph.D. thesis, Wageningen Agricultural University, Wageningen, Netherlands.
- Van Genuchten, M. Th., 1980. A closed form for predicting the hydraulic conductivity of unsaturated soils. *Soil Sci. Soc. Am. J.* 44: 892-898.
- Van Grinsven, J.J.M., 1988. Impact of acid atmospheric deposition on soils. Quantification of chemical and hydrological processes. Ph.D. thesis, Wageningen Agricultural University, Wageningen, Netherlands, pp. 215.
- Van Grinsven, J.J.M., N. Van Breemen and J. Mulder, 1987. Impacts of acid atmospheric deposition on woodland soils in the Netherlands. I.: Calculation of hydrological and chemical budgets. *Soil Sci. Soc. Am. J.* 51:1629-1634.
- Van Grinsven, J.J.M., J. Kros, N. van Breemen, W.H. van Riemsdijk and E. van Eek, 1989. Simulated response of an acid forest soil to acid deposition and mitigation

- measures. *Neth. J. Agric. Sci.* 37:279-299.
- Van Grinsven, J.J.M., C.T. Driscoll and A. Tiktak, 1995. Comparison of Forest-Soil-Atmosphere models and application to the Norway spruce site in Solling, Germany. *Ecol. Model.* 83:1-6.
- Wesselink, L.G., 1994. Time trends and mechanisms of soil acidification. Ph.D. thesis, Wageningen Agricultural University, Wageningen, Netherlands, pp.129.
- Wösten, J.H.M, G.J. Veerman en J. Stolte, 1994. Waterretentie- en doorlatendheidskarakteristieken van boven- en ondergronden in Nederland: De Staring reeks. Vernieuwde uitgave 1994. Technisch document 18, SC-DLO, Wageningen, Netherlands, pp. 66 (In Dutch with English summary).

Chapter 3 is a slightly revised version of:

Groenenberg, J.E., J. Kros, C. van der Salm and W. de Vries, 1995. Application of the model NUCSAM to the Solling spruce site. *Ecological Modelling*, 83: 97-107.

3 Application of the model NuCSAM to the Solling spruce site

Abstract

The Nutrient Cycling and Soil Acidification Model (NuCSAM) was applied to a spruce site at Solling, Germany, within the scope of a workshop on comparison of forest soil atmosphere models. Simulated trends and dynamics in the concentrations of SO_4 , Al and base cations and in pH between 1970 and 1990 compared favourably with time series of measured data during that period. Dynamics and concentrations of NO_3 in the subsoil were overestimated.

Simulation results for the period 1990-2090 for two deposition scenarios showed ongoing acidification (pH decrease) of the soil at the present acid load and a rapid response of soil solution chemistry to reduced acid input, but there was a long time delay before favourable Al/Ca ratios were reached.

3.1 Introduction

The *Nutrient Cycling and Soil Acidification Model* (NuCSAM) is derived from the Regional Soil Acidification Model (ReSAM) (De Vries *et al.*, 1995). ReSAM is used to evaluate the long-term (decades) impact of various emission/deposition scenarios on forest soils on a regional scale. The time resolution of this model is one year. In contrast to ReSAM, NuCSAM has been developed for application on the scale of a forest stand, including inter annual variability. The main extensions of NuCSAM compared with ReSAM are (i) implementing transport of solutes on a daily basis in both upward and downward directions, (ii) linking with a detailed hydrological model, (iii) describing the biochemical and geochemical processes on a daily basis including the modelling of temperature influences, and (iv) adding the elements phosphorus and iron.

This paper describes the application of NuCSAM to an intensively monitored spruce site in Solling, Germany. This application was done within the scope of a workshop on forest soil atmosphere models (Van Grinsven *et al.*, 1995)

3.2 Model principles and key equations

3.2.1 Model structure

NuCSAM simulates the major hydrological and biogeochemical processes in the forest canopy, litter layer, and mineral soil. The change in soil solution and solid phase chemistry is calculated from a set of mass balance equations, describing the input, output and interactions in each compartment. Vertical heterogeneity is taken into account by differentiating between soil layers. The soil layers are considered as homogeneous

compartments of constant density and the constituent input mixes completely within each soil layer.

3.2.2 Hydrological processes

An adapted version of SWATRE (Belmans *et al.*, 1983) was used as hydrological sub-model. This model provides a finite difference solution to the Richard equation.

In this version the distribution with depth for water uptake is calculated to a given fixed root distribution. Potential evapotranspiration is calculated with the Makkink equation (Makkink, 1957). Rainfall interception is calculated according to Gash (1979), using daily evaporation rates instead of an annual average value:

$$I = P_s \times sc + \frac{E * fE_{wt}}{R} \times (P - P_s) \quad (1)$$

For an explanation of used symbols see Annex 1. The calculation of water storage in the canopy at the end of the day was added according to:

$$C_t = C_0 * \exp\left(-\frac{E * fE_{dr}}{S} * t_d\right) \quad (2)$$

with

$$t_d = 1 - \frac{P}{R} \quad (3)$$

Factors (fE_{wt} and fE_{dr}) were introduced to account for the difference in evaporation rates during wet and dry periods.

A snow module based on the Birkenes model (Christophersen *et al.*, 1983) was added. Partitioning precipitation into snow and rain was calculated as a function of the average day temperature. Snow melt was calculated according to Bergstrom (1975) and sublimation of snow was calculated as a fraction of daily evapotranspiration.

3.2.3 Biogeochemical processes

Foliar uptake was simulated for NH_4 and H by a linear relation with the dry deposition. Foliar exudation of base cations is forced by foliar uptake of NH_4 and H. When precipitation exceeds the interception capacity, accumulated dry deposition and exudated base cations are leached from the canopy (throughfall), this is modelled with by a first order equation.

The nutrient cycle is modelled as a steady state, which implies that the maintenance uptake (uptake to resupply nutrients in foliage and roots) equals the sum of litter fall,

root decay and foliar exudation. Net uptake for stem, branch, leaf and root growth is forced by a logistic growth function. The nutrient contents in the tree compartments are constant, except for N, which is a function of total N deposition. Root uptake per soil layer is proportional to a given root distribution. Litter fall, root decay and root uptake are distributed over the year by given monthly varied coefficients. Reallocation of nutrients prior to litter fall and root decay is only included for N, and is a function of the N content in leaves and roots. Mineralization from various humus compartments is described by a set of first order equations. N is released as NH_4 only. Organic anions, produced during mineralization, are calculated from the charge balance of mineralized constituents (NH_4 , Ca, Mg, K, SO_4). Both nitrification and denitrification are described using first order kinetics. Rate constants (and fractions) describing biochemical processes (mineralization, nitrification and denitrification) are described in NuCSAM as maximum values, which are reduced for environmental factors such as soil moisture, temperature and pH. Mineralization rate constants for N are also reduced at low N contents (high C/N ratios) to take account of immobilization by microbes, according to Janssen (1983).

Dissolution of Al and base cations from primary minerals and Al hydroxides is described by rate expressions according to:

$$FX_{we,pm} = \rho \cdot T \cdot kX_{we,pm} \cdot ctX_{pm} [H]^\alpha \quad (4)$$

$$FAl_{we,ox} = \rho \cdot T \cdot kEl_1 \cdot \exp(kEl_2 \cdot ctAl_{ox}) \cdot ([Al]_e - [Al]) \quad (5)$$

Use of the Elovich equation for the dissolution of Al hydroxide (Eqn. 5) is based on laboratory experiments on acid neutralization by Al mobilization (Van Grinsven *et al.*, 1992). Cation exchange for H, Al and base cations is treated with equilibrium (Gaines-Thomas) equations. SO_4 sorption is modelled with a Langmuir isotherm. Aluminium speciation was not considered. Speciation of inorganic carbon is computed from known equilibrium equations. All the chemical equilibrium and rate equations, except for the weathering of silicates, are solved with the chemical equilibrium module EPIDIM (Groenendijk, in prep.)

3.3 Derivation of input data

3.3.1 Hydrological data

Parameters used to calculate interception were derived by calibration on the 1988 throughfall data by selecting the run with the lowest sum of squared residuals out of 50 runs, except for the storage capacity which was taken from Bouten (1992) for Douglas fir in the Netherlands with a comparable leaf area index as the stand in Solling (Table 3.1).

Table 3.1 Parameters used to calculate interception

Parameter	Value	Unit
$\frac{S}{R}$	2.0×10^{-3}	m
fE_{wt}	5.5×10^{-3}	m day ⁻¹
fE_{dr}	0.8	-
sc	3.0	-
	0.85	-

The main parameters used by SWATRE, i.e. water retention characteristics and hydrological conductivity, were taken from the data set (Tiktak *et al.*, 1995). For the litter layer, characteristics of the upper mineral soil layer were used. Conductivity parameters for the subsoil (deeper than 60 cm) (Table 3.2) were calibrated visually by selecting the run with the closest fit for the (1988) winter period when transpiration was negligible.

Values for the crop factor and water uptake distribution (Table 3.3) were subsequently derived in the same way using the summer period. Parameters for transpiration reduction were taken from Tiktak and Bouten (1990).

Table 3.2 Water retention and hydrological conductivity characteristics used in the simulation

Pressure head (m)	Depth					
	60 - 100 cm		100 - 150 cm		> 150 cm	
	water content	K (m day ⁻¹)	water content	K (m day ⁻¹)	water content	K (m day ⁻¹)
0	0.37	1.6×10^{-1}	0.38	1.0×10^{-1}	0.38	1.8×10^{-3}
0.10	0.35	5.0×10^{-2}	0.36	2.5×10^{-2}	0.35	1.3×10^{-3}
0.30	0.34	1.5×10^{-2}	0.34	5.0×10^{-3}	0.34	1.2×10^{-3}
1.00	0.33	4.0×10^{-3}	0.32	5.0×10^{-4}	0.30	5.0×10^{-4}
10.0	0.30	2.0×10^{-4}	0.30	7.0×10^{-5}	0.27	7.5×10^{-5}

Table 3.3 Values for the crop factor and root uptake distribution used in the simulation

Parameter	Value
crop factor	0.85
root uptake distribution:	
litter	0.03
0 - 10 cm	0.10
10 - 20 cm	0.18
20 - 30 cm	0.25
30 - 40 cm	0.24
40 - 60 cm	0.14
60 - 80 cm	0.06

3.3.2 Biogeochemical data

For deposition, the annual values for wet and dry components as described in the data set (Tiktak *et al.*, 1995) were used. Data related to the vegetation, such as element contents in stems, branches, needles and litter, are based on measurements described in the data set. Initial values for amounts in primary minerals (Ca, Mg, K, Na), amorphous Al hydroxides (oxalate extractable) and CEC were directly derived from the data set. CEC values from 1983 were used for the upper 80 cm and for the deeper layers we took the 1986 values. An overview of the various layer-independent parameters is given in Table 3.4. Parameters for root decay, reallocation, mineralization and root uptake were taken from De Vries *et al.* (1994). An overview of soil parameters used for the various soil layers is given in Table 3.5. Most data were derived indirectly from the Solling data set. The values for exponent α (Eqn. 4) were taken from Wesselink *et al.* (1994): 0.69 for Mg, 0.5 for Ca and 0.0 for K and Na. Langmuir parameters for SO_4 sorption were derived from Meiwes (1979).

An initialization period (1961-1970) was used to estimate solute concentrations for 1970 and to equilibrate solute concentrations with exchangeable cations and sorbed SO_4 . During that period amounts of exchangeable cations and sorbed amount of SO_4 were continuously updated while cation amounts in primary minerals and Al hydroxides were kept constant. For the initialization period we assumed a linear increase in deposition for N and S of 1864 and 4622 in 1961 to 2148 and 5811 $\text{mol}_c \text{ ha}^{-1} \text{ yr}^{-1}$ in 1970 respectively. With the assumed deposition during the initialization period, a significant amount of the exchangeable cations was desorbed in the topsoil, transported to the subsoil and exchanged for sorbed Al. This resulted in too high concentrations of base cations in the subsoil during the simulation run. Therefore, initial amounts of exchangeable base cations were lowered to 70% of the values given in the data report. The scenario analyses were carried out using meteorological data over the period 1976-1989. These were repeated until 2090. All other parameters and initial values of variables were the same as those used for the time series.

Table 3.4 Values for soil-layer independent model parameters used in the simulation based on the Solling data set (Bredemeier et al., 1995)

Process	Parameter	Unit	Value
Foliar uptake [†]	$frNH_{4,ft}$	-	0.11
	frH_{fu}	-	0.33
Foliar exudation [†]	$frCa_{fe}$	-	0.49
	$frMg_{fe}$	-	0.09
	frK_{fe}	-	0.42
	kr_{grl}	yr ⁻¹	0.10
Tree growth [‡]	Am_{stmax}	kg ha ⁻¹	3.8x10 ⁵
	t_{05}	yr	66.0
Litter fall [§]	k_{lf}	yr ⁻¹	0.19
Nitrification [¶]	$k_{ni,max}$	yr ⁻¹	100.0
Al dissolution [#]	KAl_{ox}	l ² mol ⁻²	1.0x10 ⁹

[†] Based on average throughfall and deposition data over the period 1974 - 1990

[‡] Derived by curve fitting of the biomass measurements, which were corrected for thinning (62.9%).

[§] Average needle fall rate over the period 1967-1973, taking into account that 92.5% of the litter fall is needle fall.

[¶] Derived from average throughfall and mineralization fluxes over the period 1970-1985, assuming that all mineralized N is released as NH₄.

[#] Average IAP for Al(OH)₃ at 90 cm over the period 1973-1991. The value given, is the value at 25°C, which is derived from the value at field temperature (10°C).

Table 3.5 Elovich constants for Al dissolution, base cation weathering rate constants, Gaines Thomas exchange constants and SO₄ sorption parameters used in the simulation

Soil layer (cm)	kEl_1 (10 ⁻⁷ m ³ kg ⁻¹ yr ⁻¹)	Weathering rate [§] constants (10 ⁻³ yr ⁻¹)					Exchange constants [¶] (mol l ⁻¹) ² x ⁻²					SSC (mmol _c)	$KeSO_{4qd}$ (1 mol ⁻¹) (kg ⁻¹)
		Ca	Mg	K	Na	H	Al	Mg	K	Na	NH ₄		
0-10	0.58	6.5	93.6	0.011	0.021	5180	0.97	1.60	647	8.40	1.05	15.2	7.6x10 ³
10-20	2.00	6.0	73.2	0.008	0.015	57.5	26.2	2.56	3660	29.1	6.53	28.0	1.5x10 ⁴
20-30	5.10	5.6	66.9	0.007	0.013	57.5	8.75	0.65	7470	21.2	30.7	28.0	1.5x10 ⁴
30-40	5.10	5.4	63.7	0.006	0.010	57.5	7.37	0.42	18700	32.0	30.7	28.0	1.5x10 ⁴
40-50	5.10	5.3	61.8	0.005	0.011	57.5	26.2	1.25	16900	36.2	30.7	28.3	2.4x10 ⁴
50-60	5.10	6.2	51.7	0.005	0.011	57.5	26.2	1.25	16900	36.2	30.7	28.3	2.4x10 ⁴
60-90	5.10	10.9	25.8	0.003	0.011	57.5	26.2	1.25	16900	36.2	30.7	28.3	2.4x10 ⁴

[†] Derived from average soil solution concentrations of H and Al in 1983, assuming $KAl_{ox}=1.0x10^9$ and $KEl_2=7.5x10^{-2}$ for all soil layers

[‡] The average of values given in De Vries et al. (1994).

[§] Based on total analysis and weathering fluxes of base cations from Wesselink et al. (1994) and average H concentration in 1983.

[¶] Based on average soil solution concentration measurements in 1983 and solid phase analyses in the same year except for NH₄ which is taken from De Vries et al. (1994).

3.4 Results and discussion

3.4.1 Hydrology

The model predicted throughfall well in summer (Fig. 3.1).

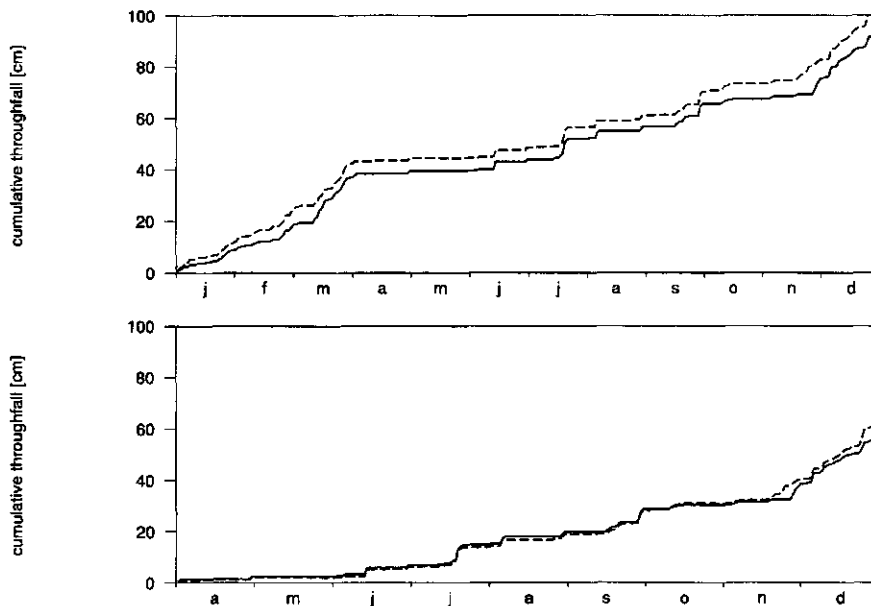


Fig. 3. 1 Measured and simulated throughfall (cm) for the whole year (top) and the summer period (bottom), --- measured throughfall, - - - simulated throughfall

Deviations occurred in winter, especially in years with heavy snowfall. These deviations are probably due to the inaccuracy of measured throughfall in winter, as in many cases measured throughfall was higher than measured precipitation.

The measured and simulated pressure heads corresponded rather well (Fig. 3.2). Simulated pressure heads at 10 cm were somewhat lower than those measured, while at 40 cm (not shown) simulated values were somewhat too high. Pressure heads at 100 cm were sometimes too low. There is considerable deviation between the calibrated water uptake distribution and the observed rooting pattern in Solling, this is probably caused by an increasing water uptake from deeper layers in dry periods, which is not taken into account in the model. Because there were no water content measurements, simulated and measured Cl concentrations were compared (Fig. 3.2). Simulated Cl concentrations were comparable with measured concentrations in both topsoil and subsoil.

Strong reduction in transpiration due to drought stress only occurred in the (extremely) dry summer of 1976 and to a lesser extent in 1982 and 1989. In many years, snow melt and heavy rainfall resulted in transpiration reduction in early spring due to anaerobiosis. However, as potential transpiration rates are relatively low in early spring, it had little effect on the total annual actual transpiration. Annual average transpiration reduction ranged from almost 0 to 14%, with 2% as the median value.

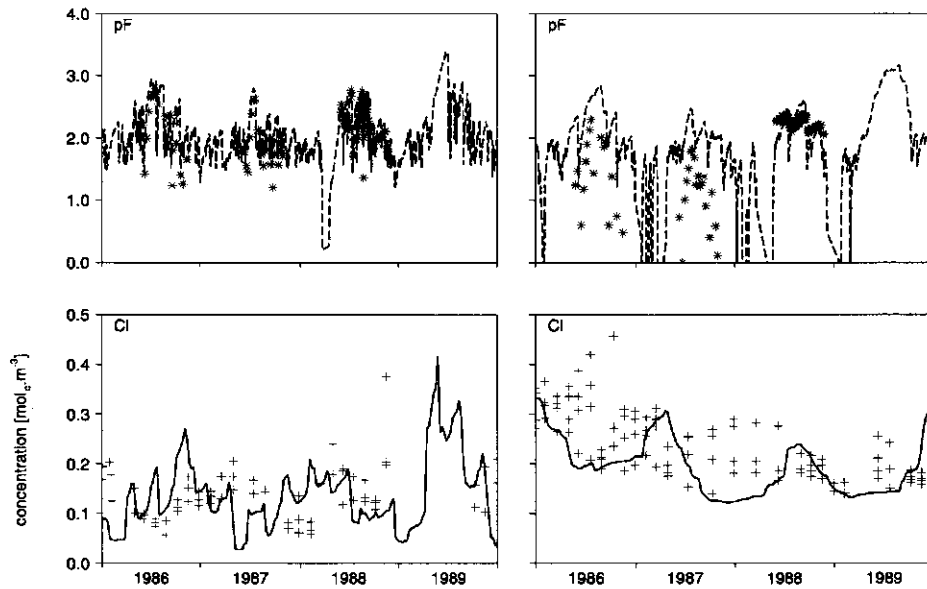


Fig. 3.2 Simulated (—) and measured (+) pF-values at 10 (left) and 100 cm (right) depth and simulated (—) and measured (+) Cl concentrations at 10 (left) and 90 cm (right) depth

3.4.2 Biogeochemistry

Validation

Discussion of the biogeochemistry is confined to interpretation and comparison of the simulated and measured solute concentrations in the mineral soil. Litter dynamics are not discussed because measured data of C and N pools, as given in the data report, are not reliable. This is concluded from the fact that the increase in C and N in the litter layer during the period 1968-1983 equals the litter fall in that period.

Simulated SO_4 concentrations (Fig. 3.3) in the topsoil and subsoil were in good agreement with measured concentrations. The rise in SO_4 from 1973 to 1978 was simulated by the model (Fig. 3.3). To simulate this behaviour the initial amount of sorbed SO_4 in the subsoil had to be set to one quarter of the sulphate sorption capacity. Simulated concentrations between 1981 and 1985 were too low. Simulated NO_3 concentrations (Fig. 3.3) in the topsoil were in the range of, and followed the same seasonal pattern as, the measured concentrations. However, calculated concentrations in 1986 and 1987 were too low. Simulated peak concentrations in the subsoil were too high. The low concentrations in the period 1982-1986 were not calculated by the model. However simulated leaching at 90 cm depth for the period 1973-1985 is in good agreement (within 5%) with the calculated leaching fluxes as given in the data report.

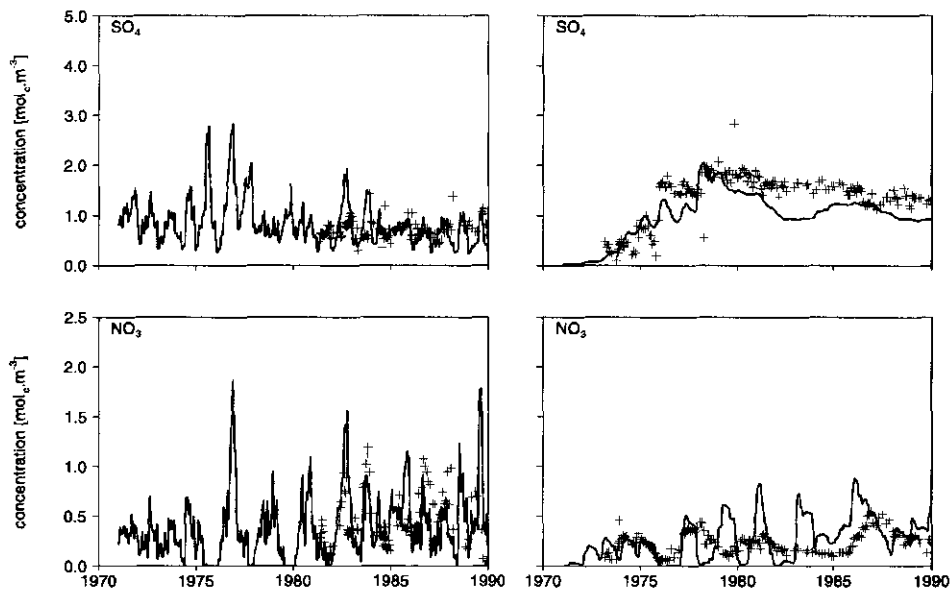


Fig. 3.3 Simulated (—) and average measured (+) concentrations of SO_4 and NO_3 at 10 cm (left) and 90 cm (right) depth

Agreement between measured and calculated Mg concentrations (Fig. 3.4) in both topsoil and subsoil was good. Concentrations of Mg in the subsoil rose from the early seventies until 1978 as a result of exchange of Al against adsorbed Mg. Weathering of Al hydroxide during this period raised the concentration of Al (Fig. 3.4). There was good agreement between measured and calculated concentrations for the topsoil. Simulated Al concentrations for the subsoil are too low but show the same trend as the measured concentrations, except for the sharp decline in simulated Al concentrations at 90 cm in 1981. This decline, which followed the SO_4 concentration, was due to precipitation of Al hydroxide which occurs instantaneously in the model if the solution is supersaturated. Decline in the Al concentration caused too strong a decline in the Mg concentration in the same period by the exchange of Mg against sorbed Al. The simulated pH values (Fig. 3.4) are on the high side of the range of measured pH values for different samples at one time. The dip in pH at 90 cm in 1974-1978 was not simulated by the model.

Scenario analysis

With the 'improved environment' (IE) scenario the Al concentration (Fig. 3.5) decreased sharply in both topsoil and subsoil. With the 'business as usual' (BU) scenario, the Al concentration gradually increased in the subsoil but decreased in the topsoil as a result of Al hydroxide depletion.

The Ca concentration remained constant with the BU scenario in both topsoil and subsoil. With the IE scenario, the Ca concentration in the entire soil profile showed

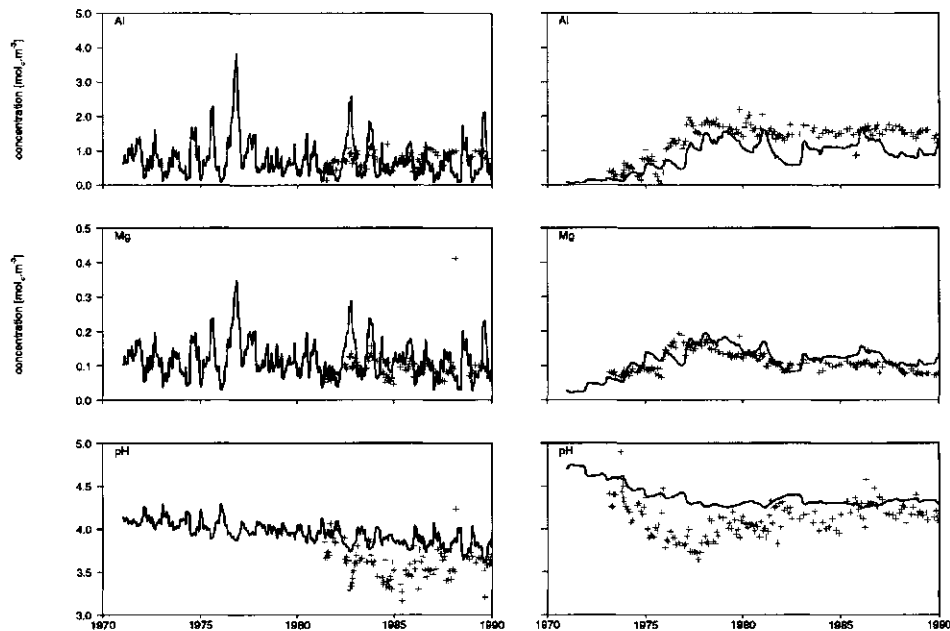


Fig. 3.4 Simulated (—) and average measured (+) concentrations of Mg, Al and pH at 10 cm (left) and 90 cm (right) depth

an initial reduction (between 2000-2030) due to exchange of adsorbed Al by Ca. Even in 2090 the Ca concentration was lower with the IE scenario than with the BU scenario. This means that the base saturation was still not in equilibrium with the deposition level at that time, due to the large CEC of the Solling site. For example, $50 \text{ kmol}_c \text{ ha}^{-1}$ Ca is needed to obtain an exchangeable Ca content of 15% for the whole profile (90 cm). This will take at least 100 years with the current net Ca input (i.e. deposition plus weathering minus net root uptake) of $0.5 \text{ kmol}_c \text{ ha}^{-1} \text{ yr}^{-1}$.

The molar Al/Ca ratio is an important indicator of the adverse effects of soil acidification on roots (De Vries, 1993). In the topsoil, this ratio showed a similar trend to the Al concentration for both scenarios and decreased below 1, which is considered to be a critical value. However, with the BU scenario this decrease was accompanied by a decrease in pH due to Al depletion. In the subsoil, the Al/Ca ratio gradually increased with the BU scenario. With the IE scenario, the Al/Ca ratio initially showed a severe increase between 2010 and 2030, although the Al concentration decreased. This was caused by the decrease in Ca concentration, as already discussed.

With the IE scenario, the pH in the entire soil profile increased. With the BU scenario, the pH in the topsoil almost decreased to a value of three in 2090, caused by Al depletion. In the subsoil the pH remained almost constant.

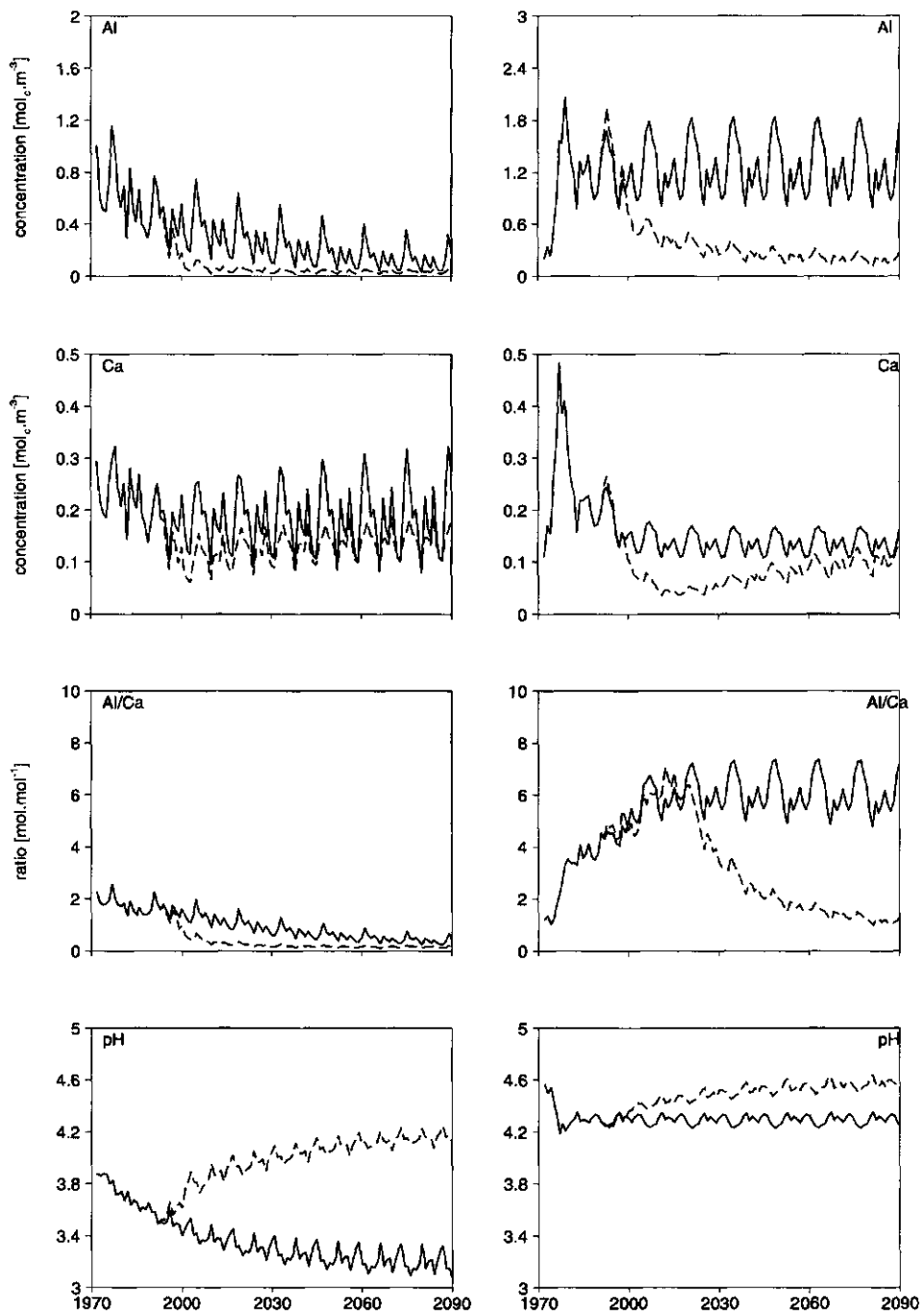


Fig. 3.5 Changes in flux-weighted Al and Ca concentration, molar Al/Ca ratio and pH in the 0-10 cm (left) and 80-100 cm (right) layers for the 'business as usual' (BU) and 'improved environment' (IE) scenarios

3.5 Conclusions

Regarding the validation of NuCSAM on the Solling site, it can be concluded that:

- (i) Agreement between measured and simulated pressure heads and Cl concentrations gives confidence in the water fluxes calculated by the model.
- (ii) Trends and dynamics of the concentrations of SO_4 , base cations and Al are reproduced well.
- (iii) Simulated peak concentrations of NO_3 in the subsoil are too high, however simulated leaching fluxes are more reliable .

Predictions with the NuCSAM model show that:

- (i) The pH in the topsoil decreases at present acid inputs because of Al depletion.
- (ii) There is a rapid response in soil solution chemistry (e.g. SO_4 , NO_3 , Al and Ca concentration) to reduced acid inputs.
- (iii) The Ca concentration decreases sharply after reduced acid inputs due to exchange of Ca against Al. Consequently, there is a long time delay before a favourable Al/Ca ratio is reached, especially in the subsoil.

References

- Belmans, C., J.G. Wesseling and R.A. Feddes, 1983. Simulation model of the water balance of a cropped soil providing different types of boundary conditions: SWATRE. *Journal of Hydrology* 63, 27-286.
- Bergström, S., 1975. The Development of a snow routine for the HBV-2 model. *Nordic Hydrology* 6, 73-92.
- Bouten, W., 1992. Monitoring and modelling forest hydrological processes in support of acidification research. Ph.D. thesis University of Amsterdam.
- Bredemeier, M, A. Tiktak and C. van Heerden, 1995. The Solling spruce site: Background information on the data set. *Ecological Modelling* 83, 7-15.
- Christophersen, N., L.H. Dymbe, M. Johannssen and H.M. Seip, 1983. A model for sulphate in streamwater at Storgama, southern Norway. *Ecological Modelling* 21, 35-61.
- De Vries, W., 1993. Average critical loads for nitrogen and sulfur and its use in acidification abatement policy in The Netherlands. *Water Air and Soil Pollution* 68, 399-434
- De Vries, W., J. Kros and C. van der Salm, 1995. Modelling the impact of nutrient cycling and acid deposition on forest soils. *Ecological Modelling* 79, 231-254.
- Gash, J.H.C., 1979. An analytical model of rainfall interception by forests. *Quarterly Journal of the Royal Meteorological Society* 105, 43-55
- Groenendijk, P., in prep. The calculation of complexation, adsorption, precipitation and weathering reactions in a soil-water system with the geochemical model EPIDIM. Wageningen. SC-DLO, Wageningen Netherlands, Report 70.
- Janssen, B.H., 1983. Organische stof en bodemvruchtbaarheid. Agricultural University Wageningen, Netherlands, Internal Report, 215 pp.
- Makkink, G.F., 1957. Testing the Penman formula by means of lysimeters. *Journal of the Institution of Water Engineers* 11, 277-288
- Meiwes, K.J., 1979. Der Schwefelhaushalt eines Buchenwald- und eines Fichtenwaldökosystem im Solling. *Göttinger Bodenkundliche Berichte*, 60.
- Tiktak, A. and W. Bouten, 1990. Soil hydrological system characterization of the two Acifom stands using monitoring data and the soil hydrological model 'SWIF'. Dutch priority programme on acidification, nr. 102.2-01.
- Tiktak, A., M.A. Bredemeier and C. van Heerden, 1995. The Solling dataset: Site characteristics, monitoring data and deposition scenarios. *Ecological Modelling* 83, 17-34.
- Van Grinsven, J.J.M., C.T. Driscoll and A. Tiktak, 1995. Workshop on comparison of Forest-Soil-Atmosphere models. *Ecological modelling* 83,1-6.
- Van Grinsven, J.J.M., W.H. van Riemsdijk, R. Otjes and N. van Breemen, 1992. Rates of Aluminum dissolution in acid sandy soils observed in column experiments. *Journal of Environmental Quality* 21, 439-447.
- Wesselink, L.G., J.J.M. van Grinsven and G. Grosskurth, 1994. Measuring and modeling mineral weathering in an acid forest soil. Solling, Germany. In: R.B. Bryant and R.W. Arnold (eds.); *Quantative Modeling of Soil Forming Processes*. Madison, Soil Sc. Soc. Am., SSSA special publication 39, 91-110.

Chapter 4 is a slightly revised version of:

Kros, J., J.E. Groenenberg, W. de Vries and C. van der Salm, 1995. Uncertainty due to time resolution in long term predictions of forest soil acidification. *Water Air and Soil Pollution* 79: 353-375.

4 Uncertainties in long-term predictions of forest soil acidification due to neglecting seasonal variability

Abstract

Soil and soil solution response simulated with a site-scale soil acidification model (NuCSAM) was compared with results obtained by a regional soil acidification model (ReSAM). ReSAM is a multi-layer model with a temporal resolution of one year. In addition to ReSAM, NuCSAM takes seasonal variability into account since it simulates solute transport and biogeochemical processes on a daily basis. Consequently, NuCSAM accounts for seasonal variation in deposition, precipitation, transpiration, litterfall, mineralization and root uptake.

Uncertainty caused by the neglect of seasonal variability in long-term predictions was investigated by a comparison of long-term simulations with ReSAM and NuCSAM. Two deposition scenarios for the period 1990-2090 were evaluated. The models were parameterized and validated by using data from an intensively monitored spruce site at Solling, Germany. Although the measured seasonal and the interannual variations in soil solution parameters were large, the trend in soil solution parameters of ReSAM and NuCSAM corresponded quite well with the data. The leaching fluxes were almost similar. Generally it appeared that the uncertainty due to time resolution in long-term predictions was relatively small.

4.1 Introduction

Various models have been developed to analyze the long-term response of surface waters and soils to acid deposition, e.g. MAGIC (Cosby *et al.*, 1985), ILWAS (Chen *et al.*, 1983), SMART (De Vries *et al.* 1989) and ReSAM (De Vries, 1991). Except ILWAS, these models have generally been developed for a regional to continental application. Consequently, these models are relatively simple and have a high degree of process aggregation to minimize data requirements for applications at large scales. The opposite is true for models having relatively complex/detailed process formulations, which are often developed for application on a site-scale. Until now, very few site-scale models are available. In particular the ILWAS model, which was originally developed as a catchment model, can be considered as a site-scale model because of its daily, or even smaller, time scale and detailed level of process formulation.

One common simplification that has been made in the large scale models is the neglect of seasonal variability of both model input and processes. Therefore these models use an annual time scale and require highly aggregated input (water routing and deposition). These simplifications may cause errors in long-term predictions. Seasonal variability is generally driven by climatic (e.g. precipitation, deposition, evaporation, snowmelt) and biotic factors (e.g. litterfall, mineralization, nutrient uptake). Georgakakos *et al.* (1989) indicated that the neglect of natural day-to-day variability, present in precipitation and other weather variables, significantly affects long-term predictions of lake alkalinity.

This was supported by Warfvinge and Sandén (1992) who showed that the long-term trend in soil solution ANC is affected by time resolution. Another problem with long-term large scale (soil) acidification models is the lack of sufficient long-term (> 50 years) series of observations, which makes these models difficult to calibrate and validate. A thorough calibration and validation on short-term (< 10 years) series is hardly possible because these models do not account for seasonal variability which plays an important role in short-time data records. However, results of the long-term large scale models can be compared with results of more detailed models which are validated on relatively short-term data sets.

Here, we report the application of a complex site-scale model including seasonal variability (NuCSAM; Chapter 2; Groenenberg *et al.*, 1995; Chapter 3) and a relatively simple regional scale model (ReSAM; De Vries *et al.*, 1995), which neglects seasonal variability, on an intensively monitored spruce site at Solling, Germany. Both NuCSAM and ReSAM were compared with observed soil solution concentrations over the period 1973-1990. The long-term simulations with both models were performed for two atmospheric deposition scenarios over a 100-year period.

The main objectives of this study are:

- (i) to characterize the effect of neglecting seasonal variability on long-term predictions of soil and soil solution response. This was done by comparing results from NuCSAM with results obtained by ReSAM.
- (ii) to validate both models, on a relatively short-term monthly observed data set from an intensively studied site in Solling, Germany.

4.2 Models used

Both NuCSAM and ReSAM simulate the major biogeochemical processes in the canopy, litter layer and mineral soil horizons. ReSAM has been developed to analyze the long term soil response to acid deposition on a regional scale. Unlike ReSAM, NuCSAM is applicable on a site-scale, since it simulates solute transport and biogeochemical processes on a daily basis, while ReSAM uses a yearly basis. Consequently, NuCSAM accounts for seasonal variation in deposition, precipitation, transpiration, litterfall, mineralization and root uptake and all the biochemical and geochemical processes are modelled as a function of temperature, whereas ReSAM neglects these effects.

4.2.1 ReSAM

ReSAM simulates all processes occurring the forest canopy, litter layer and mineral soil horizons which significantly influence the concentration of major ions in the soil solution. The model consists of a set of mass balance equations, kinetic equations and equilibrium equations. Mass balance equations describe the input-output relationship in each soil layer for all ions, except for H^+ and HCO_3^- . The concentration is determined by the CO_2 equilibrium equation (cf Annex 2), whereas the H^+ concentration is

determined from the charge-balance. Model input includes atmospheric deposition and hydrological data. The biogeochemical processes accounted for in the model are given in Annex 2, with a brief overview of the model formulations used. A complete overview of the model structure of ReSAM is given in De Vries *et al.* (1995).

Vertical heterogeneity is considered by differentiating between soil layers. The soil layers are considered as homogeneous compartments of constant density and the constituent input mixes completely within each soil layer. Horizontal heterogeneity is not considered. The time resolution is one year. However, the time-step of the model is one to five days to avoid numerical instability and to minimize numerical dispersion.

4.2.2 NuCSAM

NuCSAM (Chapter 2, Groenenberg *et al.*, 1995; Chapter 3), which has been derived from ReSAM, also simulates the major biogeochemical processes in the forest canopy, litter layer, and mineral soil but the temporal resolution is one day. Consequently, hydrological processes are also included, i.e. (i) partitioning of precipitation into rainfall and snowfall, (ii) snowpack accumulation and snowmelt, (iii) interception evaporation from the forest canopy and soil evaporation, (iv) transpiration and snowmelt, and (v) one-dimensional vertical transient water flow.

Water fluxes and soil water contents are calculated with an adapted version of the SWATRE (Belmans *et al.*, 1983) model. This model provides a finite difference solution to the Richard's equation. The adapted version (Groenenberg *et al.* 1995; Chapter 3) differs from the original model with respect to the formulation of interception evaporation and transpiration. Furthermore a snow module was added and root uptake was divided over the different soil layers according to a fixed root distribution.

The biogeochemical processes accounted for in the model are basically the same as used in ReSAM except for mineralization (cf Annex 2). In addition to ReSAM: (i) litterfall, root decay, mineralization and root uptake are distributed over the year by given monthly coefficients, (ii) both upwards and downwards solute transport is simulated and (iii) speciation of inorganic carbon is computed from known equilibrium equations. All chemical equilibrium and rate limited equations are solved with a separate chemical equilibrium module EPIDIM (Groenendijk, in prep.), which allows for the calculation of aluminium speciation by considering hydrolysis reactions and complexation with organic and inorganic anions.

4.3 Methods and data

4.3.1 Approach

To compare NuCSAM and ReSAM it is necessary to ensure that the models start under similar conditions, receive consistent inputs and use corresponding process parameters. In those cases where the two models use the same state variables and process parameters, we used the same values for both models. Parameter values and initial values of variables were either based on literature or on the NuCSAM calibration (see below). In order to exclude bias caused by a difference in process formulations we adapted NuCSAM in this comparison, so that the differences with respect to process formulations were restricted to a minimum. Mineralization formulations in NuCSAM were changed into those used in ReSAM, whereas chemical equilibria, in NuCSAM were restricted to those included in ReSAM. In doing so we ensured that the difference between the responses of the two models is caused by a difference in time resolution. To ensure that ReSAM receives the same input as NuCSAM, we accumulated the daily NuCSAM inputs to yearly values.

To obtain an insight into the effect of neglecting seasonal variability on long-term results of ReSAM, annual solute concentrations predicted by this model were compared with annual flux-weighted concentrations predicted with NuCSAM. In addition, simulated cumulative leaching fluxes were also compared. A comparison between concentrations gives an indication about differences in trends and retardation effects. A comparison of cumulative leaching fluxes gives information about differences in the net release or net retention of elements over the simulation period. This is especially important for Al, because one of the principal goals of the ReSAM model is to evaluate the effect of acidic deposition on the depletion of Al hydroxides (De Vries *et al.* 1994). To give more objective information about the performance (degree of agreement) of both models, we calculated the Normalized Mean Absolute Error (NMAE) for the model results related to the observations:

$$\text{NMAE} = \frac{\sum_{i=1}^N |P_i - O_i|}{N \cdot \bar{O}} \quad (1)$$

where: P_i and O_i denote the predicted and observed value i

\bar{O} denotes the mean of the observations

N denotes the number of observations

The NMAE quantifies the average deviation between model predictions and observations. In calculating the NMAE, the yearly ReSAM concentrations and the flux-weighted annual average NuCSAM concentrations were compared with the observed flux-weighted annual average concentrations. The latter values were generated by dividing the yearly sum of the product of observed concentrations with the cumulative simulated moisture flux over the observation period (approximation of the observed yearly leaching flux), by the yearly simulated soil moisture flux.

4.3.2 The Solling site

The Solling site (F1 plot) is a typical Norway spruce (*Picea abies*; 105 years old) plantation forest with sparse ground vegetation on a Dystric Cambisol with a well-developed humus layer (ca. 8 cm) and a 60 to 80 cm loess mineral layer lying on soliflucted material from triassic sandstone. Inputs, outputs and internal transfers of elements have been measured for more than twenty years, and were complemented by plant physiological, hydrological, micrometeorological and soil biological monitoring programmes during that time. Rainfall, throughfall and soil solution at 0 cm, i.e. below the humus layer, were collected since 1969, the soil solution at 90 cm depth since 1973 and at 10, 20, 40 and 80 cm depth since 1981 (Bredemeier *et al.*, 1995).

4.3.3 Deposition data and scenarios

For the deposition during the observation period 1973-1990 yearly values were used for wet and dry components as described in Bredemeier *et al.*, (1995).

For the characterization of the neglect of seasonal variability on long-term results of both models, we used two atmospheric deposition scenarios for the period 1990-2090, i.e. (i) *business as usual* (BU): deposition values from the Solling data set in 1990 were kept unchanged for the period 1990-2090; (ii) *improved environment* (IE): a 75% reduction was performed on the deposition values in 1990 of SO_x, NO_x and NH_x linearly between 1990 and 2000 and after that the deposition values remained constant. For all other constituents the values of 1990 were kept constant, except for H⁺, which is calculated from the charge balance. The values for the total deposition fluxes used for 1990 were: 1473 mol_c ha⁻¹ yr⁻¹ for NH₄⁺, 1410 mol_c ha⁻¹ yr⁻¹ for NO₃⁻ and 3641 mol_c ha⁻¹ yr⁻¹ for SO₄²⁻.

4.3.4 Hydrological data

Daily drainage fluxes, root uptake fluxes and water contents as calculated by SWATRE were directly used by NuCSAM. For the application of the SWATRE model to the Solling site and the data used we refer to Groenenberg *et al.*, (1995) (Chapter 3). ReSAM used annual average values for drainage fluxes, root uptake fluxes and water contents in each layer, which were kept constant during the simulation period. The annual average values were derived from the daily SWATRE calculations over the period 1973-1990.

The scenarios were evaluated by using meteorological data over the period 1973-1990. These were repeated until 2090.

4.3.5 Biogeochemical data

Biogeochemical data for NuCSAM and ReSAM (Groenenberg *et al.*, 1995; Chapter 3, Van der Salm *et al.*, 1995; Chapter 5) were mainly derived from the Solling data set of Bredemeier *et al.*, (1995).

An overview of relevant biogeochemical parameters for canopy exchange, litterfall, root decay, reallocation, mineralization, nitrification, denitrification and root uptake and their derivation are given in Table 4.1. The parameters for N cycling/transformation in NuCSAM and ReSAM were directly derived from the Solling data set of Bredemeier *et al.* (1995). Growth uptake in NuCSAM and ReSAM was calculated by multiplying a given (logistic) growth rate (Annex 2) by the element content in 1968 in stems and branches, respectively. Element contents were assumed constant with the exception of N content. N content is calculated with a linear relationship between N content and N deposition. N content is minimal at a N deposition of 1500 kmol_c ha⁻¹ yr⁻¹ and maximal at a N deposition of 7000 kmol_c ha⁻¹ yr⁻¹. During the simulation period parameters related to forest growth persisted, which means that the stand remains a mature forest with a very low net growth and a relatively high nutrient cycling. The monthly distribution fractions for litterfall, root decay, mineralization and root uptake as used in NuCSAM are given in Table 4.2. In ReSAM the fractions were evenly distributed over the year.

Table 4.1 Values for biogeochemical model parameters used in the NuCSAM and ReSAM simulations

Process	Parameter	Unit	Value
Foliar uptake ¹⁾	$fr_{NH_4\ fu}$	-	0.11
	$fr_{H\ fu}$	-	0.33
Foliar exudation ¹⁾	$fr_{Ca\ fe}$	-	0.49
	$fr_{Mg\ fe}$	-	0.09
	$fr_{K\ fe}$	-	0.42
Tree growth ²⁾	kr_{grt}	yr ⁻¹	0.10
	$Am_{st\ mx}$	kg ha ⁻¹	3.8×10 ⁵
	t_{05}	yr	69.2
Litterfall ³⁾	kr_{lf}	yr ⁻¹	0.19
Root decay	kr_{rd}	yr ⁻¹	1.4
Nitrification ⁴⁾	$kr_{ni\ mx}$	yr ⁻¹	100.0
Denitrification	$kr_{de\ mx}$	yr ⁻¹	10.0

1) Based on average throughfall and deposition data over the period 1974 - 1990

2) Derived by curve fitting of the biomass measurements, which were corrected for thinning (62.9%).

3) Based on the average needlefall rate over the period 1967-1973, taking into account that 92.5% of the litterfall is needle fall.

4) Derived from average throughfall and mineralization fluxes over the period 1970-1985, assuming that all mineralized N is released as NH₄⁺.

Table 4.2 Monthly distribution fractions (unitless) for litterfall (*lf*), root decay (*rd*), mineralization (*mi*) and root uptake (*ru*) as used in NuCSAM

Month	<i>lf</i>	<i>rd</i>	<i>mi</i>	<i>ru</i>
January	0.00	0.00	0.00	0.01
February	0.00	0.00	0.00	0.01
March	0.00	0.00	0.10	0.05
April	0.00	0.00	0.15	0.08
May	0.10	0.10	0.15	0.15
June	0.10	0.10	0.20	0.15
July	0.10	0.10	0.20	0.15
August	0.10	0.10	0.15	0.15
September	0.20	0.20	0.05	0.10
October	0.20	0.20	0.00	0.09
November	0.10	0.10	0.00	0.05
December	0.10	0.10	0.00	0.01

Dissolution parameters of Al-hydroxides in ReSAM and NuCSAM, described by an Elovich equation, are given in Table 4.3 with their derivation. Weathering rate constants for primary minerals were derived from a budget study (Wesselink *et al.*, 1994). The values for exponent α (Annex 2, Eqn. 9) were taken from Wesselink *et al.* (1994): 0.69 for Mg, 0.5 for Ca and 0.0 for K and Na.

Gaines Thomas exchange constants were based on average soil solution concentrations measurements in 1983 and solid phase analyses in the same year. SO_4^{2-} Langmuir sorption constants for both models were derived from Meiwes (1979).

Bulk density, CEC, initial values for the amounts of Ca, Mg, K and Na in primary minerals and in amorphous Al-hydroxides (oxalate extractable) were derived from Bredemeier *et al.* (1995). CEC values from 1983 were used for the first 80 cm, while values from 1986 were used for the deeper layers (Table 4.4).

An initialization period (1961-1973) was used to estimate solute concentrations in 1973 and to equilibrate solute concentrations with exchangeable cations and adsorbed SO_4^{2-} . During that period amounts of exchangeable cations and the adsorbed amount of SO_4^{2-} were continuously updated while cation amounts in primary minerals and Al hydroxides were kept constant. For the initialization period we assumed a linear increase in deposition from 67% of the value in 1973 for N (NO_2 and NH_3) and 50% of the value in 1973 for S. These percentages were derived from the average deposition trend in Western Europe.

Table 4.3 Constants for Al dissolution, base cation weathering rate constants and Gaines Thomas exchange constants, SO_4^{2-} sorption parameters used in ReSAM and NuCSAM

Soil layer (cm)	krEL ₁ ¹⁾ (10 ⁻⁷ m ³ kg ⁻¹ yr ⁻¹)	krEL ₂ ²⁾ (10 ⁻² kg mol _c ⁻¹)	KeAl _{ox} ³⁾ (l ² mol ⁻²)	Weathering rate ⁴⁾ constants (10 ⁻³ yr ⁻¹)				Exchange constants ⁵⁾ (mol l ⁻¹) ² x ⁻²				K _e SO _{4,ad} ⁶⁾ (l mol ⁻¹)		
				Ca	Mg	K	Na	H ⁺	Al ³⁺	Mg ²⁺	K ⁺		Na ⁺	NH ₄ ⁺
0- 10	0.58	7.5	1.0×10 ⁹	6.5	93.6	0.011	0.021	5180.0	1.0	1.60	647	8.4	1.1	0.5×10 ⁻³
10- 20	2.00	7.5	1.0×10 ⁹	6.0	73.2	0.008	0.015	57.5	26.2	2.56	3660	29.1	6.5	7.6×10 ⁻³
20- 30	5.10	7.5	1.0×10 ⁹	5.6	66.9	0.007	0.013	57.5	8.8	0.65	7470	21.2	30.7	14.9×10 ⁻³
30- 40	5.10	7.5	1.0×10 ⁹	5.4	63.7	0.006	0.010	153.0	7.4	0.42	18700	32.0	30.7	14.9×10 ⁻³
40- 60	5.10	7.5	1.0×10 ⁹	5.3	61.8	0.005	0.011	153.0	7.4	1.25	16900	36.2	30.7	14.9×10 ⁻³
60- 80	5.10	7.5	1.0×10 ⁹	6.2	51.7	0.005	0.011	153.0	26.2	1.25	16900	36.2	30.7	24.1×10 ⁻⁴
80-100	5.10	7.5	1.0×10 ⁹	10.9	25.8	0.003	0.011	153.0	26.2	1.25	16900	36.2	30.7	24.1×10 ⁻⁴

1) Derived from average soil solution concentrations of H⁺ and Al³⁺ in 1983, assuming KeAl_{ox}=3.5×10⁸ and krEL₂=7.5×10⁻²

2) The average of values given in De Vries *et al.* (1995).

3) Based on the average ion activity product for Al(OH)₃ at 90 cm over the period 1973-1991. The value given, relates to the a temperature of 25°C, which is derived from the value at an average field temperature (10°C).

4) Based on total analysis and weathering fluxes of base cations from Wesselink *et al.* (1994) and average H⁺ concentration in 1983.

5) Constants are defined with respect to Ca²⁺. Constants for H, Al, Mg, K and Na are based on average soil solution concentration measurements in 1983 and solid phase analyses in the same year. The NH₄ constant is taken from De Vries *et al.* (1995)

6) Derived from Meiwes (1979).

Table 4.4 Soil properties used for NuCSAM and ReSAM

Soil layer (cm)	ρ (kg.m ⁻³)	CEC (mmol _c kg ⁻¹)	ctAl _{ox} (mmol _c kg ⁻¹)	SSC (mmol _c kg ⁻¹)
0- 10	930	132.1	217	7.5
10- 20	1140	79.0	347	14.0
20- 30	1190	58.0	570	14.0
30- 40	1390	45.3	570	14.0
40- 60	1390	56.1	570	14.0
60- 80	1690	56.1	424	14.0
80-100	1690	75.9	424	14.0

4.4 Results and discussion

4.4.1 Validation of NuCSAM

To obtain an insight into the reliability of the model predictions, the NuCSAM results for the period 1973-1990 were compared with Solling field observations (see also Groenenberg *et al.*, 1995; Chapter 3). The validation is restricted to the Cl⁻, to validate the hydrology, Al³⁺, SO₄²⁻ and NO₃⁻ concentrations, because of their important role in soil acidification, and the Al³⁺/Ca²⁺ ratio, which is an important indicator for the adverse effects of soil acidification on roots. Results are presented for the topsoil (0-10 cm) and the subsoil (80-100 cm).

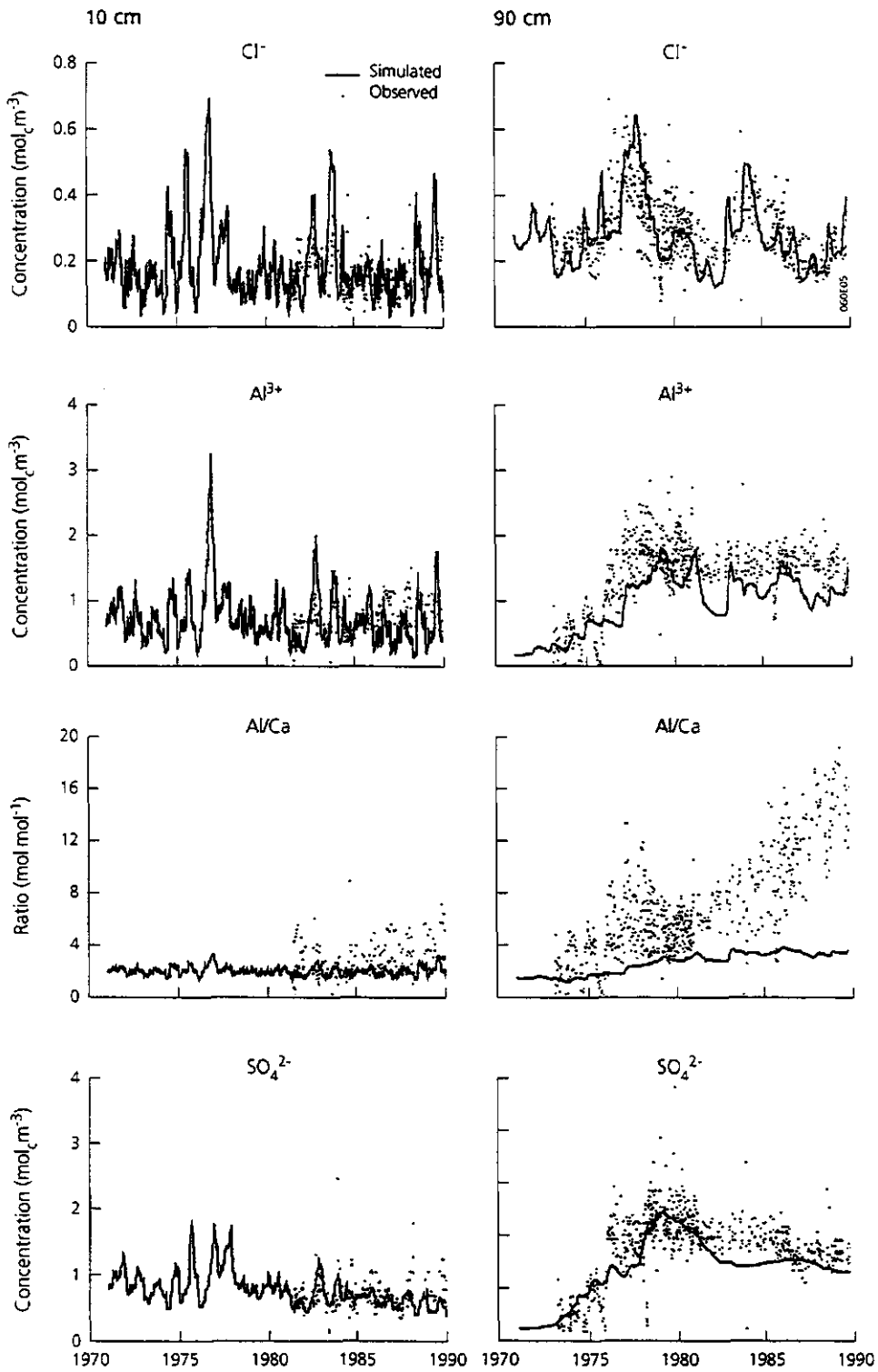
Hydrology

At the Solling site no water contents were available. Therefore, simulated and observed Cl⁻ concentrations were compared (Figure 4.1). Differences between simulated and observed Cl⁻ concentrations were rather small, both in the top soil (0-10 cm) and the subsoil (80-100 cm). Strong reduction in transpiration due to drought stress only occurred in the (extremely) dry summer of 1976 and to a lesser extent in 1982 and 1989.

Biogeochemistry

There was generally a good agreement between observed and simulated Al³⁺ concentrations for both depths (Figure 4.1). However, the sharp decline in the simulated Al³⁺ concentrations at 90 cm in 1981 was not observed. This decline, which followed the SO₄²⁻ concentration, was due to precipitation of Al hydroxide that occurs instantaneously in the model if the solution is supersaturated. Furthermore, from 1981 onwards the Al³⁺ concentrations were underestimated by the model in both the topsoil and the subsoil.

Simulated SO₄²⁻ concentrations (Figure 4.1) in the top and subsoil were in good agreement with observed concentrations. The rise of SO₄²⁻ from 1973 until 1978 was simulated by the model. To simulate this behaviour, the initial amount of sorbed SO₄²⁻ in the subsoil had to be set to one fourth of the sulphate sorption capacity. Simulated concentrations between 1981 and 1985 were too low, which corresponded with the



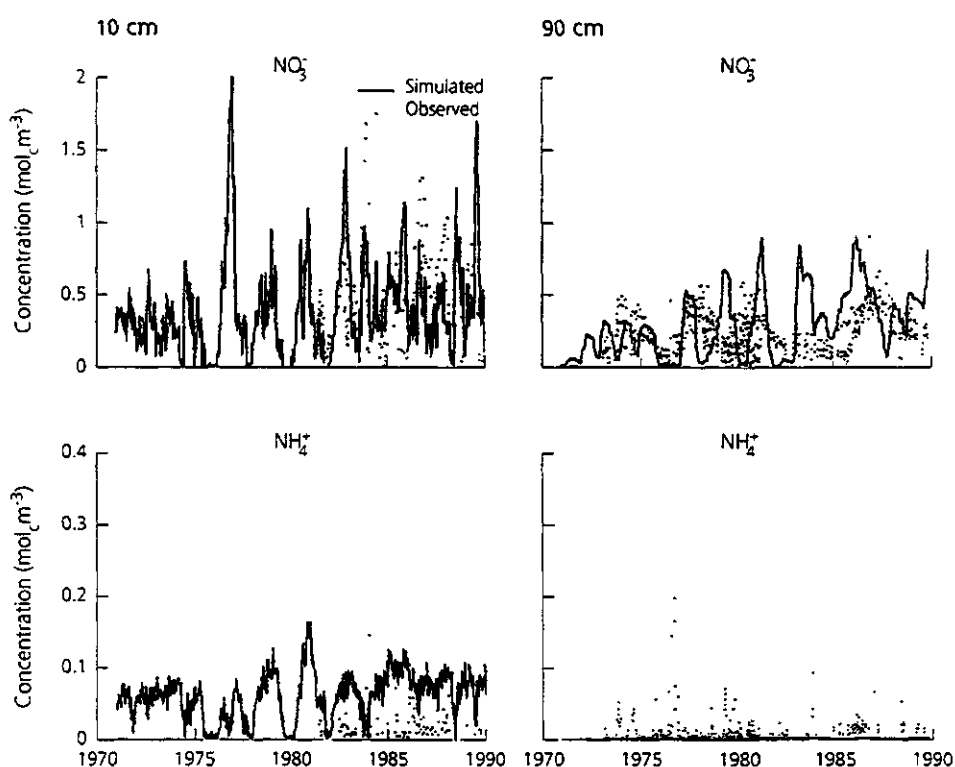


Fig. 4.1 Simulated and observed concentrations of Cl^- , Al^{3+} , Al^{3+}/Ca^{2+} ratio, SO_4^{2-} , NO_3^- and NH_4^+ at 10 cm (left-hand side) and 90 cm (right-hand side) depth

underestimation of the Al^{3+} concentration. This might be an indication that either SO_4^{2-} deposition or SO_4^{2-} desorption was underestimated during that period.

Simulated NO_3^- concentrations in the topsoil were in the range of and followed the same seasonal pattern as the observed concentrations. However, calculated concentrations in the years 1986 and 1987 were too low, while simulated peak concentrations in the subsoil were too high. The low concentrations in the period 1982-1986 were not calculated by the model.

The Al^{3+}/Ca^{2+} ratio of both the observed and the measured values followed the Al^{3+} concentration. However, the scatter in observations is much larger than with the Al^{3+} concentration. This was caused by the division of two independent, and relatively uncertain entities, resulting in an entity with a much larger uncertainty. The Al^{3+}/Ca^{2+} ratio was generally underestimated by the model, especially in the period after 1981. This was caused by the amplifying effect of an underestimated Al^{3+} and an overestimated Ca^{2+} concentration.

4.4.2 Long-term predictions with ReSAM and NuCSAM

General features

Figure 4.2 presents the flux-weighted annual average NuCSAM results and the ReSAM results for the Business as Usual (BU) scenario. Results for the Improved Environment (IE) scenario are given in Figure 4.3. Figure 4.2 and 4.3 also include the observed flux-weighted annual average values (cf Section 4.3.1).

Regarding the performance of the two models to simulate the observed concentrations and ratio in terms of the NMAE (Table 4.5), we can conclude that the results for both models are quit comparable. Inspecting the individual values of the NMAE (the closer to zero the better the predictions), results appeared to be good ($NMAE \leq 0.30$) for the Al^{3+} and SO_4^{2-} concentrations in the topsoil and in the subsoil for both models and for the NO_3^- concentration in the topsoil for NuCSAM, moderate ($0.30 < NMAE < 0.60$) for the Al^{3+}/Ca^{2+} ratio in the topsoil for both models and for the NO_3^- concentration in the topsoil and subsoil for ReSAM, and bad ($NMAE \geq 0.60$) for the Al^{3+}/Ca^{2+} ratio in the subsoil for both models and the NO_3^- concentration in the subsoil for NuCSAM.

Table 4.5 Performance of the two models during the observation period expressed as the Normalized Mean Absolute Error

	Normalized Mean Absolute Error							
	Al^{3+}		Al^{3+}/Ca^{2+}		SO_4^{2-}		NO_3^-	
	10 cm	90 cm	10 cm	90 cm	10 cm	90 cm	10 cm	90 cm
ReSAM	0.21	0.25	0.31	0.65	0.14	0.10	0.32	0.57
NuCSAM	0.30	0.21	0.33	0.64	0.16	0.15	0.26	0.70

With the IE scenario Al^{3+} concentration (Figure 4.3) strongly decreased in both the topsoil and subsoil, due to deposition reductions. With the BU scenario Al^{3+} concentration gradually increased in the subsoil. In the topsoil, however, Al^{3+} concentration decreased. In contrast to the IE scenario, this is due to a depletion of the Al hydroxide pool in topsoil. As a result of the depletion of the Al hydroxide pool, which highly determines the buffer capacity, the pH decreased (cf De Vries *et al.*, 1995).

Under the IE scenario SO_4^{2-} and NO_3^- strongly decreased in response to the decrease in atmospheric deposition. Due to SO_4^{2-} desorption and N mobilizing from the humus, there was a retardation in the concentration response, especially in the subsoil. After the period of deposition changes, the SO_4^{2-} and NO_3^- concentrations were maintained at a constant level for both scenarios.

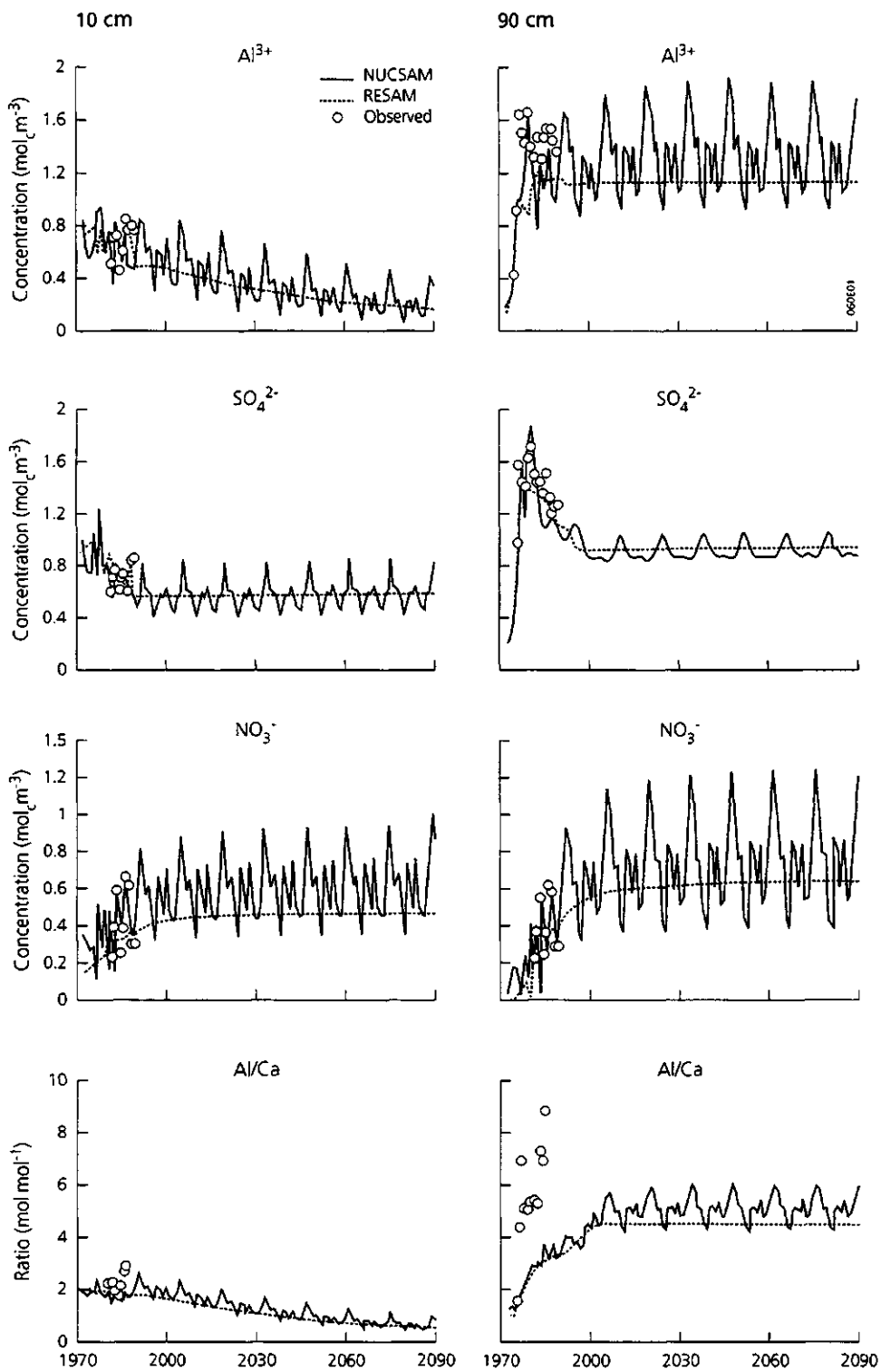


Fig. 4.2 Flux-weighted annual averaged concentrations simulated with NuCSAM and with ReSAM of Al^{3+} , SO_4^{2-} , NO_3^- , NH_4^+ and Al^{3+}/Ca^{2+} ratio at 10 cm (left-hand side) and 90 cm (right-hand side) depth, under the Business as Usual scenario. The observed flux-weighted annual averaged concentrations are also given

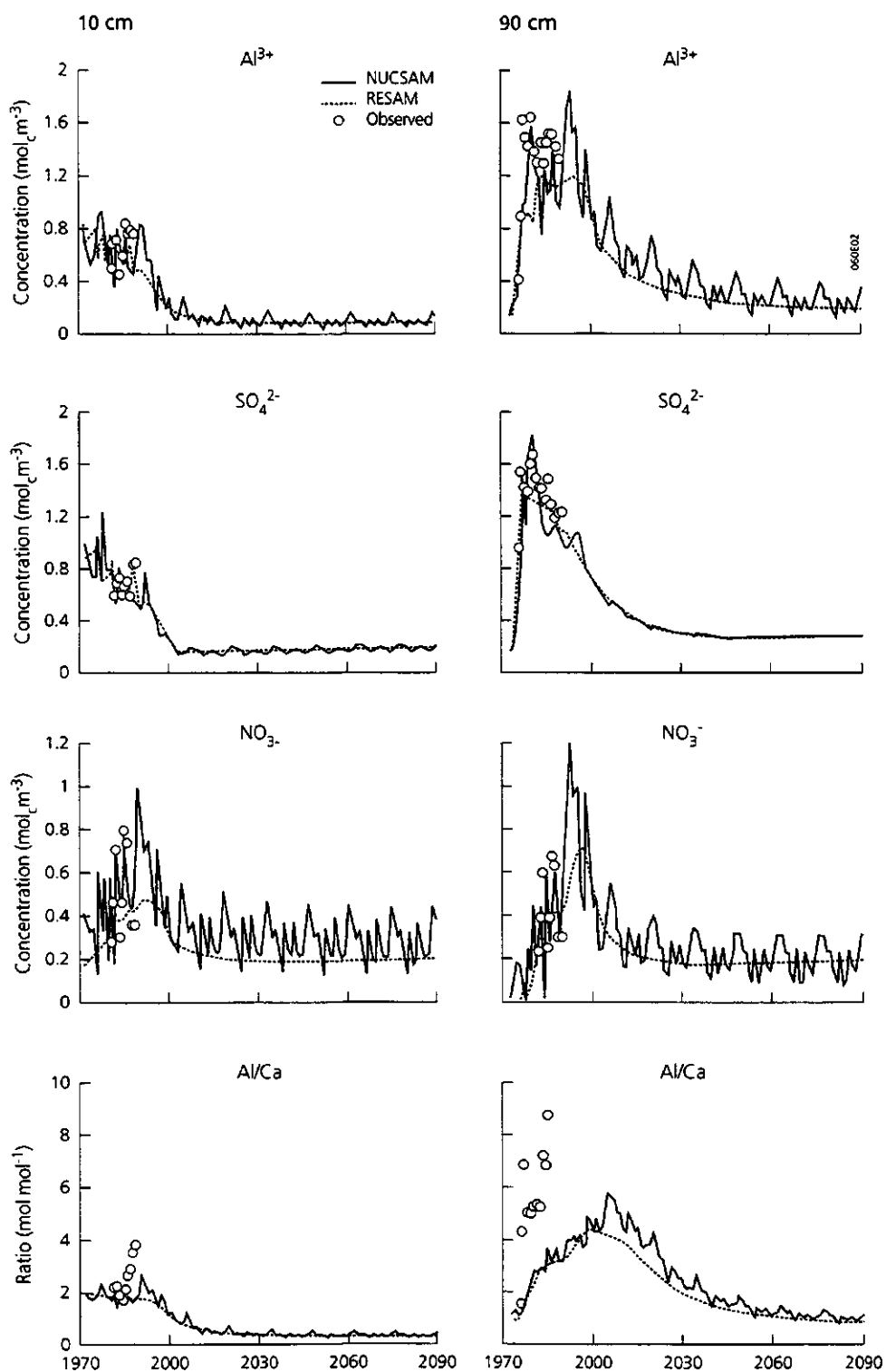


Fig. 4.3 Flux-weighted annual averaged concentrations simulated with NuCSAM and with ReSAM of Al^{3+} , SO_4^{2-} , NO_3^- , NH_4^+ and Al^{3+}/Ca^{2+} ratio at 10 cm (left-hand side) and 90 cm (right-hand side) depth, under the Improved Environment scenario. The observed flux-weighted annual averaged concentrations are also given

The molar $\text{Al}^{3+}/\text{Ca}^{2+}$ ratio in the topsoil showed a similar trend as the Al^{3+} concentration. For both scenarios the molar $\text{Al}^{3+}/\text{Ca}^{2+}$ ratio decreased below 1, which is considered a critical value. However, with the BU scenario this decrease was accompanied by a decrease in pH due to Al depletion. In the subsoil the $\text{Al}^{3+}/\text{Ca}^{2+}$ ratio gradually increased with the BU scenario. With the IE scenario the $\text{Al}^{3+}/\text{Ca}^{2+}$ ratio initially showed a severe increase between 2010 and 2030 although Al^{3+} concentration decreased. This was caused by the decrease in Ca^{2+} concentration. In the year 2090, the molar $\text{Al}^{3+}/\text{Ca}^{2+}$ ratio appeared to be slightly higher than 1, but decreased further after 2090 since the Ca^{2+} concentration was still increasing.

Differences between ReSAM and NuCSAM predictions

The agreement between flux weighted annual averaged concentration simulated by ReSAM and NuCSAM, was generally good for all presented constituents. The most remarkable difference between the two model results was that the NuCSAM outputs were fickle while the ReSAM outputs were strongly smoothed. This is, of course, inherent to the characters of the models; daily based versus annual average based. During the period 1970-1990, however, the ReSAM results also showed a slightly fickle behaviour, which was caused by using the measured yearly values for deposition during this period.

Comparing the NuCSAM results for the two scenarios in general, it was striking that seasonal variability under the IE scenario was much smaller than under the BU scenario. This especially holds for the SO_4^{2-} concentration in the subsoil, where eventually all seasonal variability was exterminated. To a lesser extent this phenomenon occurred for the SO_4^{2-} concentration in the topsoil and the Al^{3+} concentration and the $\text{Al}^{3+}/\text{Ca}^{2+}$ ratio in both considered soil layers. This was caused by the relative increase in importance of SO_4^{2-} sorption and cation exchange at lower concentration levels, resulting in a stronger buffering of concentration changes. This also explained that the seasonal variability of NO_3^- was the same for both scenarios, which is difficult to see in Figure 4.2 and 4.3. However, this was checked by normalizing the NuCSAM concentrations by dividing them by the concentrations calculated with ReSAM, which showed clearly that the seasonal variability under both scenarios was comparable.

Comparison of the long-term results of the models shows that trends for both scenarios were very similar. For most model outputs the NuCSAM result was oscillating around the ReSAM result. The $\text{Al}^{3+}/\text{Ca}^{2+}$ ratio in the subsoil, however, as predicted by ReSAM was lower from 2000 onwards for both scenarios. The maximum deviation occurred during the period of deposition reductions, between 2000 and 2010 for the IE scenario. This deviation was mainly caused by a quicker response of the adsorption complex in the ReSAM model to a change in deposition, resulting in a shorter time-delay. However, during the periods with constant deposition, when a new steady-state between deposition and the adsorption complex was achieved, the correspondence in $\text{Al}^{3+}/\text{Ca}^{2+}$ ratios improved.

Cumulative leaching fluxes of Al^{3+} , SO_4^{2-} , NO_3^- and NH_4^+ over a period of 120 years from both considered soil layers as predicted by ReSAM and NuCSAM are given in Figure 4.4 and 4.5. Results show that the leaching fluxes were similar for SO_4^{2-} . The

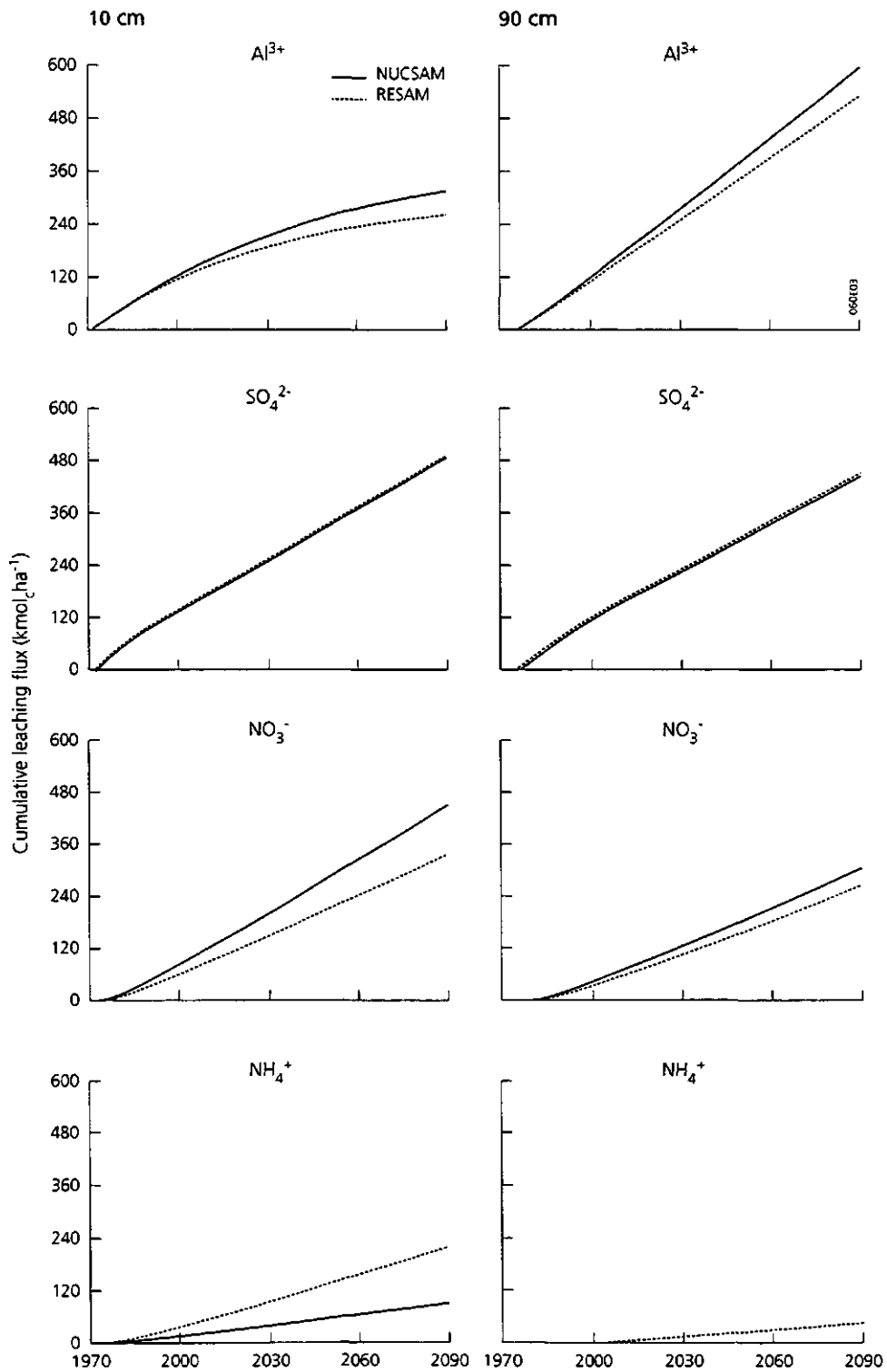


Fig. 4.4 Cumulative leaching fluxes of Al^{3+} , SO_4^{2-} , NO_3^- and NH_4^+ at 10 cm (left-hand side) and 90 cm (right-hand side) depth as simulated with NuCSAM and ReSAM, using the Business as Usual scenario

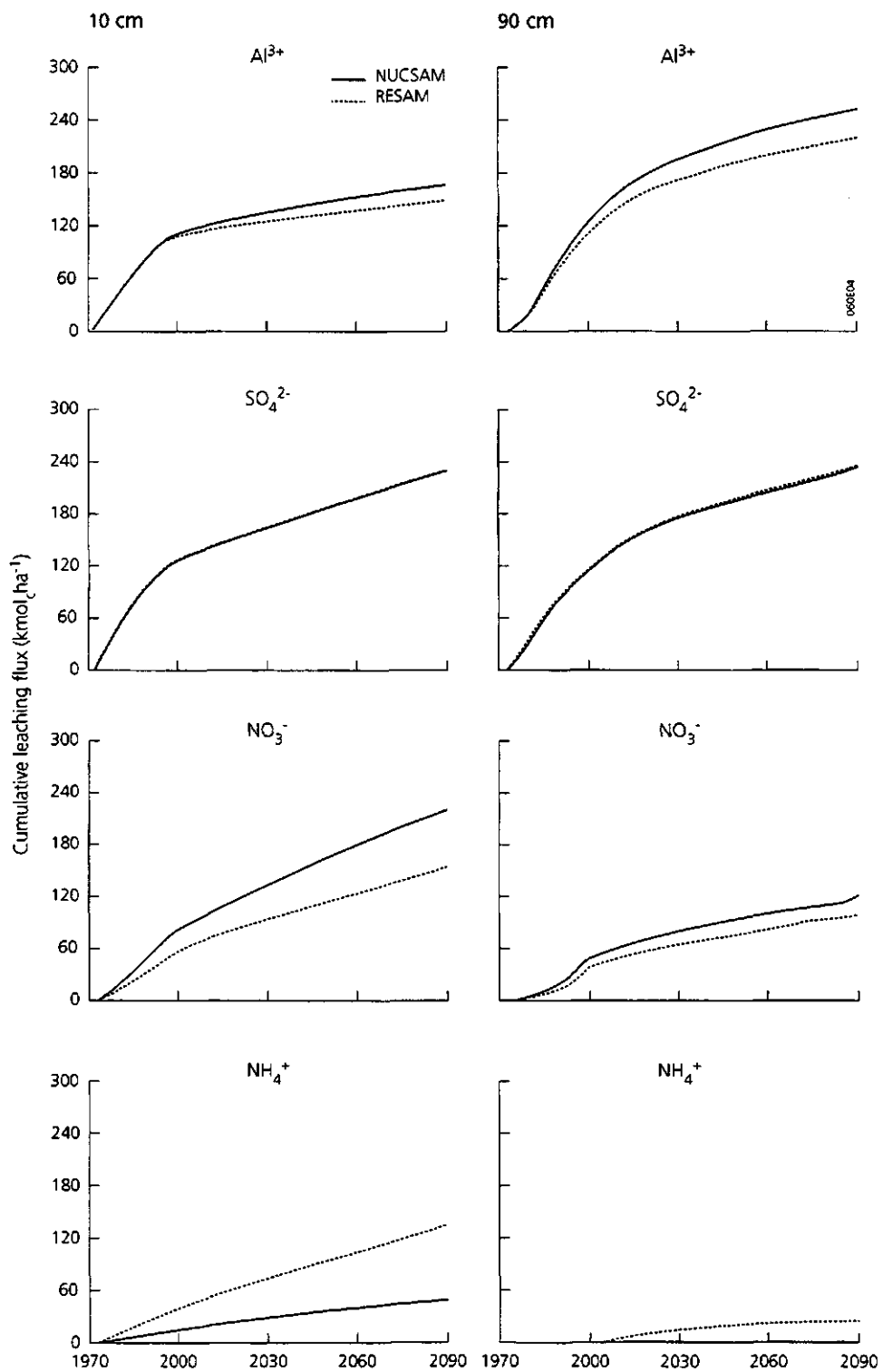


Fig. 4.5 Cumulative leaching fluxes of Al^{3+} , SO_4^{2-} , NO_3^- and NH_4^+ at 10 cm (left-hand side) and 90 cm (right-hand side) depth as simulated with NuCSAM and ReSAM, using the Improved Environment scenario

Al^{3+} and NO_3^- leaching fluxes predicted by ReSAM, however, were clearly lower than the NuCSAM fluxes, for both scenarios and both depths. The lower Al^{3+} and NO_3^- fluxes predicted by ReSAM were mainly due to a lower nitrification flux resulting in a lower Al^{3+} mobilization, lower NO_3^- leaching and higher NH_4^+ leaching (cf Figure 4.4 and 4.5). Although the neglect of seasonal variability causes an additional uncertainty in model results, it is acceptable for long-term predictions.

It must be noticed that part of the differences between the two models originates from the way the models were parameterized. All parameters used in ReSAM were exactly the same as those used in NuCSAM. However, if the models would have been compared as described by Rose *et al.* (1991), who performed a so-called input mapping procedure in order to specify consistent input values for each of the models, the parameterization of ReSAM would be different. Especially, the nitrification rate parameter ($kr_{ni\ mx}$) of ReSAM would be adjusted to a higher value, resulting in lower NH_4^+ and higher NO_3^- concentrations, and (through a higher acid production) to higher Al^{3+} concentrations. This would lead to more corresponding leaching fluxes of Al^{3+} , NO_3^- and NH_4^+ than those expressed in Figures 4.4 and 4.5.

Regarding the effect of time variability, this study showed that time resolution has only a rather small effect on the uncertainty in long-term (> 100 year) soil acidification. On a smaller time scale (10-50 years), during strong changes in deposition, the effect is more significant, especially when the $\text{Al}^{3+}/\text{Ca}^{2+}$ ratio is considered. However, when focusing on a relatively small time scale (< 1 year) to judge daily or seasonal values of concentrations or ratios it is clear that it is absolutely necessary to consider seasonal variability.

4.5 Conclusions

Regarding the validation of NuCSAM on the Solling site, it can be concluded that the model reproduces the main features of the concentration variations over time for most concentrations. In particular:

- (i) the agreement between measured and simulated pressure heads and Cl concentrations gives confidence in the water fluxes calculated by the model;
- (ii) trends and dynamics of the concentrations of SO_4^{2-} and Al^{3+} are reproduced well;
- (iii) simulated NO_3^- concentrations in the subsoil are too high which is of concern since NO_3^- leaching is important for the determination of critical N loads;
- (iv) simulated $\text{Al}^{3+}/\text{Ca}^{2+}$ ratios in the subsoil are too low which is of concern since the $\text{Al}^{3+}/\text{Ca}^{2+}$ ratio is important for the determination of critical acid loads.

Regarding the capability of ReSAM to simulate the observed flux-weighted annual averaged concentrations (and ratios) we can conclude that this is comparable or even better than NuCSAM.

Because the uncertainties in long-term predictions of soil and soil solution response induced by neglecting seasonal variability are rather small, it can be concluded that ReSAM, which neglects seasonal variability, is acceptable for making long-term annual

average predictions. A model such as NuCSAM proved to be a valuable link between relatively short data records and long term predictions generated with ReSAM.

Acknowledgements

This work was carried out with financial support from the Dutch Priority Programme on Acidification. The authors would like to thank Dr. M. Bredemeier from the University of Göttingen for the provision of the Solling data.

References

- Belmans, C., Wesseling, J.G. and Feddes, R.A.: 1983, *J. Hydrol.* **63**, 271.
- Bredemeier, M, A. Tiktak and C. van Heerden: 1995, *Ecol. Model.* **83**, 7.
- Chen, C.W., Gherini, S.A., Mok, L., Hudson, R.J.M., and Goldstein, R.A.: 1983 *The integrated Lake-Watershed Acidification Study Volume 1: Model principles and application procedures*, EPRI EA - 3221, Volume 1, Project 1109-5, Final report.
- Cosby, B.J., Hornberger, G.M., Galloway, J.N. and R.F. Wright: 1985, *Water Resour. Res.*, **21**, 51.
- De Vries, W., Posch, M. and J. Kämäri, J.: 1989, *Water, Air and Soil Pollut.* **48**, 349.
- De Vries, W., Kros, J. Van der Salm, C. and Voogd, J.C.: 1994, *Water Air and Soil Pollut.* **75**, 1.
- De Vries, W., Kros, J. and Van der Salm, C.: 1995, *Ecol. Model.* **79**, 231.
- Georgakakos, K.P., Valle-Filho, G.M., Nikolaidis, N.P. and Schnoor, J.L.: 1989, *Water Resour. Res.* **25**, 1511.
- Groenenberg, E.J., Kros, J., Van der Salm, C. and De Vries, W.: 1995, *Ecol. Model.* **83**, 97-107.
- Groenendijk, P.: in prep, *The calculation of complexation, adsorption, precipitation and weathering reactions in a soil-water system with the geochemical model EPIDIM*. Wageningen. DLO Winand Staring Centre Report nr. 70.
- Meiwes, K.J.: 1979, *Der Schwefelhaushalt eines Buchenwald- und eines Fichtenwaldökosystem im Solling*. Göttinger Bodenkundliche Berichte, 60.
- Rose, K.A., Cook, R.B., Brenkert, A.L., Gardner, R.H. and J.P. Hettelingh: 1991, *Water Resour. Res.* **27**, 2577.
- Van der Salm, C., J. Kros, J.E. Groenenberg, W. de Vries and G.J. Reinds, 1995: Validation of soil acidification models with different degrees of process aggregation on an intensively monitored spruce site, in Trudgill, S. (ed.), *Solute modelling in catchment systems*, Wiley, Chichester:327-346.
- Warfvinge, P. and Sandén, P.: 1992: Sensitivity analysis, in Sandén, P. and Warfvinge, P. (eds.), *Modeling groundwater response to acidification*, SMHI, Norrköping, Sweden.
- Wesselink, L.G., Van Grinsven, J.J.M. and Grosskurth, G.: 1994, *Soil Sci. Soc. Am. J.* **39**, 91 (special publication).

Chapter 5 is a slightly revised version of:

Salm, C. van der, J. Kros, J.E. Groenenberg, W. de Vries and G.J. Reinds, 1995.
Validation of soil acidification models with different degrees of process aggregation
on an intensively monitored spruce site. In: S. Trudgill (Ed.): Solute modelling in
catchment systems, John Wiley, Chichester: 327-346.

5 Application of soil acidification models with different degrees of process description on an intensively monitored spruce site

Abstract

A one-layer (SMART) and a multi-layer (ReSAM) soil acidification model with a resolution of one year and a multi-layer soil acidification model with a temporal resolution of one day (NuCSAM) were applied to an intensively monitored spruce site at Solling, Germany. Simulated concentrations and leaching fluxes were compared with measured values at this site during the period 1973-1989. The major aim was to study the influence of model simplifications, especially with respect to process formulation and the reduction of temporal and vertical resolution, on the simulation of soil solution concentrations.

Input parameters were derived from measured data at the Solling site. Values for the one-layer model SMART were derived by depth averaging the measured amounts and concentrations.

Results showed that all models were able to simulate most of the concentrations during the examined period reasonably. However, the one-layer model, SMART, had some difficulties to simulate strong changes in soil solution concentrations due to a lower retardation in the soil system. When applying the one-layer model SMART care should be taken at shallow depth as mineralization was not included in this model. This caused, for example, an underestimation of NO_3 and base cation concentrations at 10 cm depth. ReSAM simulated a somewhat stronger rise and fall in base cation and SO_4 concentrations in the subsoil, which is caused by slight differences in hydrology.

5.1 Introduction

At present various dynamic simulation models exist to predict acidification of soil and surface waters. These models have been designed for use on a continental to national scale, such as MAGIC (Cosby *et al.*, 1985) and SMART (De Vries *et al.*, 1989), or on a national to regional scale, such as ReSAM (De Vries *et al.*, 1995a) or for use on a catchment or site scale, such as ILWAS (Chen *et al.*, 1983) and NuCSAM (Chapter 2, Groenenberg *et al.*, 1995; Chapter 3).

Models designed for regional predictions tend to be more simplified than site scale models to minimize input requirements. These simplifications can consist of i) the use of less complex/detailed process formulations, ii) the reduction of temporal resolution, for example using an annual time resolution and thereby neglecting variability within a year of both model input and processes and iii) the reduction in vertical resolution, by using a smaller number of soil compartments. All these simplifications may cause errors in the predictions. Georgakos *et al.* (1989), for example, found that natural day-to-day variability in meteorological variables significantly affects long-term predictions of lake and stream acidification.

The objective of this study is to characterize the effect of model simplifications on soil solution response, with emphasis on the influence of temporal and vertical resolution. Therefore we compared the results derived with a one layer model SMART (Simulation Model for Acidification's Regional Trends), the multi layer models ReSAM (Regional Soil Acidification Model), with a temporal resolution of one year and NuCSAM (Nutrient Cycling and Soil Acidification Model), with a temporal resolution of one day, with measured concentrations of an intensively monitored spruce site at Solling, Germany. At this site inputs, concentrations and amounts of elements in the soil system have been measured continuously for more than twenty years and were completed by plant physiological, hydrological, micrometeorological and soil biological monitoring programmes during that time.

5.2 Models used

The three considered soil acidification models are dynamic simulation models. SMART is a one-layer model, whereas ReSAM and NuCSAM distinguish a litter layer and several mineral soil layers. The temporal resolution of SMART and ReSAM is one year, whereas NuCSAM has a temporal resolution of one day. Although, ReSAM has a temporal resolution of one year, the model uses a numerical time step of 5 days to avoid oscillations. ReSAM and NuCSAM simulate the major biogeochemical processes occurring in the canopy, litter layer and mineral horizons. SMART distinguishes only one soil layer and litterfall, root decay and mineralization are not explicitly taken into account. Only a net uptake rate of N and base cations and a net N-immobilization rate are included. In ReSAM and NuCSAM a description for litterfall, root decay and mineralization is incorporated in the models. An overview of the considered processes in the three models is given in Table 5.1. Annex 2 gives a brief overview of the model formulations.

Table 5.1 Overview of the considered processes

Process	SMART	ReSAM	NuCSAM
Canopy interaction	-	+	+
Growth uptake	+	+	+
Maintenance uptake	-*	+	+
Litterfall	-*	+	+
Root decay	-*	+	+
Mineralization	-*	+	+
(De)Nitrification	+	+	+
Carbonate weathering	+	+	+
Silicate weathering	+	+	+
Al hydroxide weathering	+	+	+
Cation exchange	+	+	+
Sulphate adsorption	+	+	+

* not explicitly included in SMART, instead overall N immobilization was included.

5.2.1 SMART

SMART simulates the concentrations of Al, divalent base cations (Ca + Mg), monovalent base cations (Na + K), NH_4 , SO_4 and NO_3 in the soil solution. In SMART most of the geochemical processes are incorporated (weathering, cation exchange, sulphate adsorption). However, only a (very) limited number of biological processes are taken into account (Table 5.1).

Nutrient cycling processes are not included because the model is based on the assumption that the amount of organic matter is in equilibrium. However, net N immobilization is taken into account to include the effect of an increase in N content in organic matter due to high N deposition.

Cation exchange, sulphate adsorption, dissolution of carbonates and Al-hydroxides are treated as equilibrium reactions (Annex 2). Weathering of base cations and (de)nitrification are described as first-order reactions. An overview of a former version of the model is given in De Vries *et al.*; 1989. Since then the description of N dynamics has been changed (De Vries *et al.*, 1995b).

5.2.2 ReSAM

In contrast to SMART, ReSAM not only simulates the major geochemical processes but biochemical processes occurring in the forest canopy, litter layer and mineral soil horizons as well (Table 5.1).

Foliar exudation, litterfall, root decay, nitrification, denitrification, protonation of organic anions and weathering are described by first-order reactions. Foliar uptake is considered to be a fraction of the dry atmospheric deposition. Root uptake is assumed to be equal to the sum of litterfall, foliar exudation and root decay minus foliar uptake plus a given net growth. Net growth is described by a logistic function. Root uptake per soil layer is assumed to be proportional to the fraction of roots in each soil layer. The dissolution of Ca and Al from carbonates and hydroxides, are described with a first-order rate equation and an Elovich equation respectively, which are both rate-limited by the degree of undersaturation. If supersaturation occurs, the Ca or Al concentration is set to equilibrium. Cation exchange and sulphate sorption are treated as equilibrium reactions, using Gaines Thomas exchange equations and a Langmuir isotherm, respectively. Speciation/dissolution of inorganic C is computed from equilibrium equations using a constant value for $p\text{CO}_2$. A complete overview of the model structure of ReSAM is given in De Vries *et al.* (1995a)

5.2.3 NuCSAM

NuCSAM has been derived from the ReSAM model. The main difference between the two models is the temporal resolution used, NuCSAM has a temporal resolution of one day instead of one year. The version of NuCSAM used for this comparison uses practically the same biogeochemical process formulations as ReSAM. However, in contrast to ReSAM, (i) litterfall, root decay and root uptake are distributed over the year by given monthly coefficients and (ii) both up- and downward transport of solutes is taken into account.

5.3 Methods and data

5.3.1 Methods

General Approach

To compare differences in model predictions, due to differences in process aggregation, temporal or vertical resolution objectively, it is necessary to minimize differences in parameterization. Data for the models were derived from the Solling dataset (Bredemeier *et al.*, 1995). In those cases where the models use the same state variables and process parameters with the same vertical or temporal resolution, we simply used the same values for both models. Parameters for SMART were derived by depth averaging the values which were used for ReSAM and NuCSAM (input mapping: Rose *et al.*, 1991). Annual deposition and water fluxes, which are input to the model ReSAM and SMART, were derived by accumulating the daily NuCSAM values to annual values.

Vertical configuration and simulation period

At the Solling site NuCSAM and ReSAM considered a litter layer of 7 cm (at the start of the simulations) and seven mineral soil layers up to a depth of 90 cm (Table 5.4). For SMART, in which one mineral soil compartment is distinguished, two simulations were run: (i) with a mineral soil layer of 10 cm thickness and (ii) with a layer of 90 cm thickness.

All models were run for the period 1971-1990. ReSAM and NuCSAM used the period 1961-1970 as an initialization period to estimate solute concentrations in 1970 and to equilibrate solute concentrations with exchangeable cations and adsorbed SO_4 . During that period, amounts of exchangeable cations and adsorbed amounts of SO_4 were continuously updated while cation amounts in primary minerals and Al hydroxides were kept constant.

SMART did not use an initialization period. Initial amounts of base cations were input to the model. Initial adsorbed amounts of SO_4 were calibrated on the amounts simulated by NuCSAM/ReSAM in 1970.

Model adaptations

In regional applications, SMART and ReSAM use annual average hydrological fluxes which are constant throughout the simulation period. This study focuses on the influence of differences in biogeochemical process descriptions and their vertical and temporal resolution (one day versus one year). Accordingly, for this application SMART and ReSAM were slightly adapted to account for variations in hydrological fluxes between the years.

The SMART model is normally applied to calculate concentrations at the bottom of the root zone. To apply the SMART model at shallow depth (10 cm), the calculation of N-immobilization was slightly adapted. In the standard version of SMART, N-immobilization is supposed to occur in the upper 20 cm of the soil. For the simulation of concentrations at 10 cm depth, the total N immobilization flux was multiplied by the ratio of the amount of organic C in the considered layer and the amount up to 20 cm depth.

Model comparison

NuCSAM simulates daily concentrations and leaching fluxes, whereas SMART and ReSAM simulated flux-weighted annual average concentrations and annual leaching fluxes. A comparison of simulated data of SMART and ReSAM with measured data is complicated as flux-weighted annual average concentrations can not be measured. A comparison of results of the three models with measured data, on the same basis, can be made by comparing: (i) measured concentrations (once a month) with simulated values. In this case monthly concentrations for ReSAM and SMART were derived by linear interpolation between annual values; (ii) estimated flux-weighted annual average measured concentrations (or leaching fluxes) with simulated values. 'Measured' leaching fluxes were calculated by multiplying measured concentrations with (monthly) simulated water fluxes (cf Section 5.3.2). Flux-weighted annual average concentrations were derived by dividing the 'measured' leaching flux by the annual water fluxes.

In this study a combined approach was used: simulated concentrations were compared with measured concentrations (according to i) and simulated cumulative annual leaching fluxes were compared with (calculated) measured annual leaching fluxes. A comparison of measured concentrations with simulated concentrations gives a good impression of the performance of the models and the ability of the models to simulate trends and extreme values. A comparison of cumulative fluxes shows whether the models tend to underestimate or overestimate total leaching fluxes for the simulation period.

To give more objective information concerning the performance of the models two statistical measures were calculated: the Normalized Mean Absolute Error (NMAE) and the Coefficient of Residual Mass (CRM) (Table 5.2). NMAE quantifies the average deviation between model prediction and measurements. CRM gives an indication of the tendency of the model to under- or overestimate (negative value) the measured data. NMAE and CRM for the three models were calculated using monthly concentrations for model results and measurements.

Table 5.2 Statistical measures for evaluation of model results

Measure	Symbol	Formulation	Optimum
Normalized Mean Absolute Error	NMAE	$\frac{\sum_{i=1}^N P_i - O_i }{N \cdot \bar{O}}$	0
Coefficient of Residual Mass	CRM	$\frac{\sum_{i=1}^N O_i - \sum_{i=1}^N P_i}{\sum_{i=1}^N O_i}$	0

P_i is the modelled value, O_i is the observed value, \bar{O} the average of the observations and N the number of observations.

5.3.2 Hydrological data

For all models used, hydrological fluxes and water contents were calculated by the model SWATRE (Belmans *et al.*, 1983). This model provides a finite difference solution to Richard's equation. The version which is used here (Groenenberg *et al.*, 1995; Chapter 3), differs from the original model with respect to the formulation of interception evaporation and root uptake. Furthermore a snow module was added. Root uptake was divided over the different soil layers according to a given fixed root distribution.

Drainage fluxes, root uptake fluxes and water contents calculated by SWATRE were directly used by NuCSAM. ReSAM and SMART use annual values and discard year to year changes in storage of soil water. Annual root uptake fluxes were derived by accumulating the daily root uptake fluxes to annual values. To keep water contents constant throughout the simulation period, annual drainage fluxes were calculated by subtracting the root uptake fluxes from the input flux for each layer. For use in ReSAM, water contents for each layer were averaged over the simulation period. The data for SMART were derived by depth averaging the water contents which were used for ReSAM. An overview of the main hydrological fluxes and water contents is given in Table 5.3.

Table 5.3 Average drainage fluxes and water contents used in NuCSAM, ReSAM and SMART

Soil layer (cm)	Average drainage fluxes (cm a ⁻¹)			Average moisture content (m ³ m ⁻³)	
	NuCSAM	ReSAM	SMART	NuCSAM/ ReSAM	SMART
0-10	73.5	73.6	73.6	0.398	0.398
10-20	70.0	70.1	-	0.394	-
20-30	64.0	64.0	-	0.362	-
30-40	55.6	55.7	-	0.363	-
40-60	47.6	47.7	-	0.367	-
60-80	42.9	43.0	-	0.336	-
80-90 ¹⁾	40.9	41.0	41.0	0.338	0.362

¹⁾ SMART soil layer 0-90 cm.

5.3.3 Geochemical data

Data used in NuCSAM and ReSAM

Geochemical data for NuCSAM and ReSAM (Groenenberg *et al.*, 1995; Chapter 3, Kros *et al.*, 1995; Chapter 4) were directly derived from the Solling dataset (Bredemeier *et al.*, 1995). An overview of the main parameters is given in Table 5.5 to 5.7. Gaines Thomas exchange constants (for all three models) were based on average soil solution concentrations measurements in 1983 and solid phase analyses in the same year. Sulphate adsorption constants for NuCSAM and ReSAM were directly derived from Meiwes (1979).

Weathering fluxes of primary minerals in NuCSAM and ReSAM were described by a first-order equation (Annex 2). Rate constants for this equation (Table 5.5) were derived from a budget study (Wesselink *et al.*, 1994). Dissolution parameters of Al-hydroxides (Elovich equation, Annex 2) in ReSAM and NuCSAM, are given in Table 5.5 together with their derivation.

SMART

Table 5.4 Soil properties used for NuCSAM, ReSAM and SMART

Soil layer (cm)	ρ (kg m ⁻³)	CEC (mmol _c kg ⁻¹)	ctAl _{ox} (mmol _c kg ⁻¹)	SSC ⁵⁾
NuCSAM and ReSAM				
0-10	930	132.14	96.5	0.99
10-20	1140	78.95	96.5	4.46
20-30	1190	57.98	185.3	4.46
30-40	1390	45.32	185.3	4.46
40-60	1390	56.12	185.3	4.46
60-80	1690	56.12	175.5	6.70
80-90	1690	75.90	93.7	6.70
SMART				
0-10	930	132.14	96.5	0.99
0-90	1389	78.95	140.0	5.05

Most data for SMART were derived by depth averaging the data which were used for NuCSAM and ReSAM (Table 5.4 and 5.5). Some parameters which were only used in SMART were directly obtained from the Solling dataset. Soil properties which were used in SMART, i.e. bulk density, CEC, sulphate sorption capacity (SSC), Al (hydr)oxide content (Table 5.4) were derived by depth averaging the data used in NuCSAM and ReSAM (Table 5.4). To calculate Gaines- Thomas exchange constants for SMART (Table 5.7) concentrations and solid phase analyses were depth averaged for the 10 cm and 90 cm soil compartment. A Depth weighted sulphate adsorption constant for SMART was derived as follows: first adsorbed amounts of sulphur were calculated for all layers, considered in NuCSAM/ReSAM, using a Langmuir equation (Annex 2) and the sulphate adsorption constants from Meiwes (1979). In calculating these amounts we assumed the same range in SO_4 concentrations in the soil solution with depth. Next the calculated adsorbed amounts were depth weighted. Finally the depth weighted sulphate adsorption constant was derived by fitting the depth weighted adsorbed SO_4 amounts against the SO_4 concentration range considered.

In SMART weathering fluxes are input to the model and were directly derived from the above mentioned budget study. In SMART dissolution of Al-hydroxide is described by equilibrium with an Al-hydroxide. Solubility products for the Al-hydroxide at 10 and 90 cm depth were derived from average soil solution concentrations of H and Al in 1983 at these depths. The solubility product for Al-hydroxide at 90 cm depth was also used in ReSAM and NuCSAM to calculate the Al concentration at equilibrium.

5.3.4 Biological data

An overview of the biological data and their derivation is given in Table 5.6. The parameters for N cycling in NuCSAM/ReSAM and SMART were derived independently from the Solling data set as the process description in the models is different. An important difference does exist in the parameterization of the nitrification process between ReSAM/NuCSAM and SMART, although parameters for both models were based on an input-output budget (Table 5.6). ReSAM/NuCSAM use an overall nitrification rate which is reduced by moisture content, pH and organic matter content. For the simulations with SMART separate nitrification fractions, based on input-output budgets, were used for the topsoil and the subsoil. The relationship between moisture content, pH, organic matter content and nitrification rate, which was used in NuCSAM/ReSAM was not calibrated on the site data.

Growth uptake in NuCSAM and ReSAM was calculated by multiplying a given (logistic) growth rate (Annex 2) by the element content in 1968 in stems and branches respectively. Element contents were assumed constant with exception of the N content. N content is calculated with a linear relationship between N content and N deposition. N content is minimal at a N deposition of $1500 \text{ kmol}_c \text{ ha}^{-1} \text{ a}^{-1}$ and maximal at a N deposition of $7000 \text{ kmol}_c \text{ ha}^{-1} \text{ a}^{-1}$. The growth uptake fluxes for SMART are input to the model. Growth uptake fluxes at 90 cm depth were derived by multiplying the growth

Table 5.5 Elovich constants for Al dissolution, base cation weathering rate constants and Gaines Thomas exchange constants, SO_4 sorption parameters used in the simulation by NuCSAM and ReSAM

Soil layer (cm)	$krEL_1^{-1}$ ($10^{-7} m^3 kg^{-1} yr^{-1}$)	$krEL_2^{-2}$ ($10^{-2} kg mol_c^{-1}$)	$KeAl_{ox}^{3-}$ ($l^2 mol^{-2}$)	Weathering rate ⁴⁾ constants ($10^{-3} yr^{-1}$)			Exchange constants ⁵⁾ ($mol l^{-1} yr^{-2}$)					$KeSO_4^{ad}$ ($l mol^{-1}$) ⁶⁾		
				Ca	Mg	K	Na	H ⁺	Al ³⁺	Mg ²⁺	K ⁺		Na ⁺	NH ₄ ⁺
0- 10	0.58	7.5	1.0×10^9	6.5	93.6	0.011	0.021	5180.0	1.0	1.60	647	8.4	1.1	0.5×10^{-3}
10- 20	2.00	7.5	1.0×10^9	6.0	73.2	0.008	0.015	57.5	26.2	2.56	3660	29.1	6.5	7.6×10^3
20- 30	5.10	7.5	1.0×10^9	5.6	66.9	0.007	0.013	57.5	8.8	0.65	7470	21.2	30.7	14.9×10^3
30- 40	5.10	7.5	1.0×10^9	5.4	63.7	0.006	0.010	153.0	7.4	0.42	18700	32.0	30.7	14.9×10^3
40- 60	5.10	7.5	1.0×10^9	5.3	61.8	0.005	0.011	153.0	7.4	1.25	16900	36.2	30.7	14.9×10^3
60- 80	5.10	7.5	1.0×10^9	6.2	51.7	0.005	0.011	153.0	26.2	1.25	16900	36.2	30.7	24.1×10^4
80-100	5.10	7.5	1.0×10^9	10.9	25.8	0.003	0.011	153.0	26.2	1.25	16900	36.2	30.7	24.1×10^4

1) Derived from average soil solution concentrations of H⁺ and Al³⁺ in 1983, assuming $KAl_{ox} = 3.5 \times 10^8$ and $krEL_2 = 7.5 \times 10^{-2}$

2) The average of values given in De Vries *et al.* (1995c).

3) Based on the average ion activity product for Al(OH)₃ at 90 cm over the period 1973-1991. The value given, relates to the a temperature of 25°C, which is derived from the value at an average field temperature (10°C).

4) Based on total analysis and weathering fluxes of base cations from Wesselink *et al.* (1994) and average H⁺ concentration in 1983.

5) Constants are defined with respect to Ca²⁺. Constants for H, Al, Mg, K and Na are based on average soil solution concentration measurements in 1983 and solid phase analyses in the same year. The NH₄ constant is taken from De Vries *et al.* (1995a)

6) Derived from Meiwes (1979).

rates of stems and branches with the element content in stems and branches, using the same values and the formulations as used by NuCSAM/ReSAM. Growth uptake fluxes at 10 cm depth were derived by multiplying the total growth uptake fluxes by the fraction of roots in the upper 10 cm.

Table 5.6 Values for soil-layer independent model parameters used in the simulation based on the Solling dataset (Bredemeier *et al.*, 1995)

Process	Parameter	Unit	Value	Model
Foliar uptake ¹⁾	$frNH_{4, fu}$	-	0.11	NuCSAM, ReSAM
	frH_{fu}	-	0.33	NuCSAM, ReSAM
Foliar exudation ¹⁾	$frCa_{fe}$	-	0.49	NuCSAM, ReSAM
	$frMg_{fe}$	-	0.09	NuCSAM, ReSAM
	frK_{fe}	-	0.42	NuCSAM, ReSAM
Tree growth ²⁾	$krgrl$	a ⁻¹	0.09	NuCSAM, ReSAM, SMART input
	A_{stmax}	kg ha ⁻¹	2.5×10 ⁵	NuCSAM, ReSAM, SMART input
	t_{05}	a	66.0	NuCSAM, ReSAM, SMART input
Litterfall ³⁾	k_{lf}	a ⁻¹	0.19	NuCSAM, ReSAM
Nitrification ⁴⁾	$k_{ni,max}$	a ⁻¹	100.0	NuCSAM, ReSAM
	$frni$	-	0.88	SMART 10 cm
	-	-	0.98	SMART 90 cm
Denitrification ⁵⁾	$frde$	-	0.10	SMART
N immobilization ⁶⁾	C/N	-	19.5	SMART
Al dissolution ⁷⁾	KAl_{ox}	l ² mol ⁻²	3.5×10 ⁸	NuCSAM, ReSAM

1) Based on average throughfall and deposition data over the period 1974 - 1990

2) Derived by curve fitting of the biomass measurements.

3) Average needlefall rate over the period 1967-1973, taking into account that 92.5% of the litterfall is needlefall.

4) $k_{ni,max}$ is derived from average throughfall and mineralization fluxes over the period 1970-1985, assuming that all mineralized N is released as NH_4^+ . $frni$ is derived from average throughfall and average drainage fluxes and calculated average root uptake fluxes for the period 1973 - 1990

5) Derived from De Vries *et al.* (1995b).

6) Based on 1973 data for C_{org} and N_{org}

7) Average IAP for $Al(OH)_3$ at 90 cm over the period 1973-1991. The value given, is the value at 25°C, which is derived from the value at field temperature (10°C).

Table 5.7 Geochemical parameters for SMART

Parameter	Unit	Values	
		10 cm	90 cm
KAl_{ox} ¹⁾	l ² mol ⁻²	4.0×10 ⁷	2.0×10 ⁹
FBC_{we} ²⁾	mol _c m ⁻³ a ⁻¹	0.039	0.043
$FBC1_{we}$ ²⁾	mol _c m ⁻³ a ⁻¹	0.011	0.012
KAl_{ex}	l mol ⁻¹	0.7	3.5
KH_{ex}	mol l ⁻¹	4786	1862
$KSO_{4 ad}$	l mol ⁻¹	4.2×10 ³	3.9×10 ³

1) Average IAP for $Al(OH)_3$ at 10 and 90 cm based on measured Al and H concentrations in the period 1973-1990

2) for 10 cm based on NuCSAM weathering rates and average H conc at 10 cm depth for the period 1973-1990, for 90 cm depth directly based on weathering fluxes from Wesselink *et al.* (1994)

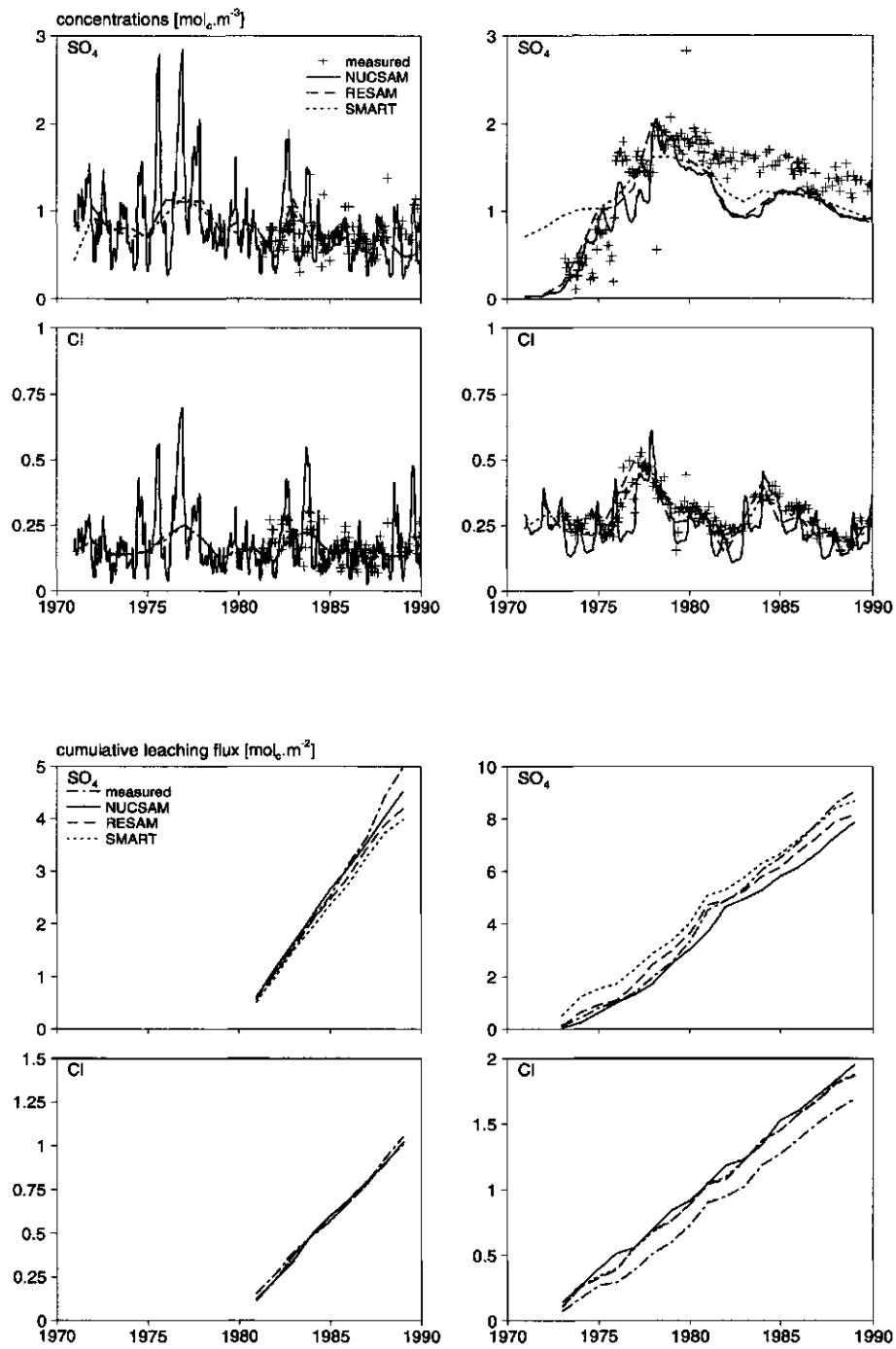


Fig. 5.1 Measured and simulated SO_4 and Cl concentrations and leaching at 10 (left) and 90 cm depth (right)

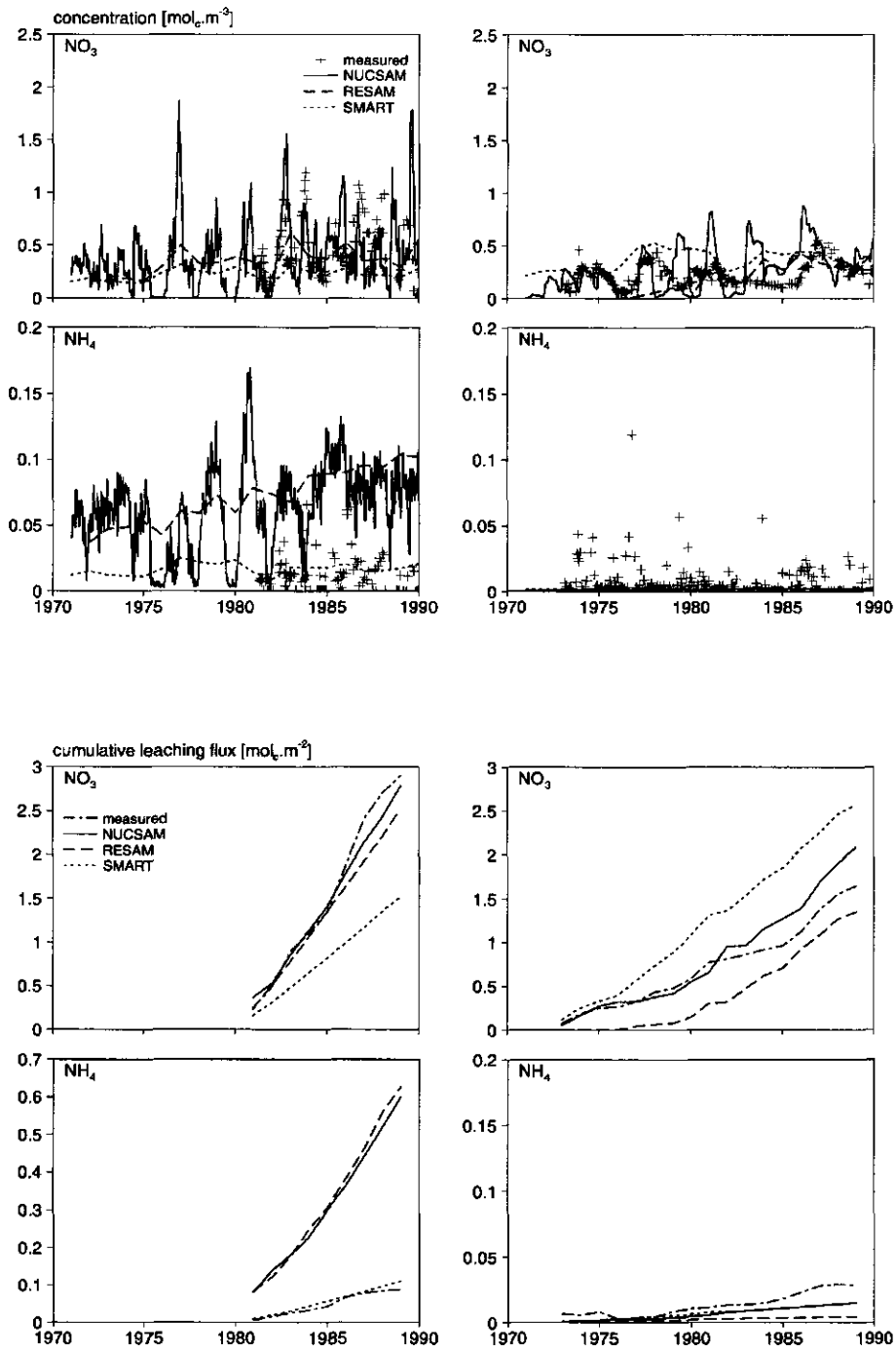


Fig. 5.2 Measured and simulated NO_3 and NH_4 concentrations and leaching at 10 (left) and 90 cm depth (right)

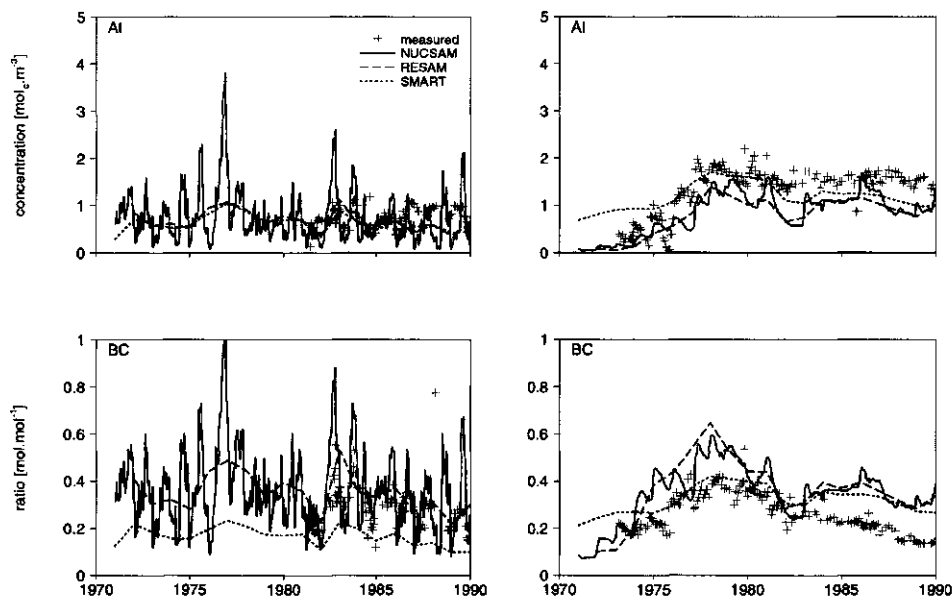


Fig. 5.3 Measured and simulated Al and BC concentrations and leaching at 10 (left) and 90 cm depth (right)

5.4 Results and discussion

To characterize the effects of differences in vertical and temporal resolution and process aggregation in the models, the simulated concentrations and leaching fluxes were compared with measured concentrations and leaching fluxes in the topsoil (10 cm) and subsoil (90 cm). Results were limited to major anions and cations, i.e. SO_4 , Cl, NO_3 , NH_4 , Al and BC (divalent base cations). Simulated and measured concentrations are shown in Figure 5.1 (SO_4 and Cl), Figure 5.2 (NO_3 and NH_4) and Figure 5.3 (Al and BC). An overview of the statistical measures, NMAE and CRM, for the various substances in topsoil and subsoil is given in Table 5.8. The figures and the statistical measures show that all models were able to reasonably simulate the measured concentrations during the examined period. Differences between ReSAM and NuCSAM, the multi-layer models, were rather small. Somewhat larger differences did occur between the concentrations simulated by SMART and those simulated by the multi-layer models. A more detailed discussion on the performance of the models to simulate the individual ions is held in the following Sections where the influence of the model differences is presented.

5.4.1 Influence of vertical resolution

The influence of vertical resolution is most clearly shown by the SO_4 concentrations and leaching fluxes, as SO_4 concentrations are mainly governed by deposition and adsorption, which is described in all models in practically the same way. Measured and simulated concentrations and leaching fluxes of SO_4 are shown in Figure 5.1. The trends in SO_4 concentrations, as simulated by NuCSAM and ReSAM, were generally in good agreement with measured data. SMART, however, overestimated SO_4 concentrations at 90 cm depth during the period 1972-1978 in which a strong rise in SO_4 concentrations took place at this depth. This overestimation, is caused by a larger dispersion of the SO_4 front in a one-layer system compared to a multi-layer system. In a multi-layer system the rise in SO_4 input initially leads to a rise in the absorbed amounts in the upper soil layers, whereas in the subsoil absorbed amounts remain unchanged. In a one-layer system, a rise in the input immediately leads to a (small) rise in the absorbed amounts and concentrations at greater depth. For all models, the performance for SO_4 in the topsoil was comparable. NMAE values were somewhat higher for NuCSAM compared to the other models (Table 5.8), as the simulated variation within the year was larger than the measured variation. Cumulative leaching fluxes at 10 cm depth were somewhat underestimated by all models in the period 1985 to 1989, due to an underestimation of SO_4 concentrations in this period with high water fluxes. Although concentrations were overestimated by SMART in the subsoil, during the period 1973-1975, the overall performance was comparable with the multi-layer models. Total leaching fluxes in 1989, simulated by SMART, were comparable with the measurements.

As a result of the smoothed SO_4 front, the rise in Al due to weathering in the period 1972 -1978 is less pronounced in SMART. This causes a lower exchange of adsorbed base cations against Al compared to the other models. This lower BC desorption in turn leads to a lower rise of the BC concentrations in the subsoil, as simulated by SMART.

Table 5.8 Normalized mean Absolute Error (NMAE) and Coefficient of Residual MASS (CRM) for simulated concentrations

Component	Depth	NMAE			CRM		
		SMART	ReSAM	NuCSAM	SMART	ReSAM	NuCSAM
SO_4	10	0.23	0.25	0.37	0.10	0.05	-0.01
	90	0.26	0.24	0.25	0.06	0.12	0.18
NO_3	10	0.56	0.50	0.62	0.48	0.10	-0.04
	90	0.84	0.63	0.76	-0.79	0.36	-0.25
NH_4	10	1.00	6.17	5.17	-0.34	-5.96	-4.92
	90	0.89	0.89	0.89	0.73	0.93	0.80
BC	10	0.47	0.25	0.41	0.46	0.21	-0.21
	90	0.29	0.16	0.45	-0.27	0.02	-0.43
Al	10	0.32	0.33	0.52	0.20	0.13	0.02
	90	0.24	0.37	0.33	0.01	0.34	0.30
H	10	0.45	0.47	0.53	0.41	0.45	0.51
	90	0.38	0.49	0.48	0.30	0.48	0.47
Cl	10	0.27	0.28	0.40	0.05	0.03	-0.04
	90	0.11	0.16	0.23	0.04	0.06	0.16

5.4.2 Influence of process description

The main differences in process description between the models occur in the description of processes involving nutrient cycling. In SMART a net N immobilization flux is calculated, whereas ReSAM and NuCSAM account for storage of N in the litter layer and for mineralization. Furthermore nitrification is described in a different way in SMART.

Figure 5.2 shows that SMART overestimated NO_3 concentrations in the subsoil (negative CRM) during the entire period, whereas concentrations in the topsoil were underestimated (positive CRM). The deviation between measured and simulated concentrations in the topsoil is due to the neglect of mineralization in the topsoil. To obtain a closer fit between simulated and measured NO_3 concentrations, a slight change in the parameters describing N immobilization in the topsoil would have been useful.

NH_4 concentrations (Figure 5.2) were generally overestimated in the topsoil. However, the overestimation of the concentrations in the topsoil by SMART was small compared to NuCSAM and ReSAM (see CRM values, Table 5.8). In the subsoil all models simulated comparable NH_4 concentrations, which were underestimated with respect to the measurements (see CRM values, Table 5.8). The relatively good agreement between measured concentrations and concentrations simulated with SMART, in the topsoil, is partly due to the fact that in SMART different nitrification constants at 10 and 90 cm depth were used which were directly derived from the Solling dataset. ReSAM/NuCSAM, however, use one overall nitrification parameter which is adapted for each horizon depending on pH, moisture content and organic matter content. Furthermore, in SMART, NH_4 concentrations in the topsoil tend to be lower due to the neglect of mineralization. The influence of mineralization is also shown by the simulation of divalent base cations (BC) by the models (Figure 5.3). In the topsoil SMART simulated lower BC concentrations compared to the other models.

An other difference in process description between SMART and ReSAM/NuCSAM is the way in which Al concentrations are calculated. In SMART Al concentrations are calculated from equilibrium with Al-hydroxide, whereas ReSAM and NuCSAM use a kinetic description (Annex 2). Figure 5.3 shows that results for the simulation of Al (main cation) were comparable with those for the main anion SO_4 . The way in which Al concentrations were calculated appears to have hardly any influence on the results for the chosen period. When applying the models for long-term predictions deviations between the concentrations predicted by NuCSAM/ReSAM and SMART may occur, particularly in the topsoil where the dissolution of Al-compounds is far from equilibrium with gibbsite. A decrease in Al-dissolution rate, due to exhaustion of certain Al-compounds, will lead to a lower simulated concentration by NuCSAM/ReSAM whereas concentrations simulated by SMART will remain constant.

5.4.3 Influence of temporal resolution

The influence of neglecting seasonal fluctuations in the considered process fluxes can best be derived by comparing ReSAM and NuCSAM, models with a comparable process description and a difference in temporal resolution. The most direct influence of the chosen temporal resolution is found in the simulation of Cl concentrations and fluxes. For Example, NuCSAM used daily up- and downward water fluxes to calculate solute transport. Accordingly stronger fluctuations in concentrations (Figure 5.1) were simulated by NuCSAM compared to other models. NMAE values for the Cl concentrations, however, showed that the simulation of the Cl concentrations by NuCSAM was not better than for the other models. In the topsoil the simulated fluctuation of the Cl concentration was sometimes out of phase with the measured fluctuation. In the subsoil NuCSAM underestimated Cl concentrations in wet periods (Table 5.8).

The influence of the chosen temporal resolution on model performance can particularly be expected for the simulated concentrations of NO_3 , NH_4 and base cations which are strongly influenced by seasonal processes as nutrient cycling and mineralization. NO_3 concentrations (Figure 5.2, Table 5.8) simulated with NuCSAM and ReSAM were in close agreement with the measurements in the topsoil. Although, NuCSAM simulated the seasonal peaks in NO_3 concentrations NMAE values in the topsoil were somewhat higher for NuCSAM compared to ReSAM. NO_3 concentrations in the subsoil were poorly simulated by ReSAM up to 1980. From 1980 onwards concentrations simulated by NuCSAM and ReSAM were in the same range as measured values (relatively low NMAE and CRM). However, fluctuations in simulated concentrations by NuCSAM occurred more frequent than the measured multi-year fluctuations in concentrations. The differences in simulated NO_3 concentrations in the subsoil, between NuCSAM and ReSAM is caused by the fact that in NuCSAM total N uptake is lower. N uptake in NuCSAM is lower due to a restriction of the N uptake to the growing-season, which leads in certain years to a higher N demand than available in the soil solution, causing a lower total N uptake in that year.

Cumulative leaching fluxes for NO_3 in the topsoil (Figure 5.2) were in close agreement with measured leaching fluxes both for NuCSAM and ReSAM. In the subsoil, cumulative leaching fluxes were underestimated ($-0.3 \text{ mol}_c \text{ m}^{-2}$) by ReSAM, due to the underestimation of the concentrations (positive CRM) in the period up to 1980 and overestimated ($+0.4 \text{ mol}_c \text{ m}^{-2}$) by NuCSAM due to the overestimation of seasonal peak concentrations (negative CRM).

The correspondence between simulated and measured NH_4 concentrations (Figure 5.2) was meagre for ReSAM and NuCSAM. The periodical fluctuations in concentrations in the subsoil were not simulated by NuCSAM and generally concentrations were overestimated in the topsoil. Although, both measured and simulated NH_4 concentrations were relatively low, the deviation between measured and simulated values leads to a serious overestimation (circa $0.5 \text{ mol}_c \text{ m}^{-2}$) in the period 1983 to 1989.

Base cation concentrations (Figure 5.3) are both influenced by processes with a strong seasonal magnitude, such as mineralization, solute transport and ion-exchange and by more constant processes such as weathering. The general trend in divalent base cation

concentrations in the topsoil was reasonably simulated both by NuCSAM and ReSAM. NuCSAM and ReSAM overestimated the rise in BC concentrations in the subsoil up to 1978. From 1982 onwards concentrations were overestimated by all models, which is probably due to an underestimation of tree growth during this period. ReSAM simulated a somewhat stronger rise and fall in BC concentrations in the subsoil than NuCSAM. This is caused by a stronger desorption of BC in ReSAM. The same phenomenon, however somewhat weaker, can be observed for SO_4 (Figure 5.1). ReSAM simulated slightly higher SO_4 concentrations than NuCSAM during the period 1975-1980. The deviation between ReSAM and NuCSAM is induced by slight differences in hydrology as reflected by the differences in simulated Cl concentrations in the subsoil.

5.5 Conclusions

Although, clear differences in process description do exist between SMART, ReSAM and NuCSAM, all models were able to reasonably simulate most of the concentrations during the study period. The description of the dissolution of Al-hydroxides either by a rate-limited reaction or by an equilibrium equation did not lead to differences in modelled Al concentrations during the study period. Large differences in complexity of the description of N cycling do exist between the models. In SMART mineralization is not included in the model, which led to lower concentrations of NH_4 and divalent base cation in the subsoil compared to the other models. NH_4 concentrations simulated by SMART were closer to the measurement than in the other models, ReSAM and NuCSAM underestimated NH_4 concentrations in the topsoil and overestimated these concentrations in the subsoil. The better results for SMART are a consequence of the use of separate nitrification parameters in SMART for the topsoil and the subsoil, which were directly derived from the measurements, whereas in ReSAM/NuCSAM nitrification rate was dependant on pH, water content and organic matter content. The relationship between these environmental parameters and nitrification parameters was not calibrated on the side data.

The influence of vertical resolution of the models was clearly shown by the simulation of SO_4 and base cations in the subsoil. All models were able to simulate a rise in SO_4 concentration, between 1975 and 1980, due to a decrease in sulphate adsorption. However, the one-layer model, SMART, tended to overestimate the initial rise in SO_4 concentration, due to a larger dispersion of the sulphur front in a one-layer system compared to a multi-layer system.

A strong influence of temporal resolution was expected in the simulation of NO_3 by NuCSAM compared to ReSAM. In the topsoil NO_3 concentrations simulated by the models were in the same range as the measurements. In the subsoil NO_3 concentrations were underestimated by ReSAM, as ReSAM simulated a higher N uptake compared to NuCSAM. In the subsoil NO_3 concentrations simulated by NuCSAM were in the range of the measurements, however fluctuations were poorly simulated. The NMAE values for the NO_3 concentrations in the top- and the subsoil were higher for NuCSAM than for ReSAM. In the topsoil the higher NMAE values resulted from the fact that simulated fluctuation were sometimes out of phase with the measured fluctuations. In the subsoil simulated fluctuations occurred more frequent than measured fluctuations.

References

- Belmans, C., J.G. Wesseling and R.A. Feddes, 1983. Simulation model of the water balance of a cropped soil providing different types of boundary conditions: SWATRE. *J. Hydrology* 63, 27-286.
- Bredemeier, M.A., A. Tiktak and C. van Heerden, 1995. The Solling spruce stand. Background information on the dataset. *Ecol. Model.* 83, 7-15.
- Chen, C.W., S.A. Gherini, L. Mok, R.J.M. Hudson and R.A. Goldstein, 1983. The integrated Lake-Watershed Acidification Study. Volume 1. Model principles and application procedures, EPRI EA-3221, Vol. 1, Project 1109-5. Final report.
- Cosby, B.J., R.F. Wright, G.M. Hornberger and J.N. Galloway, 1985. Modelling the effects of acid deposition: Estimation of long-term water quality responses in a small forested catchment. *Water Resour. Res.* 21, 1591-1601.
- De Vries, W., M. Posch and J. Kämäri, 1989. Simulation of the long-term soil response to acid deposition in various buffer ranges. *Water, Air and Soil Pollut.* 48, 349-390.
- De Vries, W., J. Kros and C. Van der Salm, 1995a. Modelling the impact of acid deposition and nutrient cycling in forest soils. *Ecol. Model.* 79, 231-254.
- De Vries, W., M. Posch, G.J. Reinds and J. Kämäri, 1995b. Simulation of soil response to acidic deposition scenarios in Europe. *Water, Air and Soil Pollut.* 79, 1 - 32.
- De Vries, W., M.M.T. Meulenbrugge, W. Balkema, J.C.H. Voogd and R.C. Sjordijn, 1995c. Rates and mechanisms of cation and silica release in acid sandy soils: 3. Differences between soil horizons and soil types. Submitted to *Geoderma*.
- Georgakos, K.P., G.M. Valle-Filho, N.P. Nikolaidis, J.L. Schnoor, 1989. Lake-Acidification studies: the role of input uncertainty in long-term predictions. *Water Res. Res.* 25, 1511-1518.
- Groenenberg, J.E., J. Kros, C. Van der Salm and W. De Vries, 1995. Application of the model NuCSAM to the Solling spruce site. *Ecol. Model.* 83, 97-107.
- Kros, J., J.E. Groenenberg, W. De Vries and C. Van der Salm, 1995. Uncertainties in long-term predictions of forest soil acidification due to neglecting interannual variability. *Water, Air and Soil Pollut.* 79, 353-375.
- Meiwes, K.J., 1979. Der Schwefelhaushalt eines Buchenwald- und eines Fichtenwaldökosystem im Solling. *Göttinger Bodenkundliche Berichte*, 60.
- Rose, K.A., R.B. Cook, A.L. Brenkert, R.H. Gardner, J.P. Hettelingh, 1991. Systematic comparison of ILWAS, MAGIC and ETD watershed acidification models. 1. Mapping among model inputs and deterministic results. *Water Resour. Res.* 27, 2577-2589.
- Wesselink, L.G., Van Grinsven, J.J.M. and Grosskurth, G.: 1994, Measuring and modelling mineral weathering in an acid forest soil. Solling, Germany, *Soil Sci. Soc. Am. J.* 39, 91-110.

Chapter 6 is a slightly revised version of:

De Vries, W., J. Kros, J.E. Groenenberg, G.J. Reinds, C. van der Salm and M. Posch, 1995. Scenario studies on soil acidification at different spatial scales. In: J.F.T. Schoute, P.A. Finke, F.R. Veeneklaas & H.P. Wolfert (eds.), Scenario studies for the rural environment. Kluwer, Dordrecht, Netherlands. *Environment & Policy* 5: 169-188.

6 Scenario studies on soil acidification at different spatial scales

Abstract

Three dynamic soil acidification models have been developed for application at a continental (European) scale, a national scale and a local scale, i.e. SMART, ReSAM and NuCSAM. NuCSAM was specifically developed to gain insight in the effect of acidic deposition and nutrient cycling on a local scale and to aid further research (research aim), whereas the major objective of SMART was to assist decision makers in evaluating environmental policies in Europe (management aim). ReSAM serves both aims but on a different scale (smaller compared to SMART and larger compared to NuCSAM).

This paper gives an overview of various model studies including: (i) model validation on a local and a national scale and (ii) scenario studies, which evaluate effects of different deposition scenarios for SO_x , NO_x and NH_x on soils on a local, national and continental scale. Result showed (i) a reasonable to good agreement between measured and simulated soil solution chemistry both at a local and regional scale and (ii) an improvement in the future acidification status of Dutch forest soils at given emission-deposition reductions, whereas the reverse was predicted for European forest soils. The uncertainties in model predictions and the use of the models in acidification abatement policies is addressed and the various strong and weak points of the models are evaluated. Furthermore, the limitations and possibilities to use the models in other scenario studies, such as changes in land use, hydrology and heavy metal deposition are discussed.

6.1 Introduction

Acid atmospheric deposition first became recognized as a problem in the early seventies when acidification of lakes and streams in Scandinavia and Northeastern America led to a decline in fish species (Likens and Bormann, 1974). Ulrich *et al.* (1979) were among the first to draw attention to acidification of forest soils caused by acid deposition and its potentially harmful effects on forest ecosystems. Evidence exists that the vitality of forest ecosystems in Europe is seriously endangered by changes in soil chemistry in the root zone. Examples are a decrease in pH and base saturation, an increase in toxic Al and the unbalanced availability of base cation nutrients (Ca, Mg, K) due to excessive Al and NH_4 (Roelofs *et al.*, 1985; Roberts *et al.*, 1989). Although acidification of soils, such as decalcification and podzolization, is a natural process in coarse textured (sandy) soils in areas with a precipitation excess, it is the present rate of soil acidification which is alarming. Current enhanced soil acidification due to elevated atmospheric deposition of SO_x , NO_x and NH_x has been proven by input-output budgets. (e.g. Van Dobben *et al.*, 1992). Recently enhanced soil acidification in Central and Northern Europe has also been proven by resampling forest soils at intervals of several decades (e.g. Hallbäck and Tamm, 1986; Billet *et al.*, 1988; Butzke, 1988). These studies showed that soil pH and base saturation have decreased strongly within the root zone of most forest soils in the past 20 to 30 years.

At present various dynamic simulation models exist to predict the acidification of surface waters. Examples are the Integrated Lake Watershed Acidification Study (ILWAS) model, developed for the application on single catchments (Chen *et al.*, 1983) and the Model for the Acidification of Groundwater in Catchments (MAGIC) developed for regional catchment applications (Cosby *et al.*, 1985). At the Winand Staring Centre, different soil acidification models have been developed for use on different scales, i.e. NuCSAM (Nutrient Cycling and Soil Acidification Model; Chapter 2, Groenenberg *et al.*, 1995; Chapter 3), ReSAM (Regional Soil Acidification Model; De Vries *et al.*, 1995) and SMART (Simulation Model for Acidification's Regional Trends; De Vries *et al.*, 1989). The models ReSAM and SMART were specifically developed to evaluate long-term soil responses to deposition scenarios on a regional (national to continental) scale, respectively. Consequently, ReSAM and SMART do not include seasonal dynamics. The temporal resolution of the models is one year, and the hydrologic description in these models is very simple. Simulation of the interannual variability is, however, included in NuCSAM, which is specifically developed for application (and validation) on a local scale.

ReSAM and SMART are part of integrated acidification simulation models that give a quantitative description of the linkages between emissions, deposition and environmental impacts such as soil acidification and effects on terrestrial and aquatic ecosystems. These integrated models are DAS (Dutch Acidification Simulation model) for application in the Netherlands (Olsthoorn *et al.*, 1990) and RAINS (Regional Acidification Information and Simulation model) for application in Europe (Alcamo *et al.*, 1990)

The major objective of this paper is to give a review of modelling studies with NuCSAM, ReSAM and SMART about the impact of deposition scenarios for SO_x , NO_x and NH_x on soils at various regional scales. Furthermore, various studies on model validation and uncertainties in model predictions are reviewed. Finally the strong and weak points of the models are evaluated and their possible use in predicting the mobilization of heavy metals after environmental (e.g. land use) changes is discussed (chemical time bombs).

6.2 The models NuSCAM, ReSAM and SMART

Two major groups of soil acidification models are those based on an empirical approach and those based on mechanistic descriptions of processes. A disadvantage of relatively simple empirical models is that they lack a theoretical basis for establishing confidence in the predictions. Consequently, the models NuCSAM, ReSAM and SMART described here are all characterized by a process-oriented deterministic approach. The stochastic character of input data can, however, be included in all models by a Monte Carlo approach, given a specified range of input data (e.g. Kros *et al.*, 1993). A disadvantage of relatively complex mechanistic models is, however, that input data for their application on a regional scale is generally incomplete. So, even if the model structure is correct (or at least adequately representing current knowledge), the uncertainty in the output of complex models may still be large because of the uncertainty of input data, (Hornberger *et al.*, 1986). There is thus a trade off between detail and reliability

of information obtained and regional applicability. Consequently the desired degree of spatial resolution in model output is a factor of crucial importance when selecting the level of detail in both the model formulation and its input data. A larger application scale justifies the development of a simpler model, as illustrated in Table 6.1.

Table 6.1 Characteristics of the dynamic soil acidification models used at the DLO Winand Staring Centre

Name	Complexity	Soil layering	Temporal resolution	Application scale
NuCSAM	Complex	multi-layer	one day	Site
ReSAM	Intermediate	multi-layer	one year	The Netherlands
SMART	Simple	one-layer	one year	Europe

The models SMART and ReSAM, designed for regional predictions, are more simplified than the site scale model NuCSAM to minimize input requirements. The simplifications consist of: (i) the reduction of temporal resolution, i.e. using an annual time resolution, thus neglecting interannual variability of both model inputs and processes, (ii) the reduction in spatial resolution, by using a smaller number of soil compartments and (iii) the use of less detailed process formulations. To apply a model on a regional scale, the various processes occurring in the soils have either been limited to a few key soil processes, or represented by simple conceptualizations (process aggregation). The degree of process aggregation in the models increases (complexity decreases) when the availability of data decreases, which occurs with an increase in the geographic area of application.

The major reason for developing NuCSAM was to be able to validate the model on intensively (mostly biweekly) monitored sites during a relatively short-time period. Validation of dynamic models which do not include interannual variability, i.e. ReSAM and SMART, is problematic, since long-term time series of soil chemistry data are generally lacking. However, long-term simulations with SMART and ReSAM can be compared to those made with the validated NuCSAM model, that serves as a standard. In this way an indirect model output validation can be accomplished for the regional models ReSAM and SMART.

The major reason for differentiating between the multi-layer ReSAM model and the one-layer SMART model was the trade-off between the level of detail in model outputs and the availability of model inputs. ReSAM gives insight into the spatial (vertical) variation in soil (solution) chemistry within the rootzone. Since the hydrologic description in the one-layer model SMART is simplified to the use of an annual precipitation excess draining from the rootzone, this model only predicts soil solution chemistry at the bottom of the rootzone. Important acidification indicators such as the Al concentration and Al/Ca ratio, however, increase with depth due to Al mobilization, transpiration and Ca uptake. Since most fine roots, responsible for nutrient uptake, occur in the upper soil layer (0-30 cm soil depth), it is important to obtain reliable estimates for this layer by including water uptake with depth and nutrient cycling (foliar uptake, foliar exudation, litterfall, mineralization and nutrient uptake) within the rootzone. However, inclusion of these processes in the model requires additional data on nutrient cycling. These data are readily available for the Netherlands but not for Europe. Consequently, ReSAM, developed for application in the Netherlands, includes such processes whereas SMART, developed for application on a European scale, does not.

Table 6.2 Processes and process formulations included in NuCSAM, ReSAM and SMART

Processes	NuCSAM	ReSAM	SMART
Hydrological processes:			
Water flow	Hydrological submodel	Variable flow with depth	Precipitation excess
Biological processes:			
Foliar uptake	Proportional total deposition	Proportional to total deposition	-
Foliar exudation	Proportional to H and NH ₄ deposition	Proportional to H and NH ₄ deposition	-
Litterfall	First-order reaction	First-order reaction	-
Root decay	First-order reaction	First-order reaction	-
Mineralization/immobilization	First-order reaction ¹⁾	First-order reaction	Proportional to N deposition
Growth uptake	- Constant growth - Logistic growth	- Constant growth - Logistic growth	Constant growth
Maintenance uptake	Forcing function ²⁾	Forcing function ²⁾	-
Nitrification	First-order reaction ¹⁾	First-order reaction	Proportional to net NH ₄ input
Denitrification	First-order reaction ¹⁾	First-order reaction	Proportional to net NO ₃ input
Geochemical processes:			
CO ₂ dissociation	Equilibrium equation	Equilibrium equation	Equilibrium equation
RCOO protonation	First-order reaction	First-order reaction	-
Carbonate weathering	First-order reaction	First-order reaction	Equilibrium equation
Silicate weathering	First-order reaction ³⁾	First-order reaction ³⁾	Zero-order reaction
Al hydroxide weathering	-First-order reaction -Elovich equation	- First-order reaction - Elovich equation	Equilibrium equation
Cation exchange	Gaines Thomas equations ⁴⁾	Gaines Thomas equations ⁴⁾	Gaines Thomas equations ⁴⁾
Sulphate adsorption	Langmuir equation	Langmuir equation	Langmuir equation
Phosphate adsorption	Langmuir equation	-	-
Complexation reactions	Equilibrium equations	-	-

¹⁾ In NuCSAM, these processes are also described as a function of temperature

²⁾ In ReSAM and NuCSAM the maintenance uptake equals it the sum of litterfall, root decay and foliar exudation minus foliar uptake.

³⁾ In ReSAM and NuCSAM there is also the option to include a dependence of pH on the weathering rate.

⁴⁾ In SMART cation exchange is limited to H, Al and the sum of base cation (BC) whereas in ReSAM and NuCSAM it includes H, Al, NH₄, Ca, Mg, K and Na

Process descriptions

NuCSAM, ReSAM and SMART are all based on the principle of ionic charge balance and on a simplified solute transport description. In all models, it is assumed that: (i) a soil layer is a homogeneous compartment of constant density and (ii) the element input mixes completely in a soil layer. Furthermore, N-fixation, SO₄ reduction and SO₄ precipitation are not included and the various process descriptions for biological and geochemical interactions are simplified to minimize input data. Going from NuCSAM to SMART the degree of process aggregation increases by (i) a simpler hydrological description, (in ReSAM and SMART the annual water flux percolating through a soil layer is constant and equals the infiltration minus the transpiration, whereas NuCSAM contains a separate hydrological model), (ii) ignoring several processes (e.g. nutrient cycling), (iii) simpler descriptions of processes (e.g. equilibrium equations instead of rate limited reactions) and (iv) ignoring elements (e.g. organic anions, RCOO) or lumping elements (e.g. sum of base cations, BC, instead of Ca, Mg, K and Na separately). This is summarized in Table 6.2.

Biological processes are all described by rate-limited reactions. In most cases first-order reactions are used. Notable exceptions are the canopy interactions in NuCSAM and ReSAM that are described by linear relationships with atmospheric deposition (cf Table 6.2). In SMART, all geochemical reactions are described by equilibrium equations, except for silicate weathering which is described by a zero-order reaction (Table 6.2). In NuCSAM and ReSAM, the geochemical reactions are either described by equilibrium equations (dissociation of CO₂, cation exchange and SO₄ adsorption) or first-order reactions (protonation of organic anions and weathering of carbonates, silicates and secondary Al compounds). So, unlike SMART, NuCSAM and ReSAM account for the effect of mineral depletion on the weathering rate.

6.3 Validation and application of the models at various scales

6.3.1 Studies on a local scale

6.3.1.1 Methodology

The model NuCSAM was specifically developed for application and validation on a site scale. The major idea was to compare model predictions of the validated NuCSAM model with those of ReSAM, to have confidence in the long-term predictions with the latter model in various scenario studies. Uncertainty caused by neglecting the seasonal variability in long-term predictions was therefore investigated by a comparison of long-term simulations (1990-2090) with NuCSAM and ReSAM (Kros *et al.*, 1995a; Chapter 4), using data from an intensively monitored spruce site at Solling, Germany (Bredemeier *et al.* 1995). NuCSAM and ReSAM were also validated on that site by comparing simulated concentrations and leaching fluxes with measured values during the period 1973-1989 (Van der Salm *et al.*, 1995; Chapter 5). The SMART model was also validated on the Solling site, even though SMART (and ReSAM) was not developed for application at such a scale. The major aim was to study the influence of model simplifications, especially with respect to process formulation and the reduction

of temporal and spatial resolution, on the simulation of soil solution concentrations. A direct comparison of simulated data of SMART and ReSAM with measured data was not possible, since both models simulate flux-weighted annual average concentrations, that can not be measured. Consequently, we compared monthly measured concentrations (which were assumed to equal the monthly average concentration) with simulated values, that were derived by linear interpolation between annual values. In NuCSAM, monthly values were calculated by averaging the simulated daily concentrations.

To give more objective information concerning the performance of the models two statistical measures were calculated: the Normalized Mean Absolute Error (NMAE) and the Coefficient of Residual Mass (CRM) (Table 6.3). NMAE quantifies the average deviation between model prediction and measurements. CRM gives an indication of the tendency of the model to under- or overestimate (negative value) the measured data. NMAE and CRM for the three models were calculated using monthly concentrations for model results and measurements.

Table 6.3 Statistical measures for evaluation of model results

Measure	Symbol	Formulation	Optimum
Normalized Mean Absolute Error	NMAE	$\frac{\sum_{i=1}^N (P_i - O_i)}{N \cdot \bar{O}}$	0
Coefficient of Residual Mass	CRM	$\frac{\sum_{i=1}^N O_i - \sum_{i=1}^N P_i}{\sum_{i=1}^N O_i}$	0

P_i is de modelled value, O_i is de observed value, \bar{O} is de mean of the observed values and N the number of observations

We used two atmospheric deposition scenarios for the period 1990-2090, i.e.: (i) *business as usual* (BU): deposition at the Solling site in 1990 was kept unchanged for the period 1990-2090 and (ii) *improved environment* (IE): a linear 75% reduction was performed on the 1990 deposition values of SO_x , NO_x , and NH_x between 1990 and 2000, and after that the deposition values remained constant. For all other constituents the values of 1990 were kept constant, except for H, which is calculated from the charge balance. The total deposition fluxes for 1990 were $1470 \text{ mol}_c \text{ ha}^{-1} \text{ yr}^{-1}$ for NH_4 , $1410 \text{ mol}_c \text{ ha}^{-1} \text{ yr}^{-1}$ for NO_3 and $3640 \text{ mol}_c \text{ ha}^{-1} \text{ yr}^{-1}$ for SO_4

6.3.1.2 Model validation

Simulated and measured concentrations in the topsoil (10 cm) and subsoil (90 cm). for SO_4 , NO_3 and Al are shown in Figure 6.1. All models were able to reasonably simulate the measured concentrations during the historical period. Differences between the multi-

layer models, NuCSAM and ReSAM, were rather small. Somewhat larger differences did occur between the concentrations simulated by SMART and those simulated by the multi-layer models.

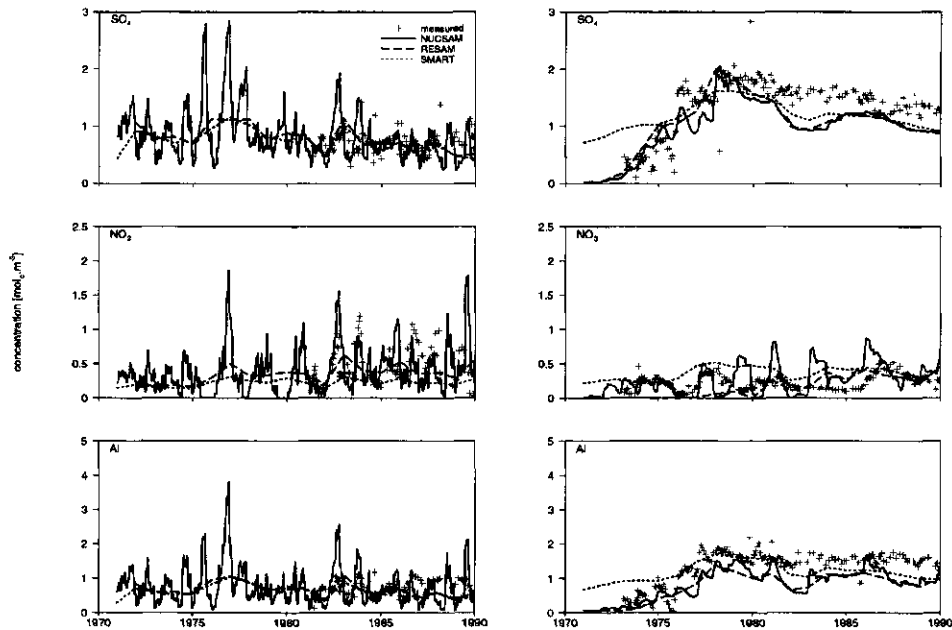


Fig. 6.1 Observed and simulated concentrations with NuCSAM, ReSAM and SMART of SO_4 , NO_3 and Al at Solling at 10 cm depth (left) and 90 cm depth (right)

The influence of vertical resolution is most clearly shown by the SO_4 concentrations. SO_4 concentrations are mainly governed by deposition and adsorption, which is described in all models in practically the same way. The trends in SO_4 concentrations, as simulated by NuCSAM and ReSAM, were generally in good agreement with measured data. SMART, however, overestimated SO_4 concentrations at 90 cm depth during the period 1972-1978 in which a strong rise in SO_4 concentrations took place at this depth. This overestimation is caused by a larger dispersion of the SO_4 front in a one-layer system compared to a multi-layer system. For all models, the performance for SO_4 in the topsoil was comparable. NMAE values were somewhat higher for NuCSAM compared to the other models (Table 6.4), since the simulated variation within the year was larger than the measured variation.

The influence of the chosen temporal resolution on model performance can be seen most clearly for the simulated concentrations of NO_3 in the topsoil, which are strongly influenced by seasonal processes, such as nutrient cycling and mineralization. NO_3 concentrations in the topsoil (Fig. 6.1) simulated with NuCSAM were in close agreement with the measurements, whereas ReSAM could not accurately simulate the seasonal peaks in NO_3 concentrations. SMART overestimated NO_3 concentrations in the subsoil (negative CRM) during the entire period, whereas concentrations in the topsoil were underestimated (positive CRM), due to the neglect of mineralization in the topsoil (cf Table 6.4).

Results for the simulation of Al (main cation) were comparable with those for the main anion SO_4 . (cf Table 6.4). The way in which Al concentrations were calculated (cf Table 6.2) appeared to have hardly any influence on the results for the chosen period. When applying the models for long-term predictions, however, deviations between the concentrations predicted by NuCSAM/ReSAM and SMART may occur, particularly in the topsoil. (cf Van der Salm *et al.* 1995; Chapter 5).

Table 6.4 Normalized Mean Absolute Error (NMAE) and Coefficient of Residual MASS (CRM) for simulated SO_4 , NO_3 and Al concentrations with NuCSAM, ReSAM, and SMART at Speuld

Component	Depth	NMAE			CRM		
		SMART	ReSAM	NuCSAM	SMART	ReSAM	NuCSAM
SO_4	10	0.23	0.25	0.37	0.10	0.05	0.01
	90	0.26	0.24	0.25	0.06	0.12	0.18
NO_3	10	0.56	0.50	0.62	0.48	0.10	0.04
	90	0.84	0.63	0.67	0.79	0.36	0.25
Al	10	0.32	0.33	0.52	0.20	0.13	0.02
	90	0.24	0.37	0.33	0.01	0.34	0.30

6.3.1.3 Model predictions

Flux-weighted annual average solute concentrations simulated by NuCSAM and ReSAM for the Improved Environment (IE) scenario are given in Figure 6.2. The agreement between observed flux-weighted annual average concentrations and those simulated by ReSAM and NuCSAM was generally good for all presented constituents (Fig. 2; see also Fig. 6.1). The most remarkable difference between the two model results was that the NuCSAM outputs were fickle, while the ReSAM outputs were strongly smoothed. This is, of course, inherent to the character of the models; daily time step versus annual averages.

Comparison of the long-term results of the models shows that trends in solute concentrations were very similar. This was also the case for the Business as Usual (BU) scenario (not shown). For most model outputs the NuCSAM result was oscillating around the ReSAM result. The Al/Ca ratio in the subsoil predicted by ReSAM, however, was lower than that predicted by NuCSAM from 2000 onwards. The maximum deviation occurred during the period of deposition reductions, between 2000 and 2010. This deviation was mainly caused by a quicker response of the adsorption complex in the ReSAM model to a change in deposition, resulting in a shorter time-delay. However, during the periods with constant deposition, when a new steady-state between deposition and the adsorption complex was reached, the correspondence in Al/Ca ratios improved. (cf Kros *et al.*, 1995a; Chapter 4)

Regarding the effect of time variability, this study showed that time resolution has only a rather small effect on the uncertainty in long-term (> 100 year) soil acidification. On a smaller time scale (10-50 years), during strong changes in deposition, the effect is more significant, especially when the Al/Ca ratio is considered. However, when seasonal or episodic values of concentrations or ratios are of importance, it is inevitable to use a short (daily) time step.

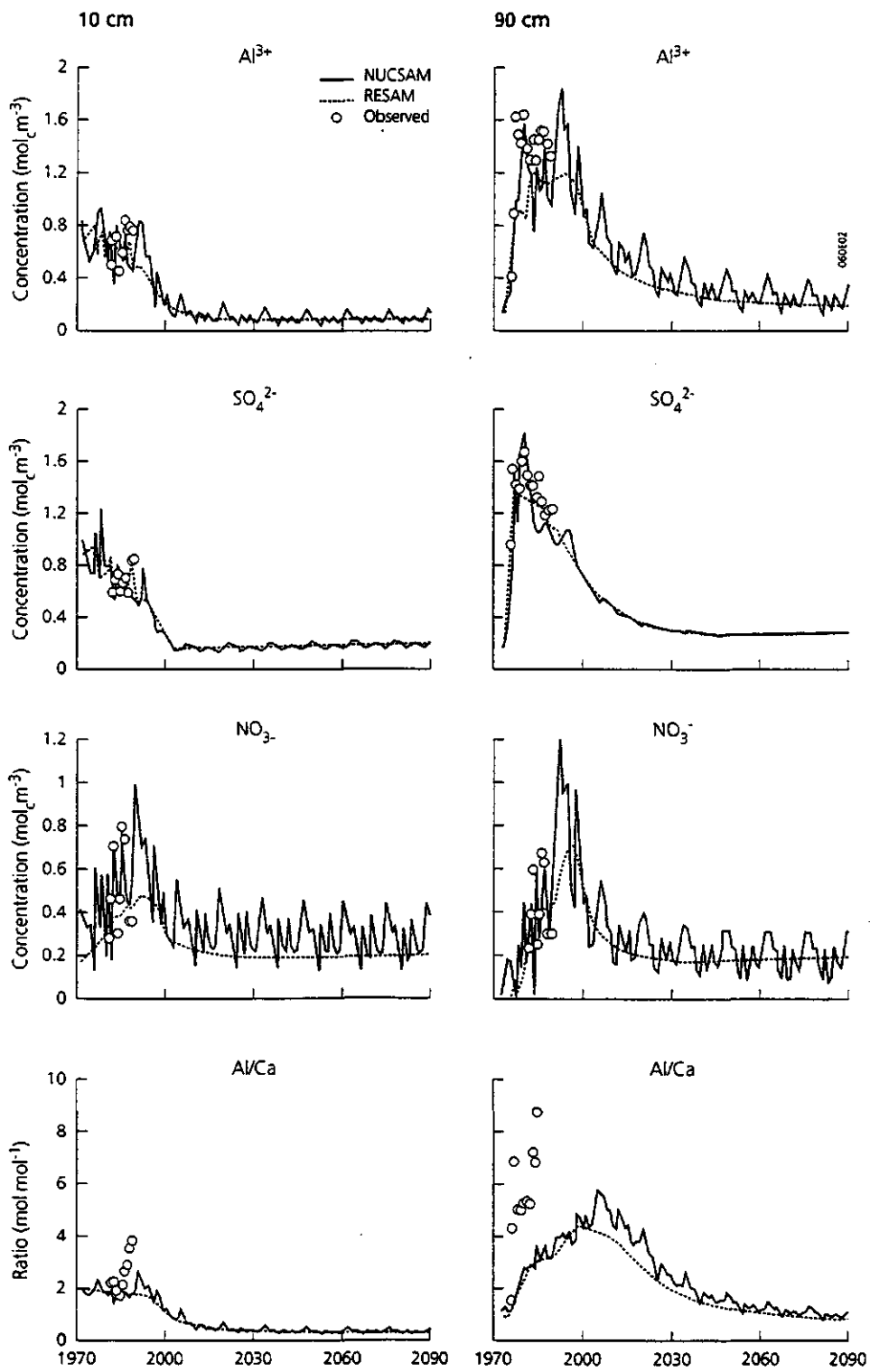


Fig. 6.2 Flux-weighted annual average concentrations simulated with NuCSAM and with ReSAM of SO_4 , NO_3 , Al and Al/Ca ratio at Speuld at 10 cm depth (left) and 90 cm depth (right), for the period 1970-2090 under the Improved Environment scenario. The observed flux-weighted annual average concentrations between 1970 and 1990 are also given

6.3.2 Studies on a national scale

6.3.2.1 Methodology

The long-term impact of atmospheric deposition on Dutch forest soils was evaluated with the ReSAM model. Three emission-deposition scenarios for SO_x, NO_x and NH_x for the period 1960-2050 were generated based on: (i) historical emission data (1960-1990), (ii) expected emissions in the near future (1990-2000) and (iii) deposition targets (2000-2050) since no emission policy has been developed for the period after 2000. For this period three scenarios were used (the scenarios were identical up to 2000) based on deposition targets that were formulated for the years 2010 and 2050 (Table 6.5).

Table 6.5 Average values used for the potential acid deposition in 2010 and 2050 for three scenarios. Official deposition targets are underlined

Receptor	Potential acid deposition (mol _c ha ⁻¹ yr ⁻¹) ¹⁾					
	scenario 1		scenario 2		scenario 3	
	2010	2050	2010	2050	2010	2050
The Netherlands	<u>2240</u> ²⁾	<u>2240</u>	<u>1400</u> ³⁾	1230	1230	<u>700</u> ⁴⁾
Forest in the Netherlands ⁵⁾	2550	2550	1600	<u>1400</u>	<u>1400</u>	800

1) Potential acid deposition in the Netherlands is defined as the sum of SO_x, NO_x and NH_x deposition minus seasalt corrected bulk deposition of base cations

2) The official target was 2400 mol_c ha⁻¹ yr⁻¹ (cf De Vries, 1993) but on the basis of the measures described in NEPP⁺ a somewhat lower value was calculated.

3) A critical acid load related to root damage caused by Al toxicity (cf De Vries, 1993).

4) A critical acid load that prevents nearly all possible negative effects including groundwater pollution (cf De Vries, 1993).

5) Increased deposition on forests, due to filtering of gaseous air pollutants, was accounted for by multiplying the average dry deposition by empirically derived correction factors, (Erisman, 1991).

Twenty deposition areas with relatively uniform deposition values were identified. In order to limit both data acquisition and computation time, the calculations within each area were restricted to seven tree species and 14 representative profiles of acid sandy soils of major importance, that comprised nearly 65% of the total Dutch forest area. The various data, such as water fluxes in soil layers (ii) weathering, growth and turnover rates, (iii) element contents in tree compartments, litter, primary minerals, hydroxides and on the adsorption complex and (iv) rate and equilibrium constants for modelled soil processes, i.e. nitrification, denitrification, protonation, base cation weathering, Al dissolution and cation exchange, were derived from literature surveys, field research, laboratory experiments and model calibration (cf De Vries et al, 1994a).

To gain insight in the reliability of the predictions of the model ReSAM on a national scale, a comparison was made between results of 550 model simulations on the soil solid phase and soil solution chemistry in 1990 with measurements in 150 forest stands during the period March to May in the same year. The tree species and soil types included in the field survey were similar to those included in the simulations. However, one should be aware of the following differences: (i) The distribution of tree species differed between the field survey and the simulation runs, (ii) ReSAM predicted water

flux-weighted annual average concentrations, whereas the field data were single measurements in early spring and (iii) ReSAM predictions for the topsoil were an average of two soil layers with a total depth varying between 20 and 30 cm, whereas the topsoil in the field data set referred to a layer of 0 to 30 cm. For the subsoil, ReSAM predictions related to the bottom of the rooting zone, varying between 50 and 80 cm, whereas the field data referred to a layer of 60-100 cm.

6.3.2.2 Model validation

A comparison of median values of important soil solution parameters is given in Table 6.6. The pH, Al concentration, molar Al/Ca ratio and molar NH₄/K ratio in the topsoil (top 20 to 30 cm) and pH, Al and NO₃ concentration are important indicators of forest stress, whereas pH, Al and NO₃ concentration in the subsoil are important indicators of potential groundwater pollution. The SO₄ concentration has been added to acquire an insight into the relative contributions of S and N in soil acidification.

Table 6.6 Median values of soil solution parameters measured in the field and simulated by ReSAM

Parameter	Unit	Topsoil		Subsoil	
		measured	simulated	measured	simulated
pH	(-)	3.6	3.7	3.9	3.8
Al	(mol _c m ⁻³)	0.7	0.5	0.6	1.2
Al/Ca	(-)	1.3	1.7	-	-
NH ₄ /K	(-)	1.7	2.8	-	-
NO ₃	(mol _c m ⁻³)	-	-	0.5	0.7
SO ₄	(mol _c m ⁻³)	-	-	1.1	1.2

The agreement between model results and field data was good (difference < 10%) for the pH and the SO₄ concentration, reasonable (difference between 10-30%) for the Al/Ca ratio, the NO₃ concentration and the Al concentration in the topsoil and poor (difference > 30%) for the NH₄/K ratio and the Al concentration in the subsoil. Comparison between model results and field data for the tracers Na and Cl in both topsoil and subsoil showed that the model results are always (slightly) lower, especially in the topsoil (De Vries *et al.*, 1994a). This partly explains the underestimation of Al concentrations in the topsoil. The overestimation of Al in the subsoil can partly be explained by an overestimation of the NO₃ and SO₄ concentration, which influences Al mobilization. The remaining difference is most probably due to the long-term effect of liming (Ca) and fertilization (mainly K) and/or a higher base cation input from the atmosphere, which will cause an increase in base cation concentration and a decrease in Al concentration. This also explains the overestimation of the molar Al/Ca ratio and molar NH₄/K ratio by ReSAM. More detailed information on the regional validation of ReSAM is given in De Vries *et al.* (1994a).

6.3.2.3 Model predictions

As an example of model predictions, trends in the forested area exceeding critical values for the Al concentration and Al/Ca ratio in the topsoil are given in Figure 6.3. Between 1990 and 2000 there is no difference in trends for the three scenarios because the deposition values are similar. In this period the estimated average deposition in The Netherlands drops from approximately 4700 to 2500 mol_c ha⁻¹ yr⁻¹. In response to this deposition reduction there is a considerable decrease in the Al concentration and Al/Ca ratio in the topsoil. The area exceeding a critical Al concentration and Al/Ca ratio of 0.2 mol_c m⁻³ and 1.0 mol mol⁻¹, respectively, is approximately 75% and 60% in 1990, whereas the percentage of forest soils exceeding both values is approximately 40% in the year 2000. A deposition reduction according to scenario 2 was enough to avoid exceedances in Al concentration or Al/Ca ratio in forest topsoils in the year 2050. The average deposition level at this time is close to 1400 mol_c ha⁻¹ yr⁻¹ which is the average critical load derived for the effects of aluminium on forests (De Vries 1993). For scenario 1 the area exceeding a critical Al concentration and Al/Ca ratio remained approximately 30% and 10% respectively, in the year 2050 (Fig. 6.3).

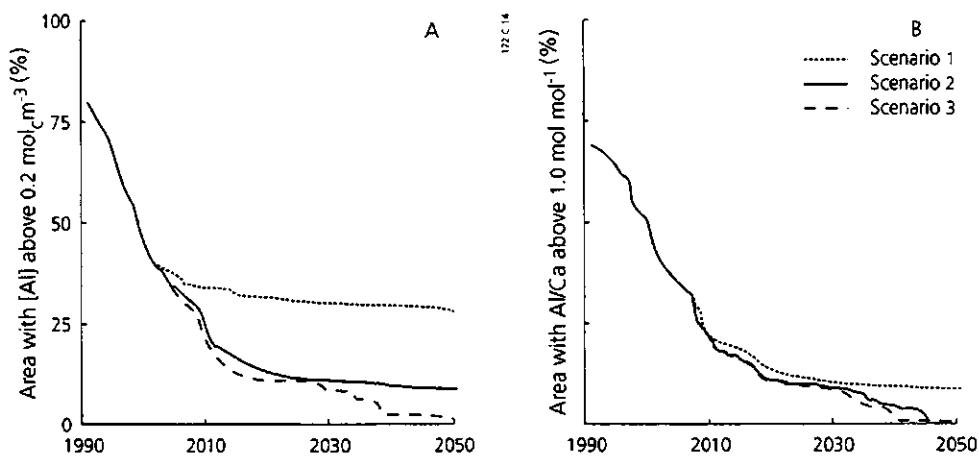


Fig. 6.3 The percentage of Dutch forest soils exceeding a critical Al concentration of 0.2 mol_c m⁻³ (A) and a critical molar Al/Ca ratio of 1.0 in the topsoil (B) in response to three scenarios

The predicted response of 'N related parameters', such as the molar NH₄/K ratio and NO₃ concentration, to a deposition reduction was small compared to the 'Al related parameters'. This was mainly due to N mobilization from litter, which in turn was caused by a decrease in the N content of leaves in response to decreased N deposition. This caused a time lag between the reduction in N deposition and the predicted concentrations of NH₄ and NO₃ (cf De Vries *et al.*, 1994a).

6.3.3 Studies on a european scale

6.3.3.1 Methodology

The SMART model was used to evaluate the long-term impact of three emission - deposition scenarios on European forest soils, i.e: (i) the 'Official Energy Pathways' scenario (OEP), based on governments projections for future energy use, (ii) the 'Current Reduction Plans' scenario (CRP) which takes into account likely reductions of emission due to proposed abatement measures, and (iii) the 'Maximum Feasible Reductions' scenario (MFR), which assesses the impacts of a radical, but technologically feasible, decrease in emissions (mostly SO₂). The resulting total emissions for Europe in the period 1960-2050 for SO₂, NO_x and NH₃ are shown in Figure 6.4.

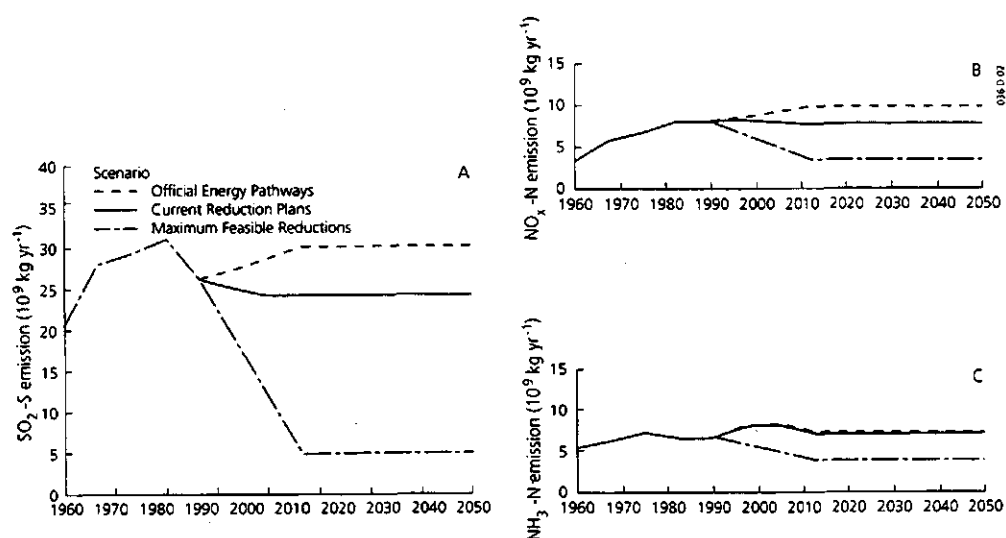


Fig. 6.4 Trends in total emissions of SO₂, NO_x and NH₃ in Europe for three scenarios, i.e. Official Energy Pathways (OEP), Current Reduction Plans (CRP) and Maximum Feasible Reductions (MFR)

Deposition areas were defined by a grid net of 1.0° longitude versus 0.5° latitude. Within each gridcell calculations were made for all major combinations of tree species and soil types. A distinction was made between coniferous and deciduous trees to account for differences in dry deposition, transpiration and growth uptake. The spatial variability of the soil was taken into account by distinguishing 80 different soil types according to the FAO-UNESCO Soil Map of the World (FAO, 1981) on the basis of the dominant soil unit, texture class and slope class (De Vries *et al.*, 1994c). Input data for SMART include system inputs and soil data. System inputs (and outputs), i.e. deposition, precipitation, evapotranspiration and growth uptake, were derived as a function of location (gridcell) and of forest type. Soil data were derived as a function of soil type irrespective of the location. Most soil data were related to readily available soil (and land) characteristics, using so-called transfer functions. Examples are the derivation of physical and chemical soil properties, such as the bulk density (ρ), volumetric moisture content (θ) and cation exchange capacity (CEC) from the (clay) and organic carbon content, (cf Table 6.7). Detailed information on the transfer functions used is given in De Vries *et al.* (1994c).

Table 6.7 Transfer functions between soil properties and soil characteristics (after De Vries *et al.*, 1994c)¹⁾

Soil property	Transfer function	Condition
$\rho^{2)}$ (kg m ⁻³)	1000 / (0.625 + 0.05 · carbon + 0.0015 · clay) 725 - 337 · log carbon	carbon ≤ 5% carbon ≥ 15%
$\theta^{3)}$ (m ³ m ⁻³)	0.04 + 0.0077 · clay 0.27	clay ≤ 30% clay ≥ 30%
<i>CEC</i> ⁴⁾ (mmol _c kg ⁻¹) 5 · clay + 27.25 · carbon		

¹⁾ Clay stands for clay content in % and carbon for organic carbon content in %

²⁾ For 5% < carbon < 15%, ρ is interpolated linearly

³⁾ Refers to the situation at field capacity

⁴⁾ Refers to a value measured at pH 6.5

6.3.3.2 Model predictions

As an example of model predictions, impacts of the different scenarios on the Al concentration and Al/BC ratio are illustrated in Figure 6.5. Predictions of the forested area exceeding a critical Al concentration (0.2 mol_c m⁻³) after 1985 showed a steady increase for the OEP scenario, a small reduction between 1985 and 2000 followed by a slight increase for the CRP scenario and a marked decrease, especially between 1985 and 2000, for the MFR scenario (Fig. 6.5A). The response of the Al/BC ratio was similar except for the CRP scenario. Unlike Al, the area exceeding a critical Al/BC ratio (1.0 mol mol⁻¹) increased after 1985 for this scenario (Fig. 6.5B). Apparently, the decrease in BC concentration, induced by a decrease in base saturation change in response to ongoing acid deposition, compensated the decrease in Al concentration. The concentrations in 2050 were not yet at steady-state with respect to the deposition level at that time. Even when using the OEP scenario, with higher total S and N emissions in 2050 compared to 1985 (cf Fig. 6.4), the predicted areas with an Al concentration and Al/BC ratio exceeding critical values in 2050 were 'only' about 28% and 14%, respectively. Calculations with a steady-state version of the model SMART showed that these areas would increase up to 43% and 30% respectively at constant 1985 atmospheric deposition (De Vries *et al.*, 1994b).

As with ReSAM, the predicted response of 'N related parameters', i.e. the C/N ratio and the NO₃ concentration, was different from the 'Al related parameters'. The predicted forested area with a C/N ratio or a NO₃ concentration above presumed critical values increased continuously after 1985, even for the maximum feasible reductions (MFR) scenario. The problem of N accumulation thus appeared to be more persistent on a European scale, than that of soil acidification (cf De Vries *et al.*, 1994c)

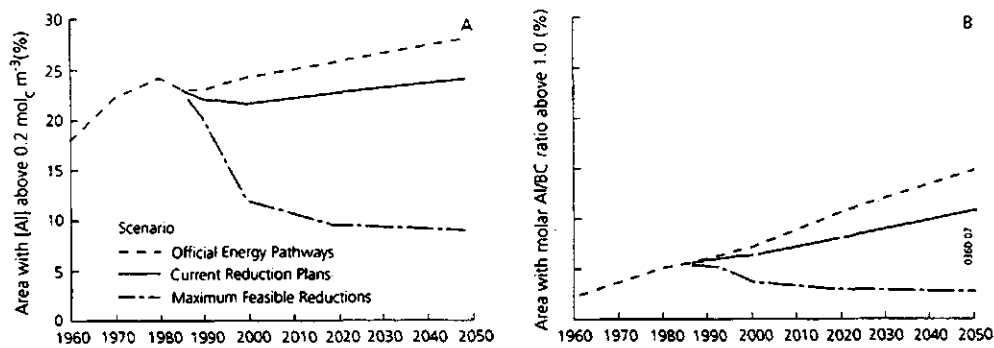


Fig. 6.5 Temporal development of the forested area in Europe (%) with Al concentrations above $0.2 \text{ mol}_c \text{ m}^{-3}$ (A) and molar Al/BC ratios above 1.0 (B) in response to three scenarios

6.4 Discussion and conclusions

6.4.1 Evaluation of model predictions

Important aspects of model evaluation are validation of model results on measured data and assessment of the uncertainty in model results due to uncertainties in model structure and model inputs. According to Janssen *et al.* (1990), model validation can be divided in: (i) a conceptual validation (are the various model assumptions and concepts justified), (ii) an operational validation (is the model suitable for the purpose aimed at, and does it produce plausible results) and (iii) a model output validation (is there a good agreement between model predictions and measured data). Even though SMART and ReSAM were validated by comparing simulations with historical observations of changes in soil solution chemistry between 1974 and 1989 in a continuously monitored spruce site in Solling, Germany (cf Section 3.1.2) the time period of the data set was too short for a rigorous validation of the model outputs. Consequently, the question about the accuracy of the long-term soil responses estimated by the SMART and ReSAM model cannot be answered satisfactorily. However, the reasonable to good agreement between measured and simulated (i) changes in soil solution chemistry on a site scale (cf Section 3.1.2) and (ii) frequency distributions of ion concentrations on a regional scale (cf Section 3.2.2) imply that SMART and ReSAM produce plausible results.

Even though model predictions are plausible, the uncertainty can be large due to the uncertainty and spatial variability in input data, especially for large scale predictions. This can be derived from a study in which the uncertainty in the response of the model ReSAM to a given deposition scenario has been evaluated in relation to uncertainty (including spatial variability) of data (Kros *et al.*, 1993). The main aim was to find out which additional data would most improve the reliability of predictions, to guide data derivation for a regional application of ReSAM. The uncertainty analysis was performed by using Monte Carlo simulation techniques in combination with regression analysis. The uncertainty in model outputs was quantified by giving frequency distributions of input data instead of deterministic values. The resulting frequency distributions of the

model output were analyzed by regression analyses to evaluate the contribution of the uncertainty of various parameters to the model uncertainty. This uncertainty analysis has been restricted to a Leptic podzol with Douglas fir, subject to a reducing deposition scenario between 1987 and 2010.

Overall results showed that the uncertainty contribution of the various parameters depended on the considered output variable, soil compartment and time. However, in most cases the uncertainty in the deposition of SO_2 , NO_x and NH_3 and parameters determining the nitrogen and aluminium dynamics played the most important role (Kros *et al.*, 1993). A simple sensitivity analysis performed earlier (De Vries and Kros, 1989) also showed that changes in the Al chemistry in the topsoil are strongly influenced by the parameters regulating nitrification and Al dissolution, because these processes mainly regulate H production and consumption, respectively. The relative unimportance of CEC and base saturation, is due to the low values (and the small range) for the base saturation of Dutch forest soils. On a European scale, these variables are likely to be more important. An important outcome of the study was, however, that average input data, used in a regional application in order to limit the number of simulations, produce adequate average model outputs for a specific soil vegetation combination.

6.4.2 Limitations of the models

The major possibilities and limitations of the three models are summarized in Table 6.8. The model limitations are related to their aim. NuCSAM was developed to reproduce soil (solution) chemistry on a site scale during a limited time period, whereas ReSAM and SMART were developed to predict long-term impacts of acid deposition on the soil on a regional scale. Consequently, unlike NuCSAM, peaks in soil solution chemistry cannot be reproduced by ReSAM and SMART. The annual time step of these models also hampers their validation, since long-term soil chemistry data are generally lacking. Unlike ReSAM and SMART, however, NuCSAM can not (hardly) be used to evaluate acidification policies on a regional scale because of the immense data needs. Large-scale application of ReSAM is already a huge task in this respect. (cf Table 6.8). Another drawback of NuCSAM is the complexity of the model, which makes it difficult for other modellers to use NuCSAM. In this respect, SMART is by far the most easy model to apply. (cf Table 6.8). A final aspect regarding model limitations, is the possibility to use the models in other scenario studies. Examples are studies on the effects of changes in hydrology (e.g lowering of groundwater tables) and in land use (e.g reforestation of former agricultural lands) on the soil (solution) chemistry. Since NuCSAM contains a separate hydrological submodel, changes in hydrology can easily be included. Changes in land use, affecting the nutrient cycle, can also relatively easy be included in NuCSAM and in ReSAM but not in the original SMART model, that excludes nutrient cycling. In principle, all models can, however, be revised such that other scenario studies are possible. For example, nutrient cycling has recently been included in SMART, together with the possibility of including seepage flow, to enable the calculation of nitrogen availability and pH in all major vegetation/ soil combinations in the Netherlands (Kros *et al.*, 1995b). Another possibility is the coupling of these soil acidification models with models on heavy metal behaviour, including pH dependent

adsorption processes. The effort that is required to adapt the models for use in other scenario studies will, however, differ as indicated in Table 6.8.

Table 6.8 Possibilities and limitations of the models NuCSAM, ReSAM and SMART

Model	Possibilities for			
	Site scale validation	large scale application	use by other modellers	use in other scenario studies
NuCSAM	Good	Limited	Limited	Reasonable
ReSAM	Limited	Reasonable	Reasonable	Limited
SMART	Limited	Good	Good	Limited

6.4.3 Use of the models to predict chemical time bombs

Chemical time bombs have been defined as a 'chain of events resulting in the delayed and sudden occurrence of harmful effects caused by the mobilization of chemicals stored in soils in response to alterations in certain environmental conditions' (after Stigliani *et al.*, 1991). Such a situation may for example occur with respect to heavy metals after afforestation of former agricultural land. Due to the EC agricultural policy, arable land is currently being transformed to forest. Apart from atmospheric input, most arable soils received considerable additional metal loads originating from long-term agricultural management practices e.g the application of animal manure and/or fertiliser. Consequently, total Cd, Zn and Cu contents of arable soils at the time of forestation are significantly higher compared to mature 'natural' forest soils. Solution concentrations in arable soils are usually low due to liming, causing a near neutral soil pH, and low organic ligand contents. The conversion of arable land to forest, however, will lead to major changes in the chemical, physical and biological properties of the soil, which increase the mobility of the stored metals. Termination of liming results in a drop of the soil pH from the actual near neutral value (5.5-6.5) to an acid value (3.5-4.5). Furthermore, the maturation of the forest enhances the development of an organic layer which leads to higher concentrations of Dissolved Organic Carbon (DOC) and organic ligands in the soil solution.

A recent study by Römken and de Vries (1995) showed that a relatively simple combined soil acidification-Cd mobility model gives comparable predictions of changes in pH and Cd concentrations as those measured in afforested stands of different ages. However, in order to predict metal mobilisation more accurately, it will be necessary to further develop the integration of knowledge concerning soil acidification, organic matter dynamics and metal behaviour in the soil. Especially the processes of acidification combined with the organic matter dynamics (development of an O_h layer, increase in DOC content, Al-organic matter interactions) need further attention in order to assess future consequences of afforestation. With respect to land use changes in general, it can be concluded that there is still a lack of information concerning the dynamics of soil chemical processes on a time-frame of 10 to 100 years.

References

- Alcamo, J., R. Shaw and L. Hordijk, 1990. The RAINS model of acidification. Science and Strategies in Europe. Dordrecht, The Netherlands, Kluwer Academic Publishers, 402 pp.
- Billet, M.F., E.A. FitzPatrick and M.S. Cresser, 1988. Long-term changes in the acidity of forest soils in North-East Scotland. *Soil Use and Man.* 4: 102-107.
- Butzke, H., 1988. Zur zeitlichen und kleinräumigen Variabilität des pH-Wertes in Waldböden Nordrhein-Westfalens. *Forst und Holzwirt* 43 (4): 81-85.
- Bredemeier, M.A., A. Tiktak and C. van Heerden, 1995. The Solling spruce stand. Background information on the dataset. *Ecol. Model.* 83:7-15.
- Chen, C.W., S.A. Gherini, R.J.M. Hudson and J.D. Dean, 1983. The Integrated Lake-Watershed Acidification Study. Volume 1. Model principles and application procedures. EPRI EA-3221, Volume 1, Research Project 1109-5, TETRA TECH INC., Lafayette, California, 194 pp.
- Cosby, B.J., G.M. Hornberger, J.N. Galloway and R.F. Wright, 1985. Modeling the effects of acid deposition. Assessment of a lumped parameter model of soil water and streamwater chemistry. *Water Resour. Res.* 21: 51-63.
- De Vries, W., 1993. Average critical loads for nitrogen and sulfur and its use in acidification abatement policy in The Netherlands. *Water Air and Soil Pollut.* 68: 399-434.
- De Vries, W. and J. Kros, 1989. The long-term impact of acid deposition on the aluminium chemistry of an acid forest soil. In: J. Kämäri, D.F. Brakke, A. Jenkins, S.A. Norton and R.F. Wright (Eds.), *Regional Acidification Models. Geographic Extent and Time Development*: 113-128.
- De Vries, W., M. Posch and J. Kämäri, 1989. Simulation of the long-term soil response to acid deposition in various buffer ranges. *Water Air and Soil Pollut.* 48: 349-390.
- De Vries, W., J. Kros and C. Van der Salm, 1994a. The long-term impact of three emission-deposition scenarios on Dutch forest soils. *Water Air and Soil Pollut.* 75: 1-35.
- De Vries, W., G.J. Reinds and M. Posch, 1994b. Assessment of critical loads and their exceedance on European forests using a one-layer steady-state model. *Water Air and Soil Pollut.* 72: 357-394.
- De Vries, W., M. Posch, G.J. Reinds, and J. Kämäri, 1994c. Simulation of soil response to acidic deposition scenarios in Europe. *Water Air and Soil Pollut.* 78: 215-246.
- De Vries, W., J. Kros and C. Van der Salm, 1995. Modelling the impact of acid deposition and nutrient cycling in forest soils. *Ecol. Model.* 79: 231-234.
- Erisman, J. W., 1991. Acid deposition in the Netherlands. Bilthoven, The Netherlands, National Institute of Public Health and Environmental Protection, Report nr 723001002, 72 pp.
- FAO, 1981. FAO-Unesco soil map of the world, 1 500 000. Volume V Europe. Unesco Paris 1981, 199 pp.
- Groenenberg, J.E., J. Kros, C. van der Salm, and W. De Vries, 1995. Application of the model NuCSAM to the Solling spruce site. *Ecol. Model.* 83:97-107.
- Hallbäck, L. and C.O. Tamm, 1986. Changes in soil acidity from 1927 to 1982-1984 in a forest area of south-west Sweden. *Scand. J. For. Res.* 1: 219-232.

- Hornberger, G.M., B.J. Cosby and J.N. Galloway, 1986. Modeling the effects of acid deposition. Uncertainty and spatial variability in estimation of long-term sulfate dynamics in a region. *Water Resour. Res.* 22 (8): 1293-1302.
- Janssen, P.H.M., W. Slob en J. Rotmans, 1990. Gevoeligheidsanalyse en onzekerheidsanalyse: een inventarisatie van ideeën, methoden en technieken. Bilthoven, Rijksinstituut voor Volksgezondheid en Milieuhygiëne. Rapport 958805001, 119 pp.
- Kros, J., W. De Vries, P.H.M. Janssen and C.I. Bak, 1993. The uncertainty in forecasting regional trends of forest soil acidification. *Water Air and Soil Pollut.* 66: 29-58.
- Kros, J., J.E. Groenenberg, W. de Vries and C. van der Salm., 1995a. Uncertainties in long-term predictions of forest soil acidification due to neglecting seasonal variability. *Water, Air and Soil Pollut.* 79:353-375.
- Kros, J., G.J. Reinds, W. de Vries, J.B. Latour and M. Bollen, 1995b. Modeling of soil acidity and nitrogen availability in natural ecosystems in response to changes in acid deposition and hydrology. DLO Winand Staring Centre Report, 95
- Likens, G.E. and F.H. Bormann, 1974. Acid rain a serious regional environmental problem. *Science* 184: 1176-1179.
- Olsthoorn, T.N., J.A. Van Jaarsveld, J.M. Knoop, N.D. Van Egmond, J.H.C. Mülschlegel and W. Van Duijvenbooden, 1990. Integrated modeling in the Netherlands. In: J. Ferhann, G.A. Mackenzie and B. Rasmussen (Eds.), *Environmental models: Emissions and consequences*: 461-479.
- Roberts, T.M., R.A. Skeffington and L.W. Blank, 1989. Causes of type 1 spruce decline. *Forestry* 62 (3): 179-222.
- Roelofs, J.G.M., A.J. Kempers, A.L.F.M. Houdijk and J. Jansen, 1985. The effect of airborne ammonium sulphate on *Pinus nigra* var. *maritima* in the Netherlands. *Plant and Soil*, 84: 45-56.
- Römkens, P.F and W. de Vries., 1994. Acidification and metal mobilization: effects of land use changes on Cd mobility. Proc. Spec. Conf. on 'Acid Rain research: Do we have enough answers?' s' Hertogenbosch, The Netherlands 12-15 october 1994.
- Stigliani, W.M., P. Doelman, W. Salomons, R. Schulin, G.R.B. Smidt and S.E.A.T.M. van der Zee, 1991. Chemical time bombs: predicting the unpredictable. *Environment* 33: 4-30.
- Ulrich, B., R. Mayer and P.K. Khanna, 1979. Die Deposition von Luftverunreinigungen und ihre Auswirkungen in Waldokosystemen im Solling. *Schriften aus der Forstl. Fak. D. Univ. Gottingen und der Nierders. Vers. Anst. Bd. 58*, 291 pp.
- Van der Salm, C., J. Kros, J.E. Groenenberg, W. De Vries and G.J. Reinds, 1995. Validation of soil acidification models with different degrees of process aggregation on an intensively monitored spruce site. In: S. Trudgill (Ed.): *Solute modelling in catchment systems*. Wiley, Chichester:327-346.
- Van Dobben, H.T., J. Mulder, H. Van Dam and H. Houweling, 1992. Impact of atmospheric deposition on the biogeochemistry of Moorland pools and surrounding terrestrial environment. Agricultural Research Report 93, PUDOC Scientific Publishers, Wageningen, the Netherlands, 232 pp.
- Van Oene, H. and W. De Vries, 1994. Comparison of measured and simulated changes in base cation amounts using a one-layer and a multi-layer soil acidification model. *Water Air and Soil Pollut.* 72: 41-66.

7 General discussion and conclusions

It is obvious that dynamic soil acidification models are the only tool available for the evaluation of acidification abatement strategies. However, the question about the accuracy of the long-term soil responses estimated by the models ReSAM and SMART is difficult to be answered. It is nearly impossible to validate the long-term behaviour unless long-term data sets are available. However, in this study we attempted to validate these models indirectly. First, the results of a daily based stand-level model NuCSAM were directly compared to observations at two sites in order to validate the short-term behaviour, including intra-annual variation. Subsequently, the long-term flux-weighted annual average results of the validated stand-level model NuCSAM were compared to those of the regional model ReSAM. Nevertheless, the observation record of the Solling Spruce site, which is an exceptional long record, appeared to be long enough for a direct validation of the models ReSAM and, to a lesser extend, SMART.

Applications of NuCSAM to the two intensively monitored sites Speuld and Solling gave problems due to the large spatial variability of throughfall, soil solution chemistry and stand structure. Consequently, it was almost impossible to get a meaningful and representative data-set for validation. This was especially the problem at the Speuld, where the monitoring followed a disciplinary approach, with separate subplots for hydrology, soil chemistry and forest growth. Either the number of sampling replicates was too small to calculate stand averages (soil chemistry), or it was impossible to select more or less homogeneous subplots (hydrology and biomass inventory). Nevertheless, there was a reasonable to good agreement between observed and simulated changes in soil solution chemistry. NuCSAM could reproduce the general magnitude and trends of measured quantities, such as soil water contents and soil solution chemistry. Contrary to the Speuld application, the seasonal trends could not always be reproduced at Solling, especially the dynamics of nitrogen cycling.

It can be concluded that leaching fluxes simulated with the yearly based model ReSAM compared well with results from the daily based model NuCSAM. This implies that ignoring seasonal variations of weather conditions and process simplification does not have a large impact for the long-term response of flux-weighted annual average soil solution chemistry to acid deposition. Consequently, the level of aggregation/simplification as used in the model ReSAM is in balance with the model purpose, i.e. making long-term predictions at a regional scale. Eventhough the Speuld and, to a lesser extend, the Solling data-set were too short for a true validation of long-term predictions with ReSAM. The acceptable results of an application of the model NuCSAM to the two sites has increased the confidence in the regional model ReSAM as an instrument for assessing long-term response of forest-soils to acidification abatement strategies. However, when major emphasis is on stress assessment, short-term temporal dynamics cannot be ignored, as both the extreme Al concentrations and the extreme Al/Ca ratios, which occur during the growing season, can not be simulated by a yearly averaged model.

Results of scenario analyses, that were carried out for Douglas fir on a Cambic podzol and Scots pine on an Haplic arenosol in areas with low, intermediate and high atmospheric

deposition, correspond with results from the 2nd phase of the DPPA, i.e. (i) a fast improvement of the SO_4^{2-} and Al concentrations after a decrease in SO_x deposition, (ii) time-delay for the NO_3^- concentration following a decrease in nitrogen deposition, (iii) higher soil solution concentrations in the soil below Douglas fir, and (iv) a decrease depletion of the pool of secondary aluminium compounds in areas with high deposition. The differences between the ReSAM results for the newly derived scenarios and the scenarios from the 2nd phase of the DPPA appeared to be rather small.

After the development, application and validation of the stand-level model NuCSAM, some uncertainties still remain, and new uncertainties arose. For further hypothesis testing and validation of the models, there is a need to continue the application and validation using data from other intensive monitoring programs. Special attention should be given to sites where the inputs have changed drastically during the observation period, e.g. roof experiments in NITREX sites such as Speuld, Ysselstein, Gårdsjön and Klosterheide and experimental manipulation (EXMAN) sites, such as Harderwijk and Speuld. Furthermore, attention should be paid to bridging the gap between models and experimental data. Models should be used to select the most important parameters for monitoring. Models can also be used to set-up sampling strategies. Besides intensive monitoring programs there is a need for extensive monitoring on a larger number of locations. Such extensive monitoring programs are mandatory for calibration of regional models. However, as with the intensive monitoring programs, much more attention should be paid to bridging the gap between models and measurements. In the near future, the present models should be used to further explore available data-sets, especially from manipulation experiments. Uncertainty analysis and calibration at both site scale and regional scale should be used to quantify and reduce the uncertainty of model results, respectively.

Major conclusions of this research are:

- (i) The daily based model NuCSAM reproduces the main features of the concentration variations over time in both Speuld and Solling for most elements.
- (ii) The capability of the yearly based model ReSAM to simulate observed flux-weighted annual averaged concentrations (and ratios) is comparable or even better than NuCSAM.
- (iii) Long-term predictions of annual average concentrations with ReSAM and NuCSAM show general agreement. This implies that ignoring seasonal variation of weather conditions does not have a large impact on the long-term response of soil solution chemistry to deposition. ReSAM, is thus acceptable for making long-term annual average predictions.
- (iv) A site scale model such as NuCSAM proved to be a valuable link between relatively short data records and long-term predictions generated with ReSAM.
- (v) Even the one-layer model SMART was able to reproduce the main dynamics in soil solution chemistry. Except for periods in which a strong change in soil solution concentrations occurred, due to a strong (numerical) dispersion effect.
- (vi) Scenario analyses showed a fast response of the sulphate and aluminium concentrations in the soil solution after a decrease of the SO_x deposition, time-delay for the NO_3^- concentration following a decrease in nitrogen deposition, and an ongoing depletion of the pool of secondary aluminium compounds in regions with high deposition.
- (vii) For further hypothesis testing and validation of the models, there is a need to continue intensive monitoring programs, but the balance between data acquisition in the

various compartments should be emphasized. For further validation, the models should be applied to experimental manipulations.

Annex 1 Annotation of used symbols in Chapter 3

Symbol	Description	Unit
$Am_{st,mx}$	Maximum amount of stem mass	kg ha^{-1}
C_o	Amount of water on the canopy at the start of the dry period	m
C_t	Amount of water on the canopy at the end of the day	m
$ctAl_{ox}$	Oxalate extractable Al content	$\text{mol}_c \text{kg}^{-1}$
ctX_{pm}	Element contents in primary minerals (X = Na, K, Ca, Mg)	$\text{mol}_c \text{kg}^{-1}$
T	Layer thickness	m
E	Daily evapotranspiration rate	m day^{-1}
$FAl_{we,ox}$	Weathering flux of Al from Al hydroxide	$\text{mol}_c \text{m}^{-2} \text{a}^{-1}$
fE_{dr}	Correction factor for evaporation from the canopy in dry periods	-
fE_{wt}	Correction factor for evaporation from the canopy during rainfall	-
frX_{fe}	Foliar exudation fraction of X (X = Ca, Mg, K)	-
frX_{fu}	Foliar uptake fraction of X (X = NH_4 , H)	-
$FX_{we,pm}$	Weathering flux of cation X from primary minerals (X = Ca, Mg, K, Na)	$\text{mol}_c \text{m}^{-2} \text{a}^{-1}$
I	Interception	m
K	Hydraulic conductivity	m day^{-1}
kEl_1	Elovich constant	$\text{m}^3 \text{kg}^{-1} \text{a}$
kEl_2	Elovich constant	kg mol_c^{-1}
k_{lf}	Leaf fall rate	$\text{kg ha}^{-1} \text{a}^{-1}$
$k_{ni,mx}$	Maximum nitrification rate	a^{-1}
k_{rd}	root decay rate	a^{-1}
$kr_{gr,l}$	Logistic growth rate	a^{-1}
$kX_{we,pm}$	Weathering rate base cations from primary minerals	a^{-1}
P	Precipitation	m
P_s	Amount of precipitation at which the canopy is saturated	m
\bar{R}	Average rainfall intensity	m day^{-1}
ρ	Bulk density	kg m^{-3}
S	Canopy storage	m
sc	Soil cover	-
t_{50}	time at which tree is half its maximum mass	a
t_d	Dry fraction of day	-

Annex 2 Description of the most important processes included in SMART, ReSAM and NuCSAM

1. Foliar uptake and foliar exudation

ReSAM and NuCSAM:

$$FNH_3_{fu} = frNH_3_{fu} \cdot FNH_3_{dd}$$

with:

FNH_3_{fu}	foliar uptake flux of NH_3
$frNH_3_{fu}$	foliar uptake fraction of NH_3
FNH_3_{dd}	dry deposition of NH_3

$$FX_{fe} = krX_{fe} \cdot Am_{lv} \cdot ctX_{lv} ; X = Ca, Mg, K$$

with:

FX_{fe}	foliar exudation flux of X
krX_{fe}	foliar exudation rate constant for X
Am_{lv}	Amount of leaves
ctX_{lv}	Content of nutrient X in leaves

SMART: not included

2. Litterfall and root decay

ReSAM and NuCSAM:

$$FX_{lf} = krX_{lf} \cdot Am_{lv} \cdot ctX_{lv} \cdot dis_{lf}(t) ; X = N, S, Ca, Mg, K$$

$$FX_{rd} = kr_{rd} \cdot Am_{rt} \cdot ctX_{rt} \cdot dis_{rd}(t) ; X = N, S, Ca, Mg, K$$

with:

FX_{lf} and FX_{rd}	litterfall and root decay flux
krX_{lf} and krX_{rd}	litterfall and root decay rate constants
Am_{lv} and Am_{rd}	amounts of leaves and fine roots
ctX_{lv} and ctX_{rt}	contents of nutrient X in leaves and fine roots
$dis_{lf}(t)$ and $dis_{rd}(t)$	distribution functions of litterfall and root decay over the year, which is uniform for ReSAM and variable for NuCSAM, with:

$$\sum_i [dis_i(t) \cdot dt] = 1$$

where dt is the time-step and i stands for the appropriate process.

SMART: not included

3. Mineralization of litter and dead roots

ReSAM and NuCSAM:

$$FX_{mi\ lt} = kr_{mi\ lt} \cdot A_{lt} \cdot ctX_{lt} \cdot dis_{mi}(t) ; X = N, S, Ca, Mg, K$$

$$FX_{mi\ rm} = kr_{mi\ rm} \cdot A_{rm} \cdot ctX_{rm} \cdot dis_{mi}(t) ; X = N, S, Ca, Mg, K$$

with:

$FX_{mi\ lt}$ and $FX_{mi\ rn}$	mineralization flux of litter and dead roots
$kr_{mi\ lt}$ and $kr_{mi\ rn}$	mineralization rate constants
Am_{lt} and Am_{rn}	amounts of litter and dead roots
ctX_{lt} and ctX_{rn}	contents of nutrient X in litter and dead roots
$dis_{mi}(t)$	distribution function of mineralization over the year, which is uniform for ReSAM and variable for NuCSAM, with:

$$\sum_t [dis_{mi}(t) \cdot dt] = 1$$

where dt is the time-step.

In NuCSAM litter is divided into three pools (litter pool, humus pool and fermentation pool)

SMART: not explicitly included instead net N immobilization is calculated from the increase in N-content in organic matter. Between a critical (C/N_{cr}) and a minimal C/N ratio (C/N_{min}) the immobilization rate N_{im} is linearly related to the prevailing C:N ratio (C/N):

$$FN_{im} = \begin{cases} 0 & \text{if } C/N \leq C/N_{min} \\ (FN_{td} - FN_{gu} - FN_{le,min}) \cdot \frac{C/N - C/N_{min}}{C/N_{cr} - C/N_{min}} & \text{if } C/N_{min} \leq C/N \leq C/N_{cr} \\ FN_{td} - FN_{gu} - FN_{le,min} & \text{if } C/N \geq C/N_{cr} \end{cases}$$

4. Net Tree Growth

ReSAM and NuCSAM:

$$dAm_{st} = kr_{gr\ l} \cdot Am_{st} \cdot \left(1.0 - \frac{Am_{st}}{Am_{st\ mx}}\right)$$

$$dAm_{br} = fr_{brst} \cdot dAm_{st}$$

$$FX_{gu} = (dA_{st} \cdot ctX_{st} + dA_{br} \cdot ctX_{br})$$

with:

Am_{st}	maximum amounts of stems
$Am_{st\ mx}$	amount of stems
dAm_{st}	stem growth
$kr_{gr\ l}$	logistic tree growth rate constant
fr_{brst}	branch stem ratio
Am_{br}	amount of branches
dA_{br}	branch growth
FX_{gu}	nutrient uptake for tree growth
ctX_{st} and ctX_{br}	contents of nutrient X in stems and branches

SMART: model input

5. Root uptake

ReSAM and NuCSAM:

$$FX_{ru} = (FX_{gu} + FX_{lf} + FX_{fe} - FX_{fu} + FX_{rd}) \cdot dis_{ru}(t) \quad ; X = N, S, Ca, Mg, K$$

with:

FX_{ru}
 $dis_{ru}(t)$

nutrient root uptake flux
distribution function of nutrient uptake over the year, which is
uniform for ReSAM and variable for NuCSAM, with:

$$\sum_t [dis_{ru}(t) \cdot dt] = 1$$

where dt is the time-step.

The distribution of N over NO_3^- and NH_4^+ is calculated as

$$FNH_{4\ ru} = fr_{prNH_4\ ru} \cdot \frac{cNH_4}{cNH_4 + cNO_3} \cdot FN_{ru}$$

$$FNO_{3\ ru} = FN_{ru} - FNH_{4\ ru}$$

with:

$fr_{prNH_4\ ru}$ preference factor for NH_4^+ uptake
 cNH_4 and cNO_3 NH_4^+ and NO_3^- concentration in the soil solution

SMART:

$$FX_{ru} = FX_{gu} \quad ; \quad X = N, BC (Ca+Mg), K+Na$$

Distribution of N over NO_3^- and NH_4^+

$$FNH_{4\ gu} = FN_{gu} \cdot \frac{FNH_{3\ td}}{FN_{td}}$$

$$FNO_{3\ gu} = FN_{gu} \cdot \frac{FNO_{x\ td}}{FN_{td}}$$

6. Nitrification and denitrification

ReSAM and NuCSAM:

$$FNH_{4\ ni} = \theta \cdot T \cdot kr_{ni} \cdot cNH_4$$

$$FNO_{3\ de} = \theta \cdot T \cdot kr_{de} \cdot cNO_3$$

with:

$FNH_{4\ ni}$ and $FNO_{3\ de}$ nitrification flux and denitrification flux
 θ soil moisture content
 T thickness of the soil layer
 kr_{ni} and kr_{de} nitrification and denitrification rate constant

SMART:

$$FNH_{4\ ni} = fr_{ni} (FNH_{3\ td} - FNH_{4\ gu} - FNH_{4\ im})$$

$$FNO_{3\ de} = fr_{de} (FNO_{x\ td} + FNH_{4\ im} - FNO_{3\ gu} - FNO_{3\ im})$$

7. Protonation of organic anions

ReSAM and NuCSAM:

$$FR_{COO_{pr}} = \theta \cdot T \cdot kr_{pr} \cdot cR_{COO}$$

with:

$FR_{COO_{pr}}$	protonation flux
kr_{pr}	protonation rate constant

SMART:

$$cR_{COO} = cR_{COO_T} \cdot \frac{K_{pr}}{K_{pr} + cH}$$

with:

cR_{COO_T}	sum of dissociated and non-dissociated organic acids
--------------	--

8. Carbonate dissolution/precipitation

RESAM and NuCSAM:

$$FCa_{we\ cb} = \rho \cdot T \cdot krCa_{we\ cb} \cdot ctCa_{cb} \cdot (cCa_e - cCa)$$

were:

$$cCa_e = KeCa_{cb} \cdot \frac{pCO_2}{cHCO_3}$$

with:

$FCa_{we\ cb}$	Ca weathering flux from carbonate
ρ	bulk density
$krCa_{we\ cb}$	Ca carbonate weathering rate constant
$ctCa_{cb}$	Ca content in carbonates
cCa	actual Ca^{2+} concentration
cCa_e	Ca^{2+} concentration in equilibrium with calcite
pCO_2	partial CO_2 pressure in the soil

SMART:

$$FBC_{we\ cb} = \theta \cdot D \cdot (cCa_e - cCa)$$

$$cCa_e = KeCa_{cb} \cdot \frac{pCO_2}{cHCO_3}$$

9. Weathering of primary minerals

ReSAM and NuCSAM:

$$FX_{we\ pm} = \rho \cdot T \cdot krX_{we\ pm} \cdot ctX_{pm} \cdot cH^{\alpha(X)} ; X = Ca, Mg, K, Na$$

$$FAl_{we\ pm} = 3 \cdot FCa_{we\ pm} + 0.6 \cdot FMg_{we\ pm} + 3 \cdot FK_{we\ pm} + 3 \cdot FNa_{we\ pm}$$

(congruent weathering of equal amounts of Anorthite (Ca), Chlorite (Mg), Microcline (K) and Albite (Na))

with:	
$FX_{we\ pm}$	weathering flux of element X from primary minerals
$krX_{we\ pm}$	weathering rate constant of element X from primary minerals
ctX_{cb}	content of element X in primary minerals
cH	actual H^+ concentration
$\alpha(X)$	unitless exponent

SMART:

$$FBC_{we} = \text{input value}$$

$$FAI_{we\ pm} = 2 \cdot FBC_{we}$$

10. Aluminium hydroxide dissolution/precipitation

ReSAM and NuCSAM:

$$FAI_{we\ ox} = \rho \cdot T \cdot krEI1 \cdot \exp(krEI2 \cdot ctAI_{ox}) \cdot (cAI_e - cAI)$$

$$cAI_e = KeAI_{ox} \cdot cH^3$$

with:

$FAI_{we\ ox}$	Al weathering flux from Al hydroxides
$krEI1$ and $krEI2$	Elovich weathering constants
$ctAI_{ox}$	Al content in hydroxides
cAI_e	Al^{3+} concentration in equilibrium with Al hydroxide
cAI	actual Al^{3+} concentration
$KeAI_{ox}$	Al hydroxide equilibrium constant

SMART:

$$FAI_{we\ ox} = \theta \cdot D \cdot (cAI_t - cAI_{t-1})$$

$$cAI = kAI_{ox} \cdot cH^3$$

11. Cation exchange

SMART, ReSAM and NuCSAM:

$$\frac{frX_{ac}}{frBC_{ac}^{z_x}} = KeX_{ex} \cdot \frac{cX^2}{cBC^{z_x}}$$

$X = H, Al, Mg, K, Na, NH_4$ and $BC = Ca$ for ReSAM and NuCSAM
 $X = H, Al$ and $BC = Ca + Mg$ for SMART

with:

frX_{ac}	fraction of cation X on the adsorption complex
KeX_{ex}	Gaines-Thomas selectivity constant for exchange of cation X against Ca^{2+}
cX	concentration of cation X in the soil solution
z_x	valence of cation X

12. Sulphate adsorption

SMART, ReSAM and NuCSAM:

$$c_{SO_4 ad} = \frac{SSC \cdot Ke_{SO_4 ad} \cdot c_{SO_4}}{1 + Ke_{SO_4 ad} \cdot c_{SO_4}}$$

with:

$c_{SO_4 ad}$	SO_4^{2-} content at the adsorption complex
SSC	SO_4^{2-} sorption capacity
$Ke_{SO_4 ad}$	SO_4^{2-} sorption constant
c_{SO_4}	SO_4^{2-} concentration in the soil solution

13. Dissolution/speciation of inorganic C

SMART, ReSAM and NuCSAM:

$$c_{HCO_3} = Ke_{CO_2} \cdot \frac{p_{CO_2}}{cH}$$

with:

Ke_{CO_2}	product of Henry's law constant and the first dissociation constant of H_2CO_3
c_{HCO_3}	HCO_3^- concentration in the soil solution
cH	H^+ concentration in the soil solution
p_{CO_2}	partial CO_2 pressure in the soil
